# Explosive Astrophysical Transients in the Multi-Messenger Era: Some Highlights


ARCO Astrophysics Research Center of the Open university

Jonathan Granot

THE GEORGE WASHINGTON UNIVERSITY WASHINGTON DC

YITP YUKAWA INSTITUTE FOR THEORETICAL PHYSICS

Open University of Israel & George Washington University & YITP


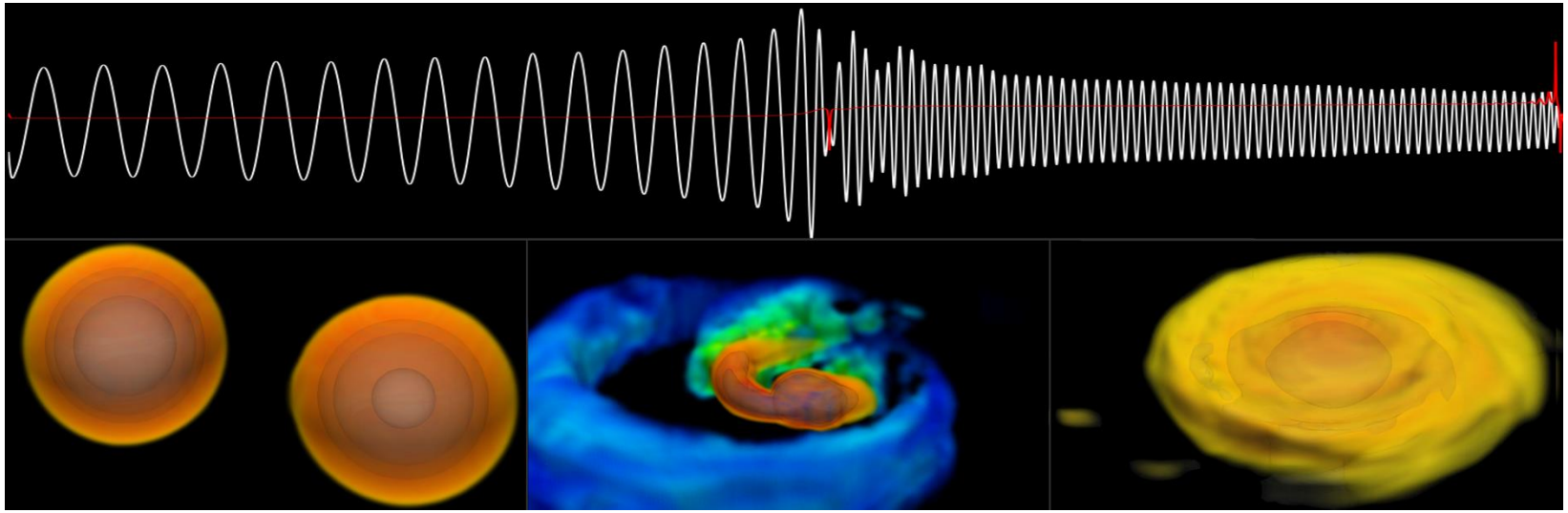

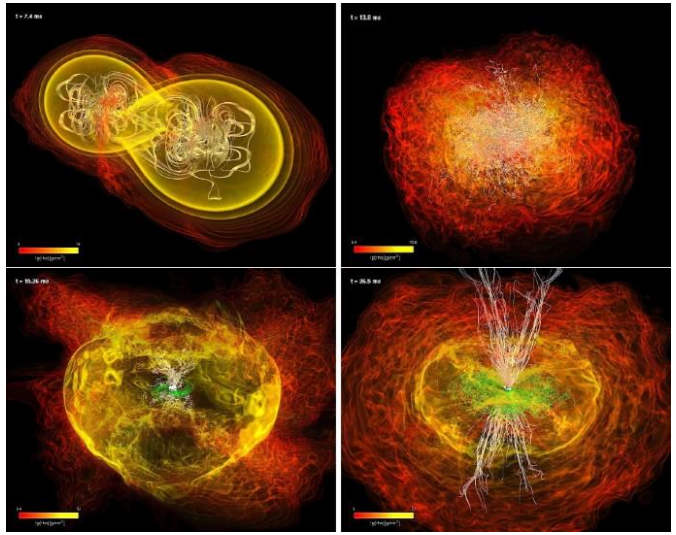

YITP long-term workshop: Multi-Messenger Astrophysics in the Dynamic Universe

Yukawa Institute for Theoretical Physics, Kyoto University, Kyoto, Japan, 26 January 2026

# Outline of the Talk: what will or will not be covered

- **GRB**s: select highlights from the recent decade
  - **GRB170817A/GW170817**: 1st EM-GW counterpart (sGRB, kilonova, afterglow), r-process elements synthesis, jet angular structure & large off-axis viewing angle
  - **Polarization**: GW170817 UL ⇒ constraints on B-field structure in the afterglow shock; GRB180720B: reverse to forward shock transition; afterglow pol. from structured jets
  - Prompt GRB: dissipation (IS/rec), emission (syn/Compt/SSC/had) (Rahaman)
  - **TeV emission**: from nearby GRBs – afterglow, reverse shock, prompt? (???)
  - **GRB 221009A** (B.O.A.T): bright in TeV, shallow jet, 6-12 MeV line (Salafia)
- **Einstein Probe** X-ray transients: mostly GRBs, start earlier, last longer (Hamidani)
- **ULGRB 250702B**: ~day long, unclear origin (some type of collapsar or TDE?)
- **Magnetar**s / **FRB**s:
  - FRBs from a Galactic magnetar, SGR 1935+2154 (28.4.2020)
  - Persistent Radio Sources (**PRS**s) associated with repeating Fast Radio Bursts (**FRB**s)
  - Extragalactic Magnetar Giant Flares- current sample and prospects

# GW170817 / GRB170817A: NS-NS merger

- First electromagnetic counterpart to a GW event
  - ❖ The short GRB 170817A (very under-luminous, 1.74 s $\gamma$-GW delay)
  - ❖ Optical (IR to UV) kilonova emission (1st clear-cut) for a few weeks
  - ❖ X-ray (> 9 d; still barely detected) to radio (>16 d) afterglow
- First NS-NS merger detected in gravitational waves (GW)
- First direct sGRB - NS-NS merger association (Eichler+ 1989)
- The $\gamma$-GW 1.74 s delay constrains GW speed: $\left|\frac{v_{GW}}{c} - 1\right| \lesssim 4 \cdot 10^{-16}$
- $D_{GW} = 43^{+2.9}_{-6.9}$ Mpc; host galaxy is elliptical: $D = 41.0 \pm 3.1$ Mpc ($z = 0.009783$) 2 kpc from host center in projection

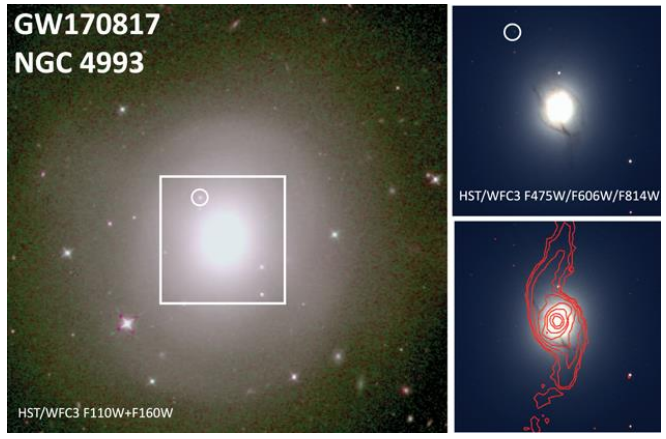


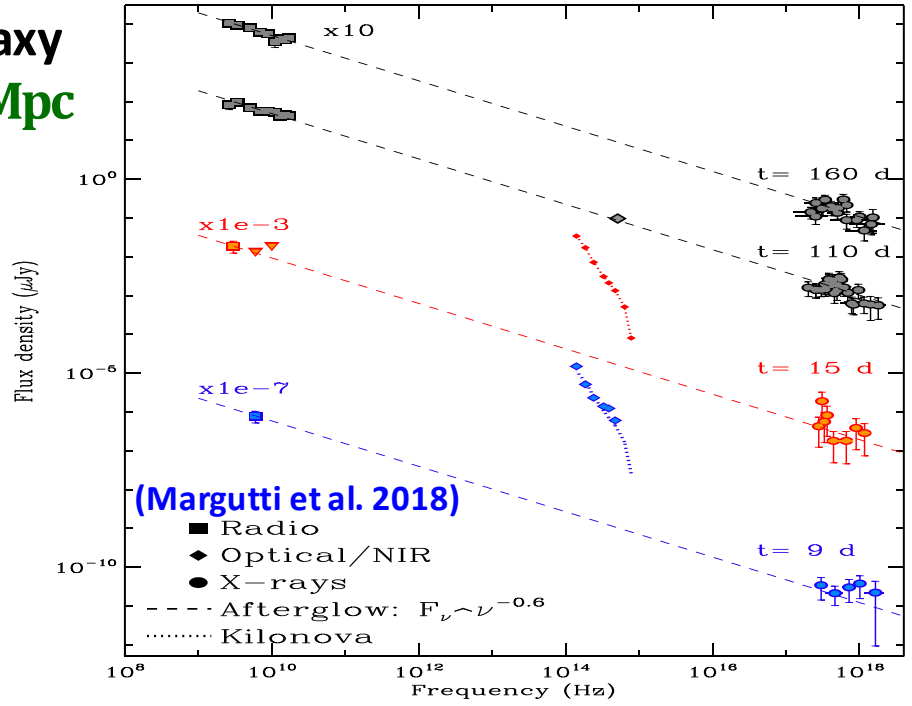


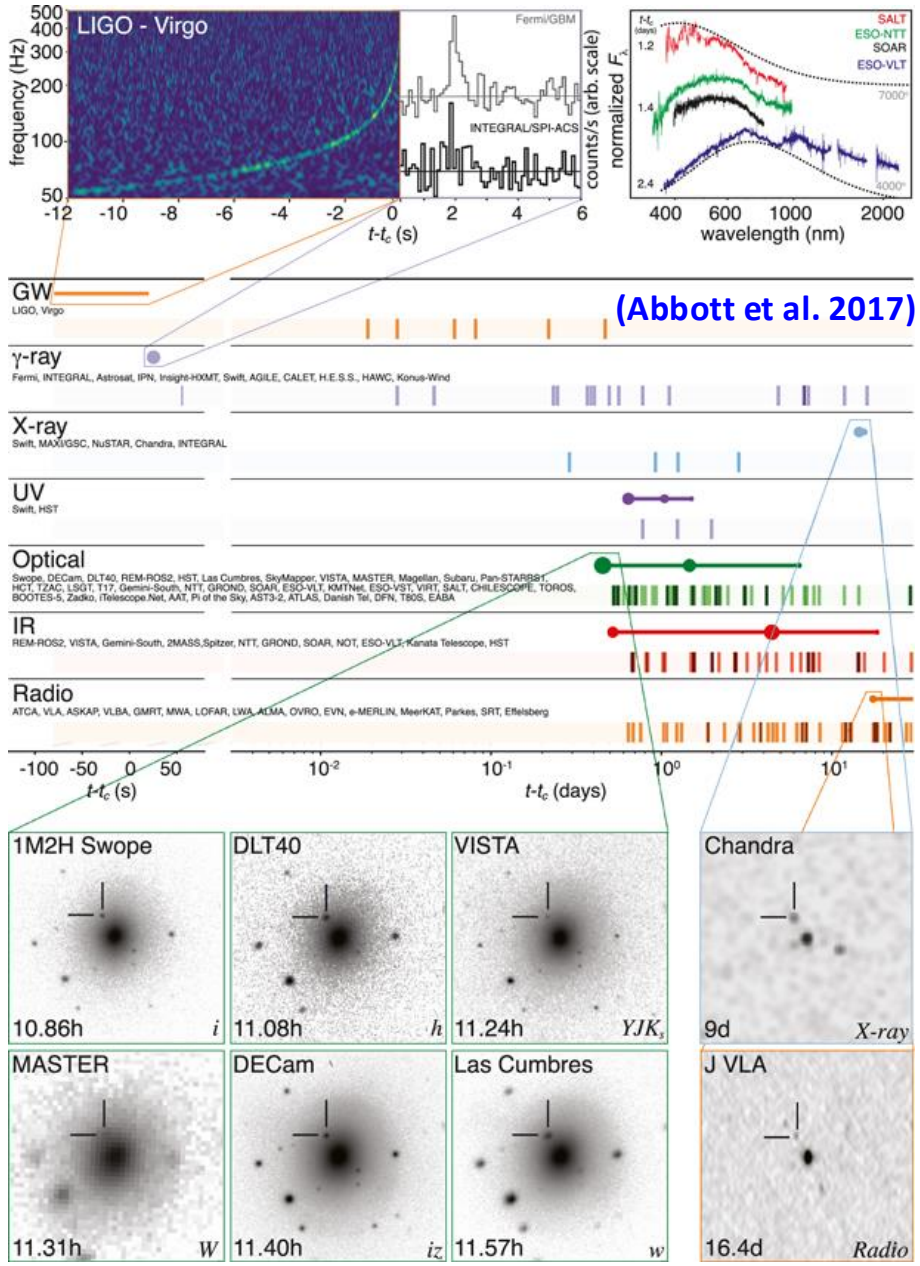

# GW170817 / GRB170817A: Kilonova

- **Observations require two components**:
  - ❖ First blue/fast, lanthanide-poor
    $M_{\rm ej} \approx (1\% - 2\%) M_\odot$ , $v_{\rm ej} \approx (0.2 - 0.3)c$
  - ❖ Second red/slow, lanthanide-rich
    $M_{\rm ej} \approx (3\% - 5\%) M_\odot$ , $v_{\rm ej} \approx (0.05 - 0.2)c$
- **Synthesized large amounts of heavy elements** (may dominate the cosmic r-process nucleosynthesis, heavy metals e.g. gold, platinum)

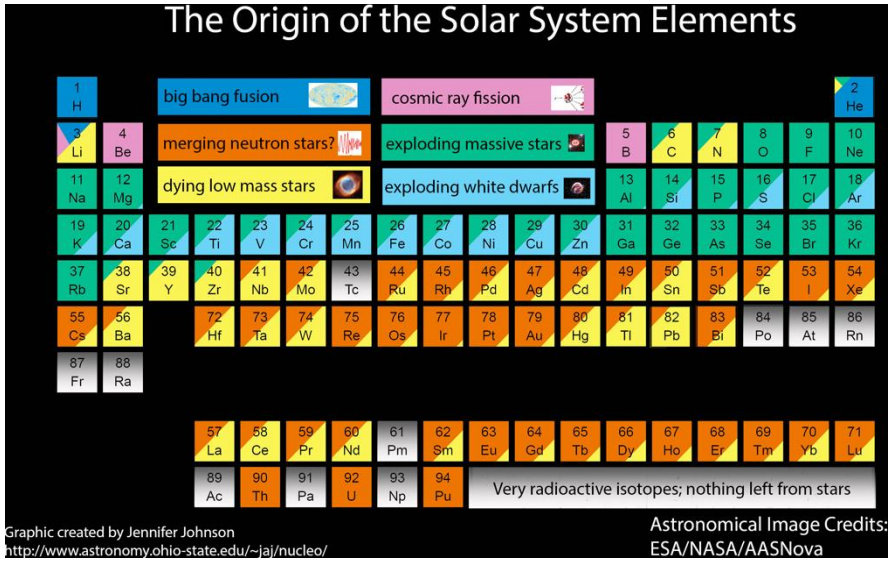


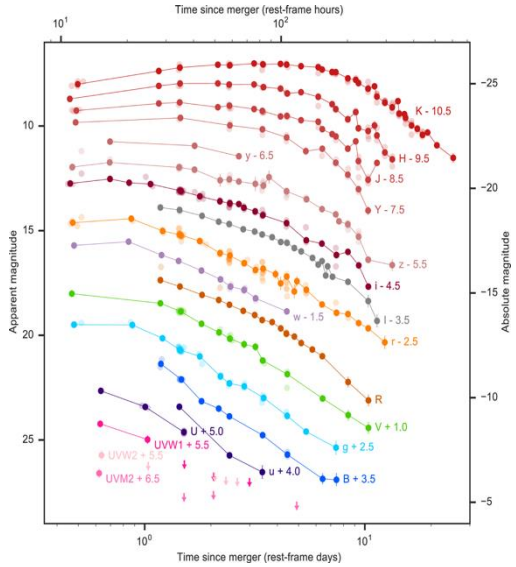


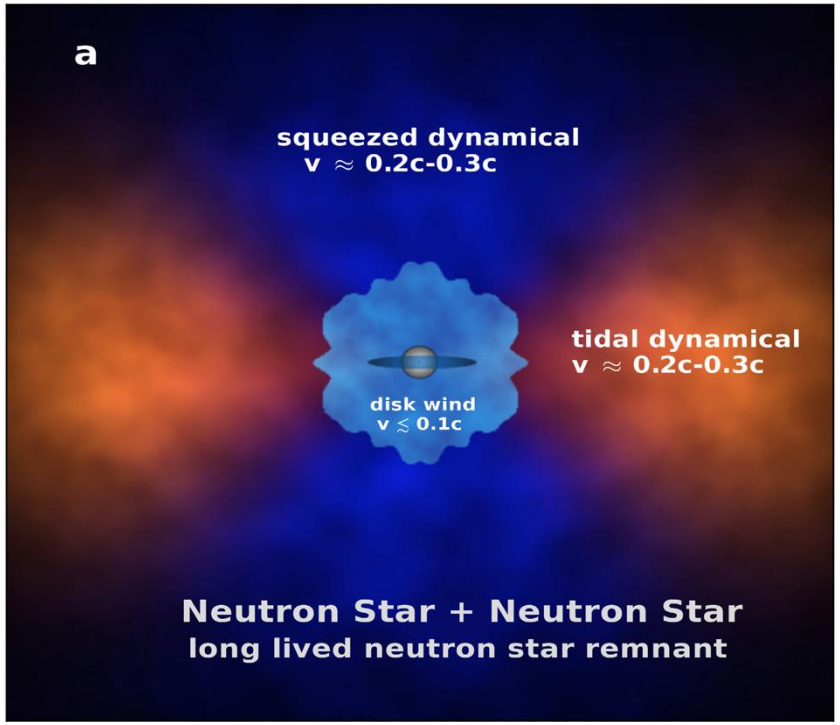


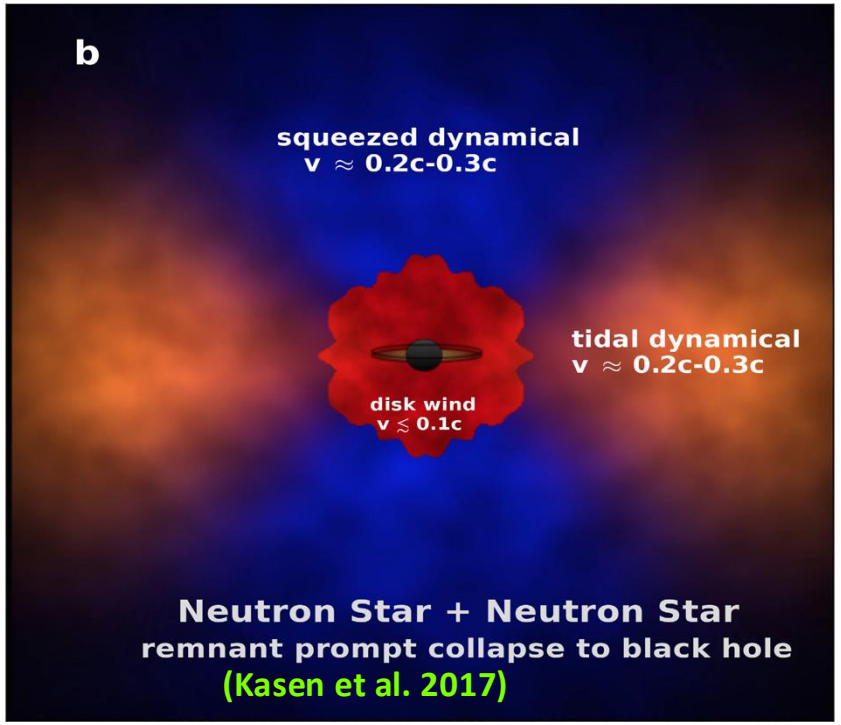


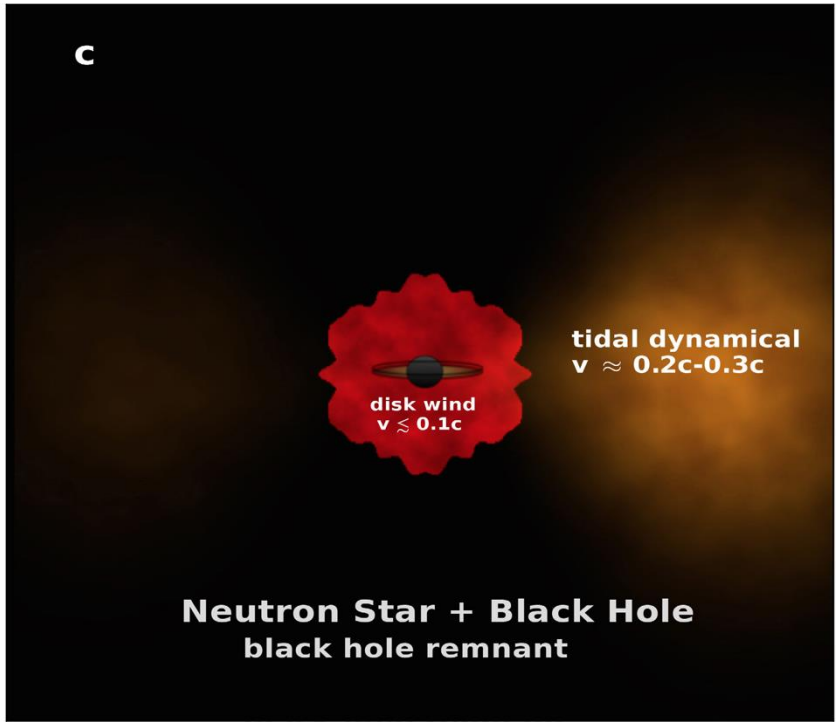

# GW170817 / GRB170817A: Remnant Type

- $M_{1,2}$ = pre-merger NS $M_{gravitational}$
- post-merger total mass: $M_i = M_1 + M_2$
- Final mass $M_f \approx 0.93 M_i$ due to:
  - ❖ GW & neutrino energy losses
  - ❖ Mass ejection during the merger
- **A stable NS or SMNS** ⇒ $P_0 \approx 1$ ms ⇒ $E_{rot} \gtrsim 10^{52.5}$ erg, $\tau_{sd} \approx 20 B_{13}^{-2}$ days ⇒ would contradict afterglow observations (also what produces the GRB/afterglow?)
- The argument can be reversed to constrain NS EoS & $M_{max} \lesssim 2.17 M_\odot$ (Margalit & Metzger 2017; Rezzolla et al. 2018)

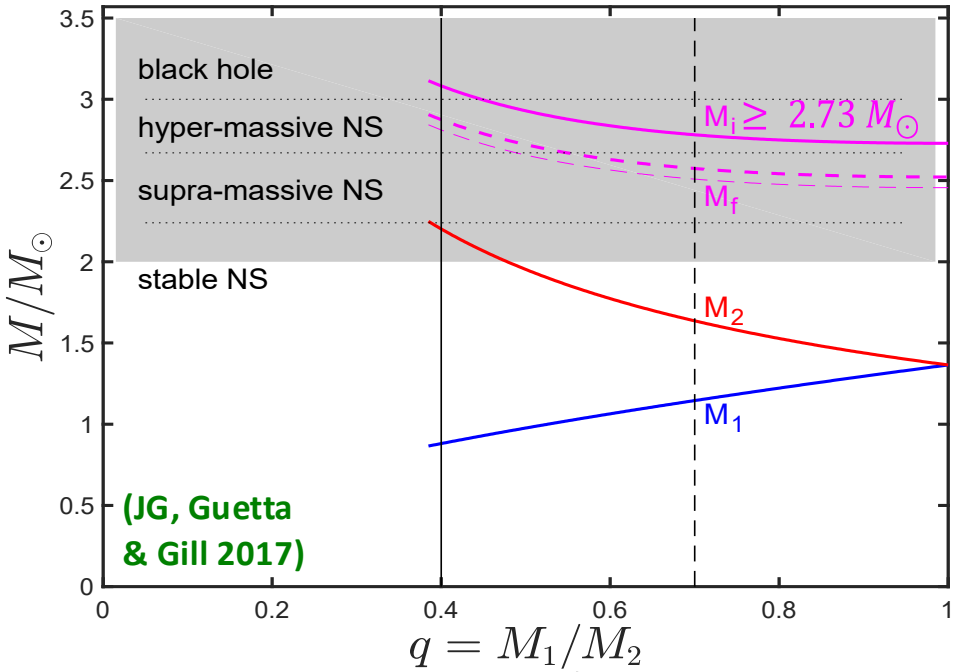


Chirp mass: $\mathcal{M} = \left(\frac{M_1^3 M_2^3}{M_1 + M_2}\right)^{1/5} = 1.188^{+0.004}_{-0.002}\, M_\odot$ (Abbott+ 2017)

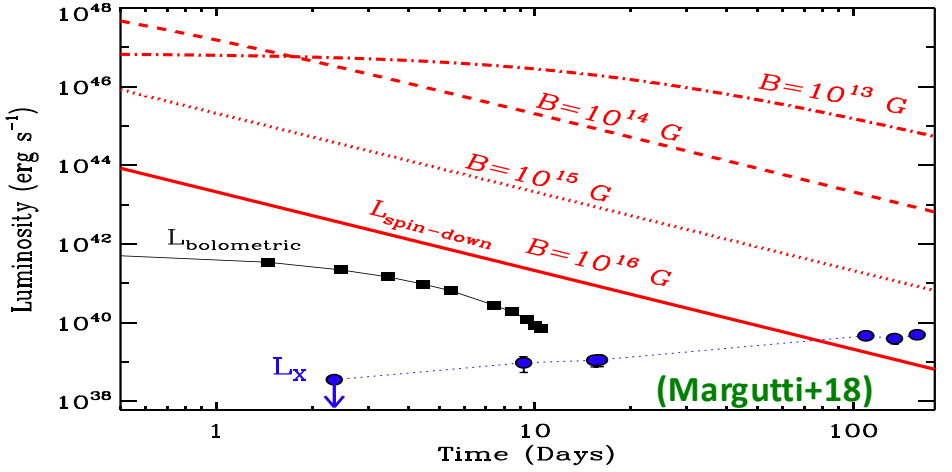

# GRB170817A: Afterglow Observations

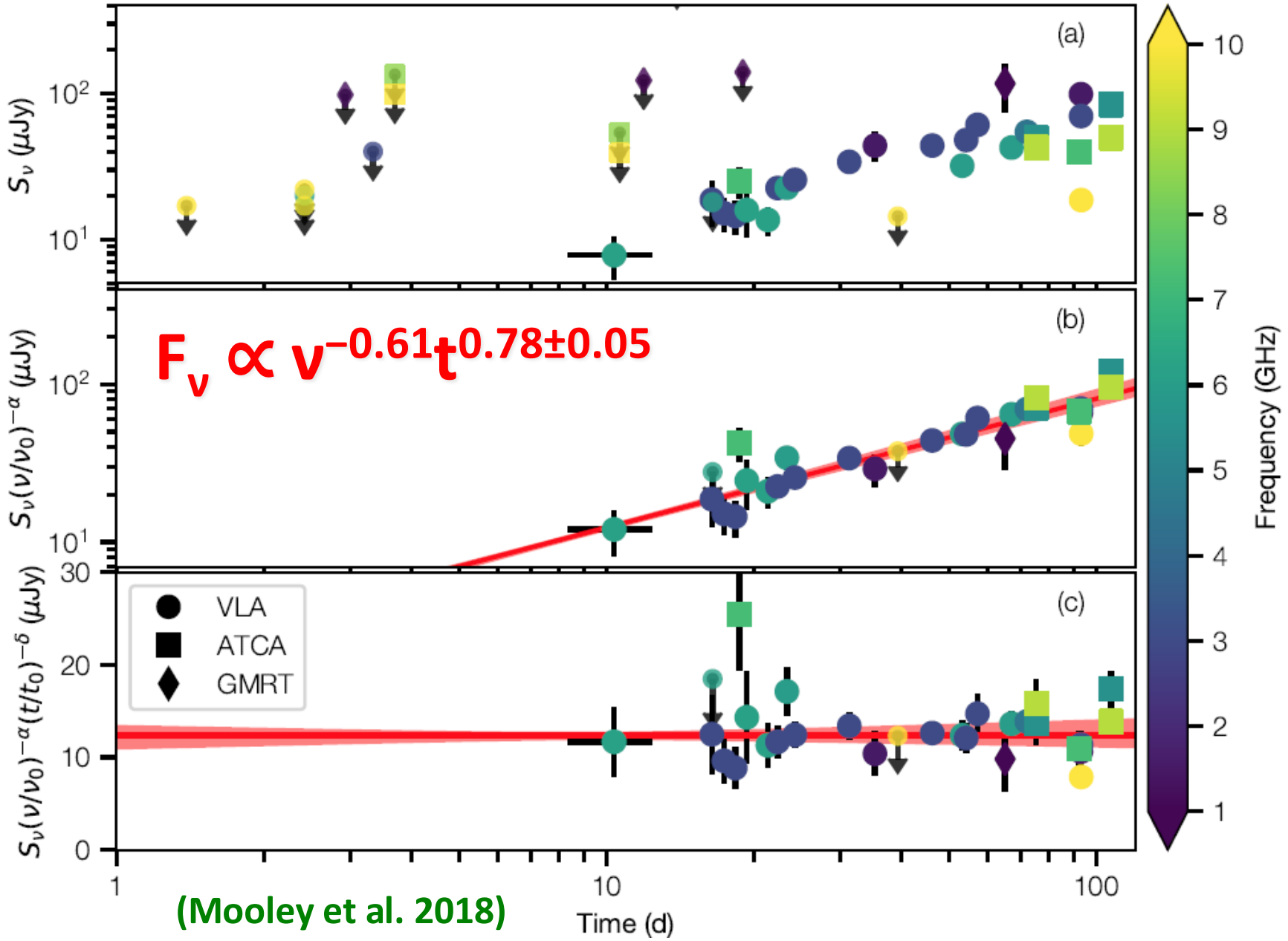


(Mooley et al. 2018)

# GRB170817A: Afterglow Observations

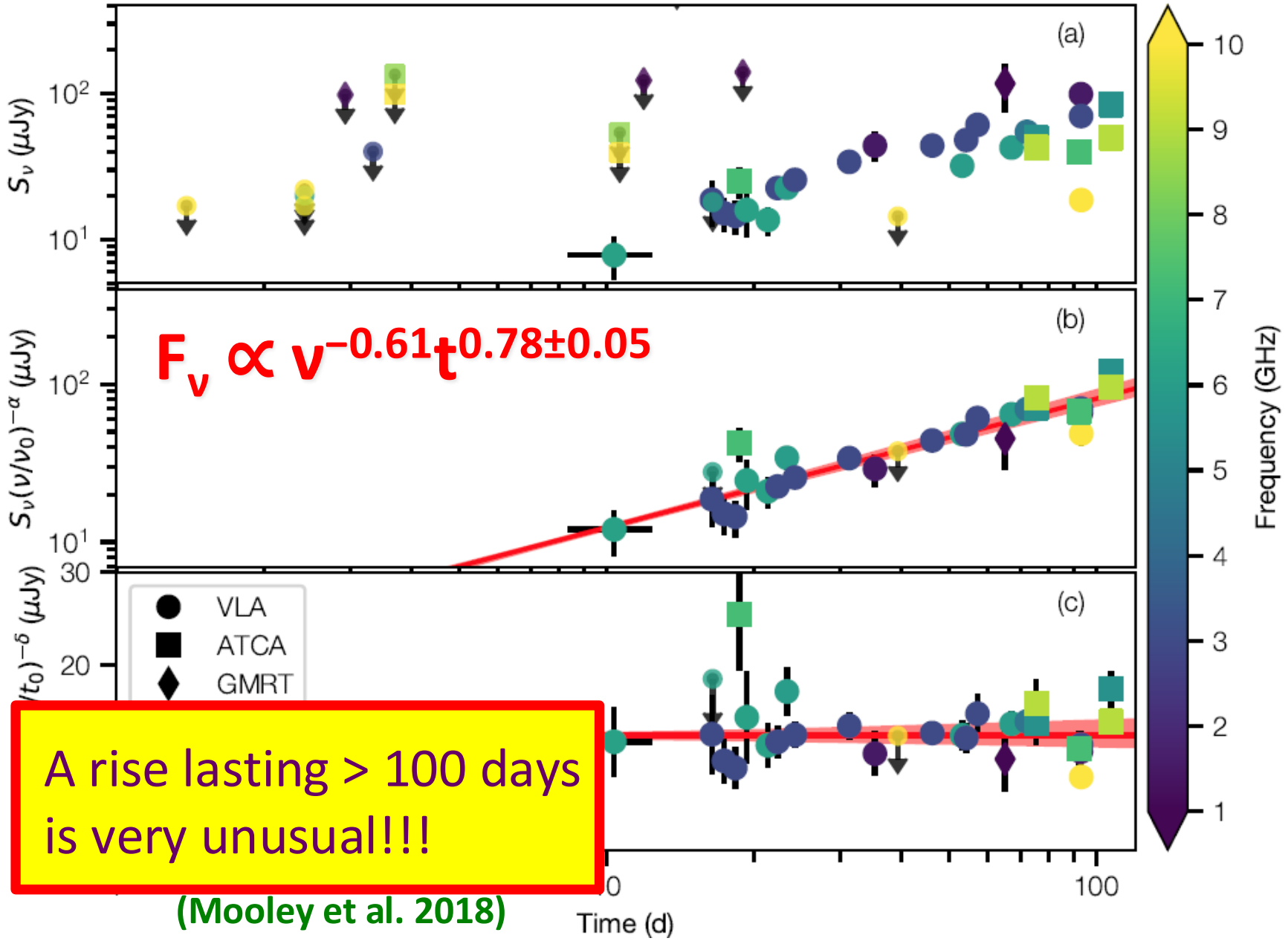


A rise lasting > 100 days is very unusual!!!

(Mooley et al. 2018)

# Analogy to rising $F_\nu$ : X-ray Plateaus

- Possible solutions:
  - Evolution of shock microphysical parameters (JG, Konigl & Piran 2006)
  - Energy injection into external shock:

1. long-lived relativistic wind
2. slower ejecta catching up
   (Sari & Meszaros 00; Nousek+ 06; JG & Kumar 06)

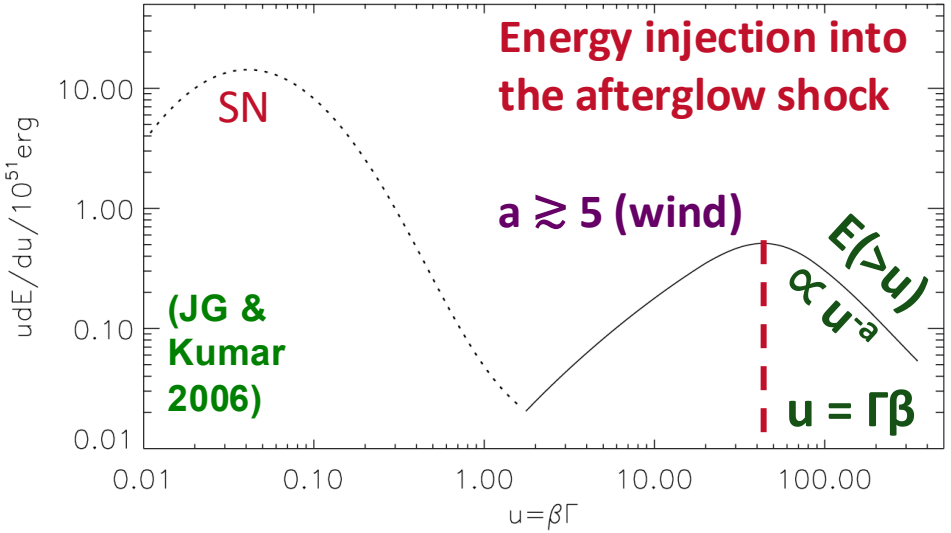


- Viewing angle effects

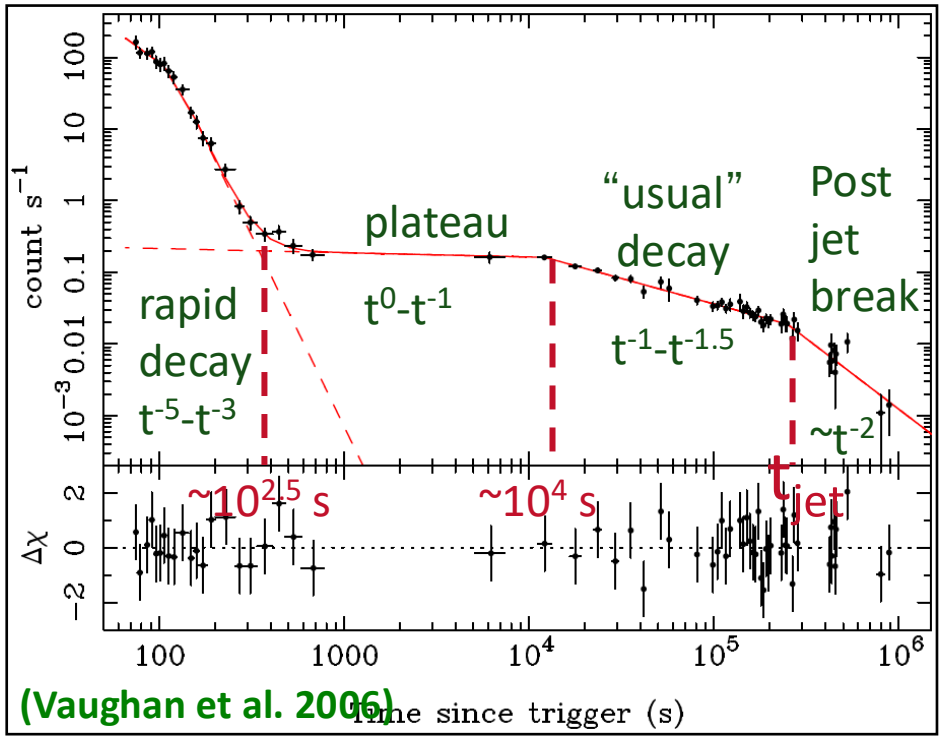


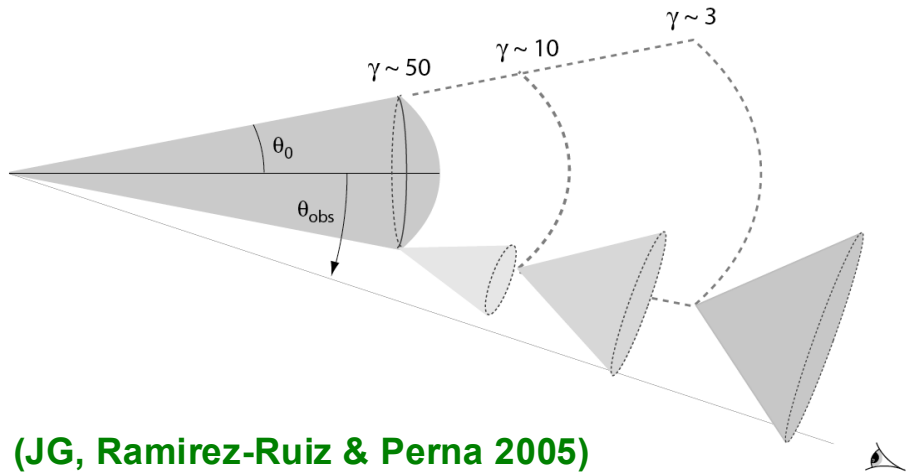

# Analogy to rising $F_\nu$ : X-ray Plateaus

- Possible solutions:
  - Evolution of shock microphysical parameters (JG, Konigl & Piran 2006)
  - Energy injection into external shock:

1. long-lived relativistic wind
2. slower ejecta catching up **radial**
   (Sari & Meszaros 00; Nousek+ 06; JG & Kumar 06)

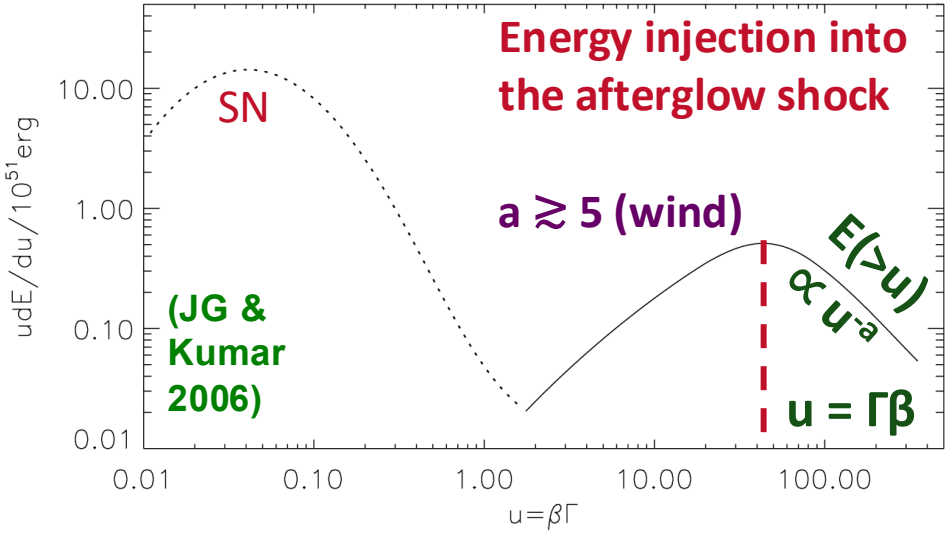


- Viewing angle effects **angular**

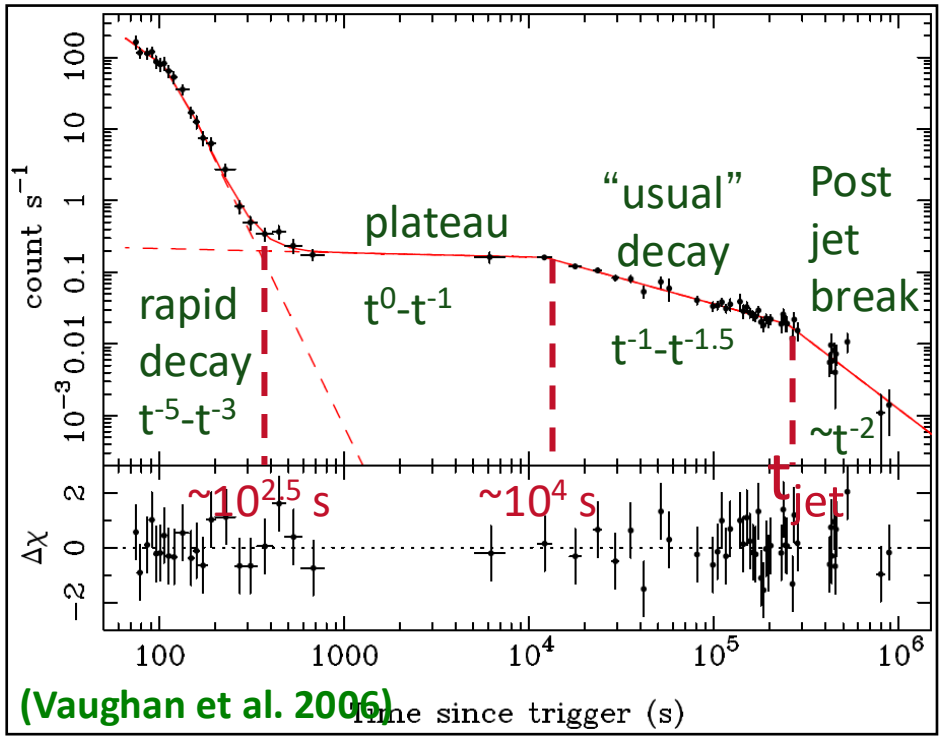


(Vaughan et al. 2006)

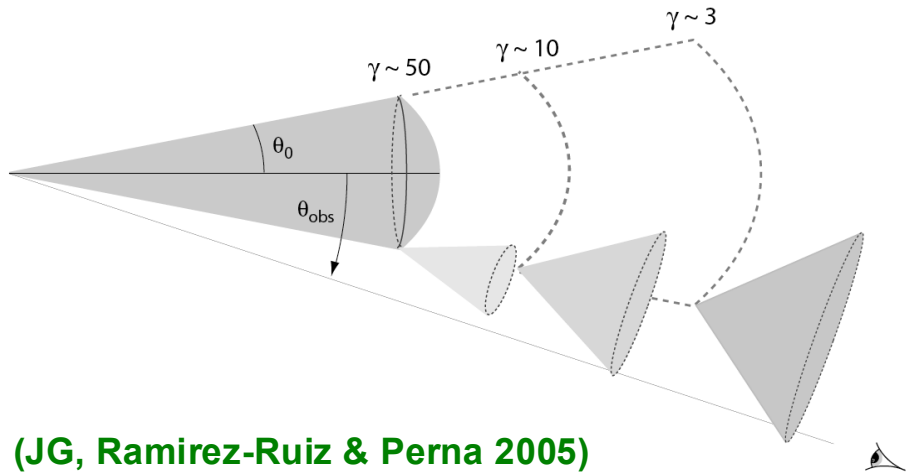


(JG, Ramirez-Ruiz & Perna 2005)

# Analogy to rising $F_\nu$ : Off-Axis Viewing

- The emission is initially strongly beamed away from our L.o.S
- $F_\nu$ rises as beaming cone widens
- When beaming cone reaches LoS $F_\nu$ peaks & approaches on-axis $F_\nu$
- The rise is much more gradual for hydrodynamic simulations due to slower matter at the jet's sides with non-radial velocities

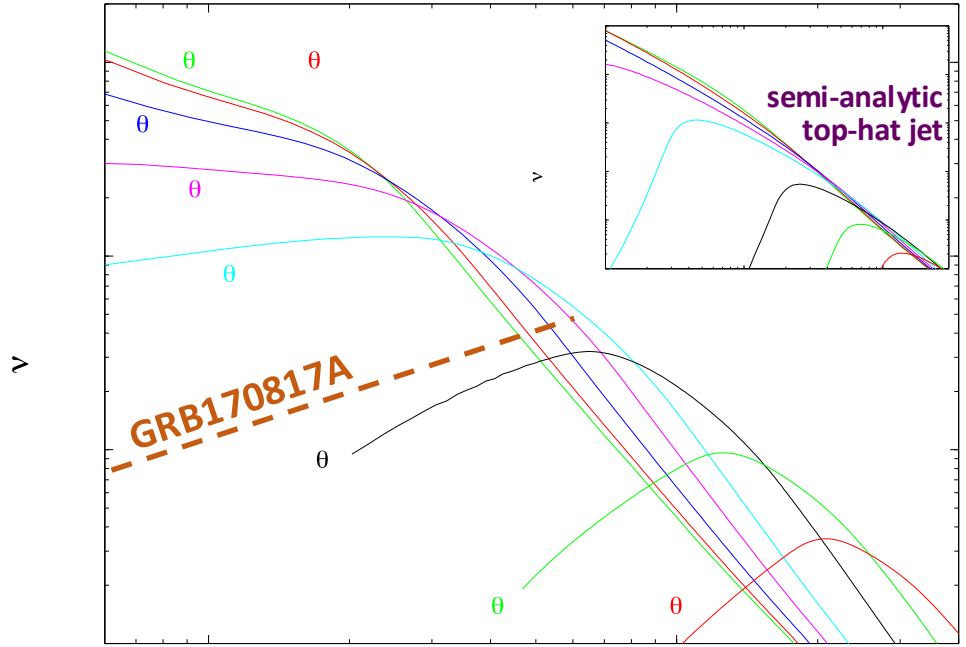


(JG et al. 2002)

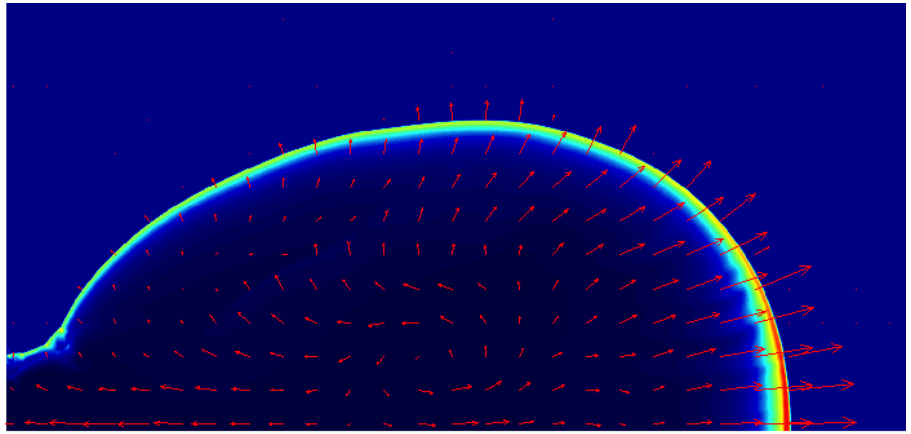


(JG et al. 2001)

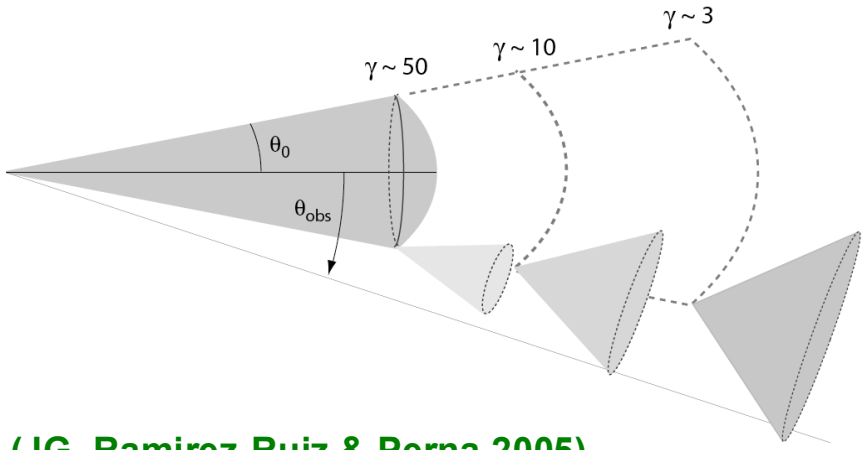


(JG, Ramirez-Ruiz & Perna 2005)

# Outflow Structure: Breaking the Degeneracy (Gill & JG 18)

- The lightcurves leave a lot of degeneracy between models
- The degeneracy may be lifted by calculation the afterglow images & polarization (e.g. Nakar & Piran 2018; Nakar et al. 2018)
- We considered 4 different models including both main types
  - Sph+$E_{inj}$: Spherical with energy injection $E(>u=\Gamma\beta) \propto u^{-6}$, $1.5<u<4$
  - QSph+$E_{inj}$: Quasi-Spherical + energy injection $E(>u) \propto u^{-s}$, $u_{min,0}=1.8$ $u_{max,0}=4$, $s=5.5$, $\zeta=0.1$

$$\frac{\epsilon(\theta)}{\epsilon_0}=\frac{u_{0,\min}(\theta)}{u_{\min,0}}=\frac{u_{0,\max}(\theta)}{u_{\max,0}}=\frac{\zeta+\cos^2\theta}{\zeta+1}$$

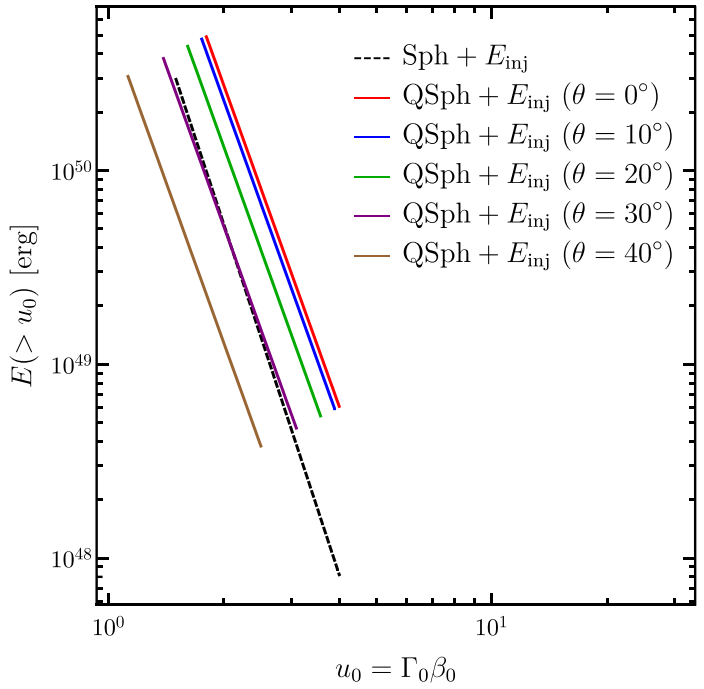


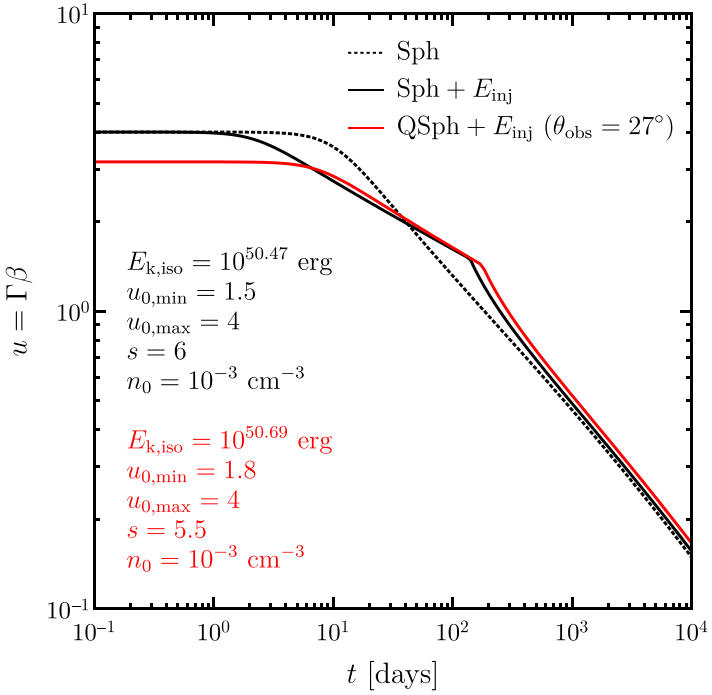

# Outflow Structure: Breaking the Degeneracy (Gill & JG 18)

- The lightcurves leave a lot of degeneracy between models
- The degeneracy may be lifted by calculation the afterglow images & polarization (e.g. Nakar & Piran 2018; Nakar et al. 2018)
- We considered 4 different models including both main types
  - GJ: Gaussian Jet (in $\varepsilon = dE/d\Omega$, $\Gamma_0 - 1$) $\Gamma_c = 600$, $\theta_c = 4.7°$
  - PLJ: Power-Law Jet; $\varepsilon = \varepsilon_c \Theta^{-a}$, $\Gamma_0 - 1 = (\Gamma_c - 1)\Theta^{-b}$, $\Theta = [1+(\theta/\theta_c)^2]^{1/2}$, $\Gamma_c = 100$, $\theta_c = 5°$, $a = 4.5$, $b = 2.5$
- As there is a lot of freedom we fixed: $p = 2.16$, $\varepsilon_B = n_0 = 10^{-3}$, $\theta_{obs} = 27°$

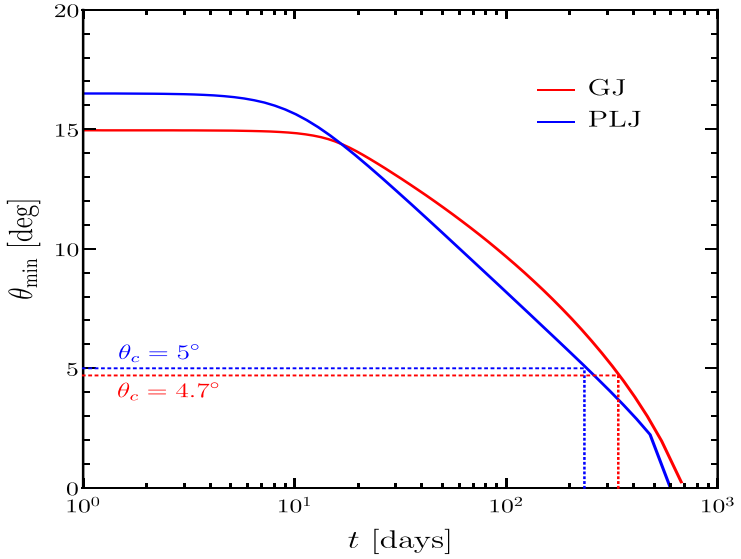


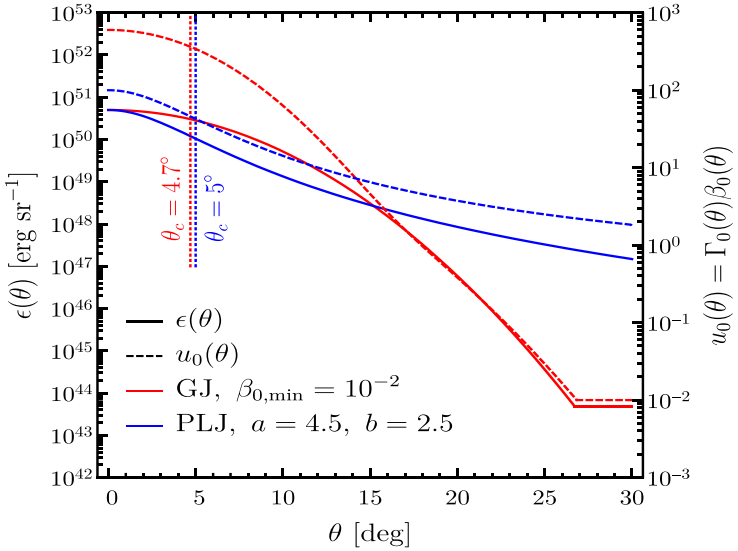

# Outflow Structure: Breaking the Degeneracy (Gill & JG 18)

- Tentative fit to GRB170817A afterglow data (radio to X-ray)

Gaussian Jet

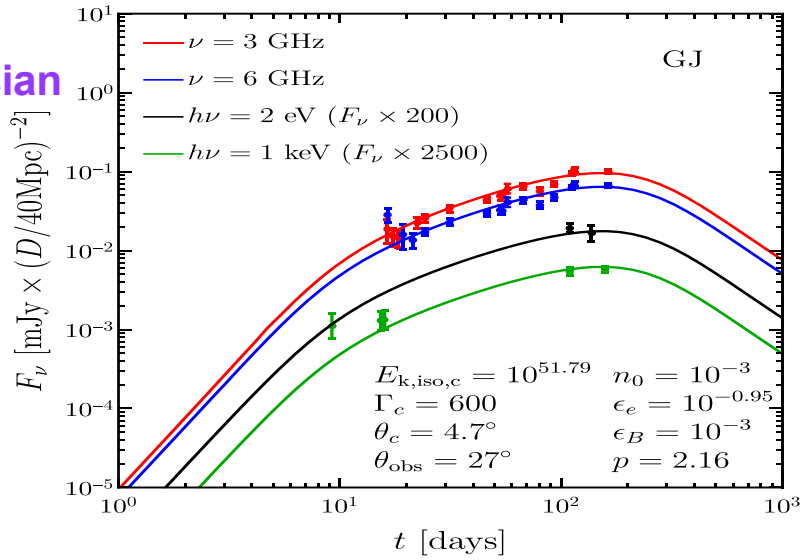


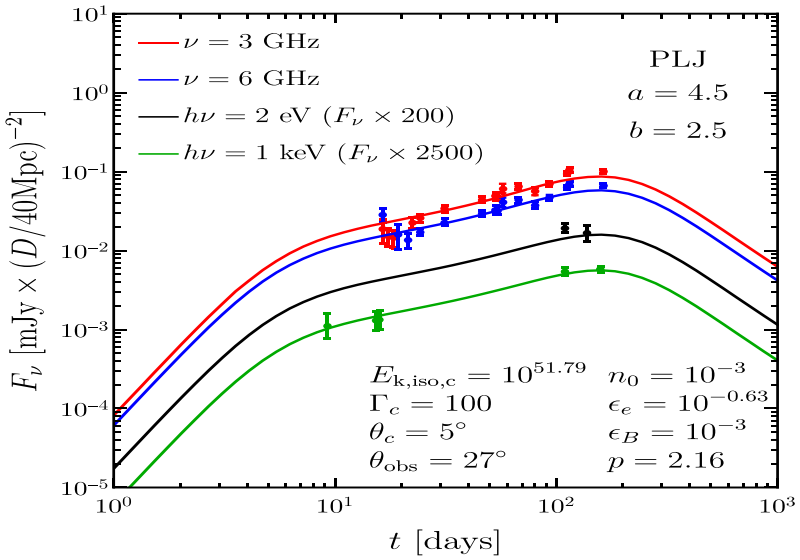


Power Law Jet

Spherical + Energy Injection

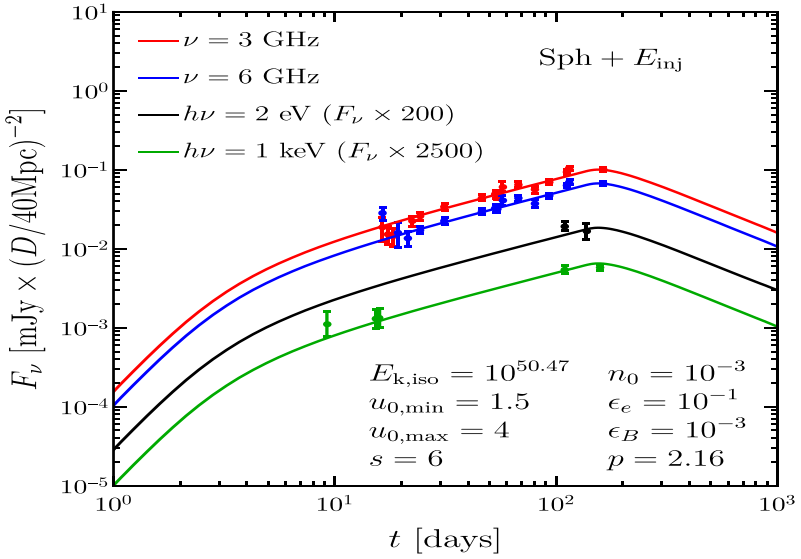


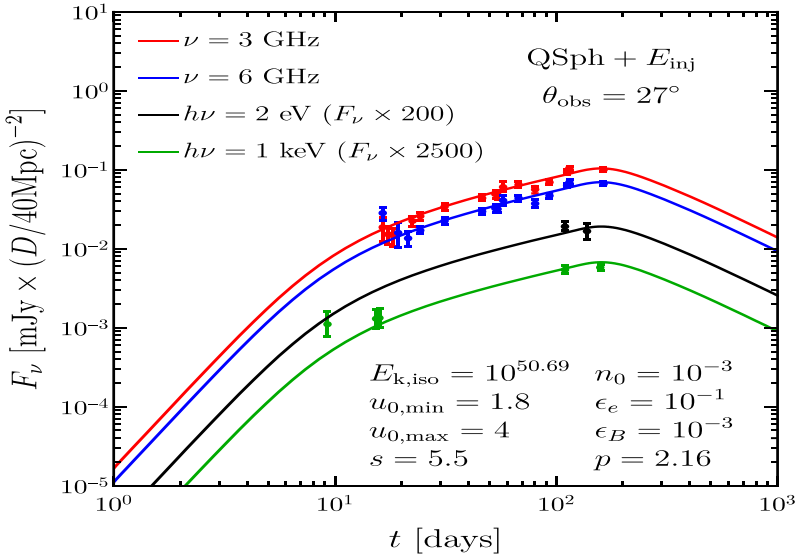


Quasi Spherical + Energy Injection

# Outflow Structure: Breaking the Degeneracy (Gill & JG 18)

- New data that came out established a peak at $t_{\rm peak} \sim 150$ days

Gaussian Jet

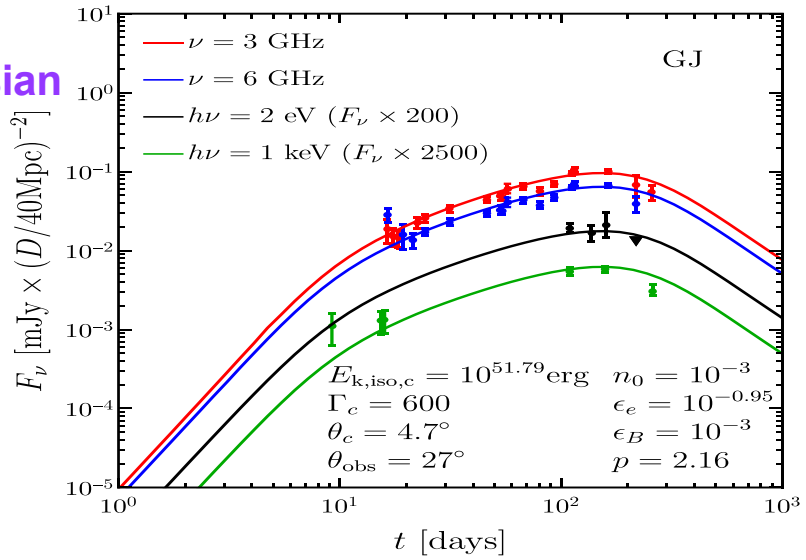


Power Law Jet

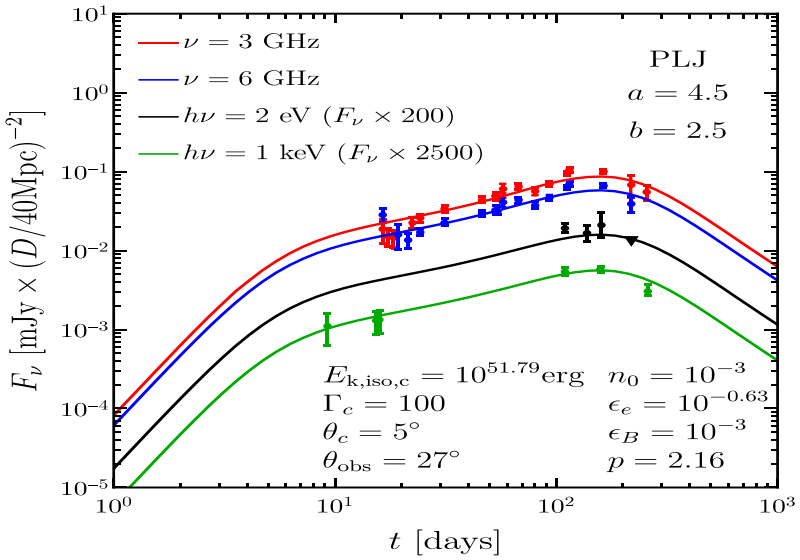


Spherical + Energy Injection

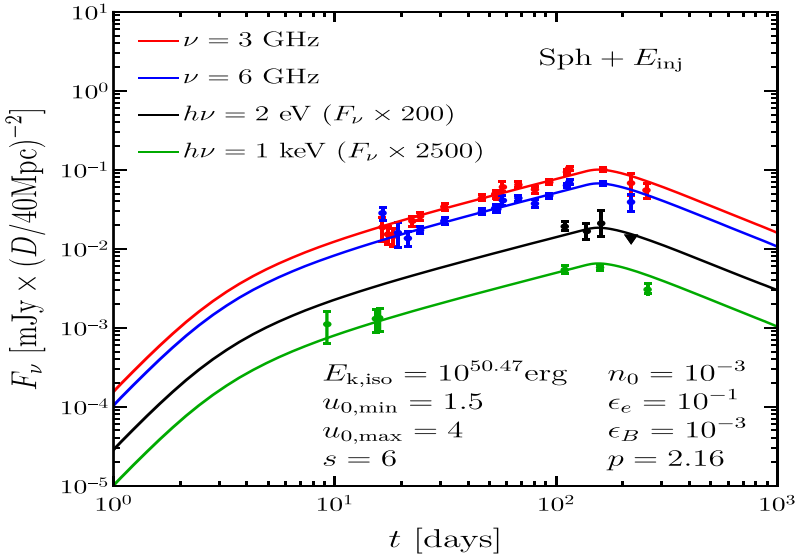


Quasi Spherical + Energy Injection

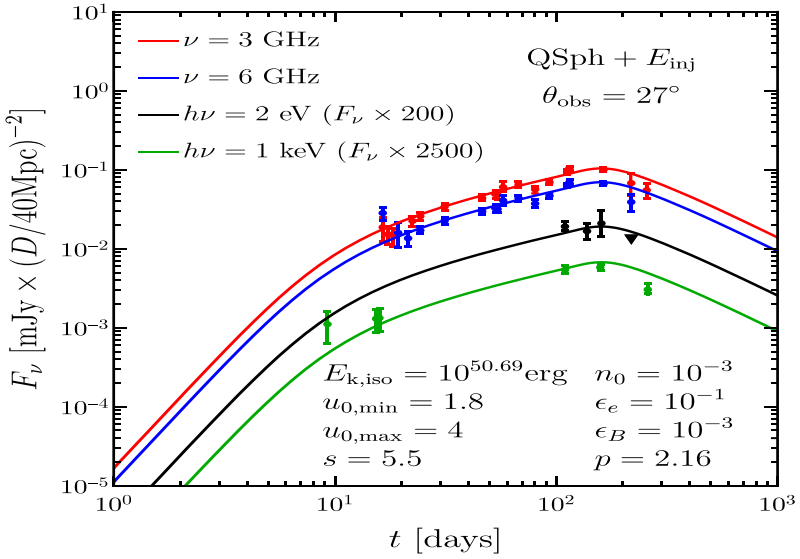

# Outflow Structure: Breaking the Degeneracy (Gill & JG 18)

- The jet models decay faster (closer to post-peak data: $F_\nu \propto t^{-2.2}$)

Gaussian Jet

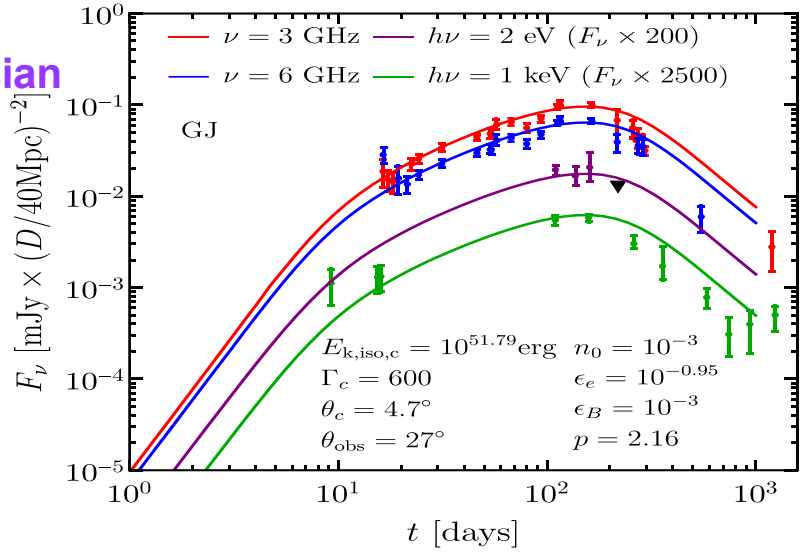


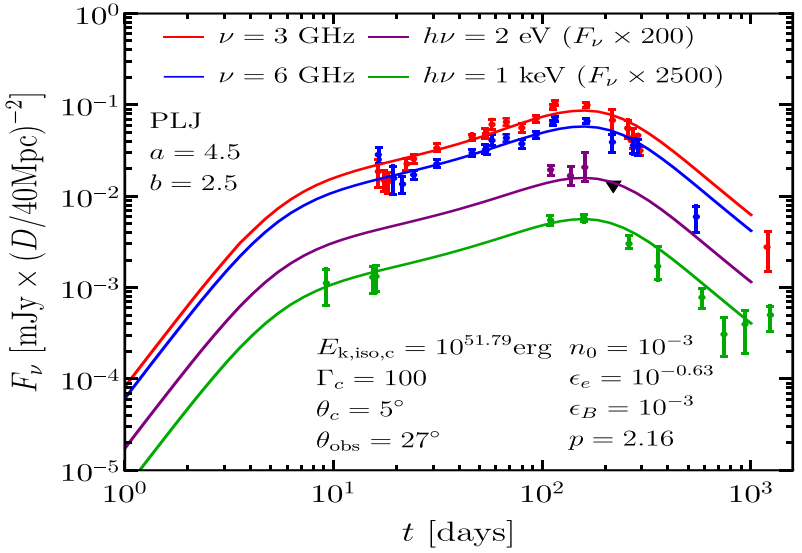


Power Law Jet

Spherical + Energy Injection

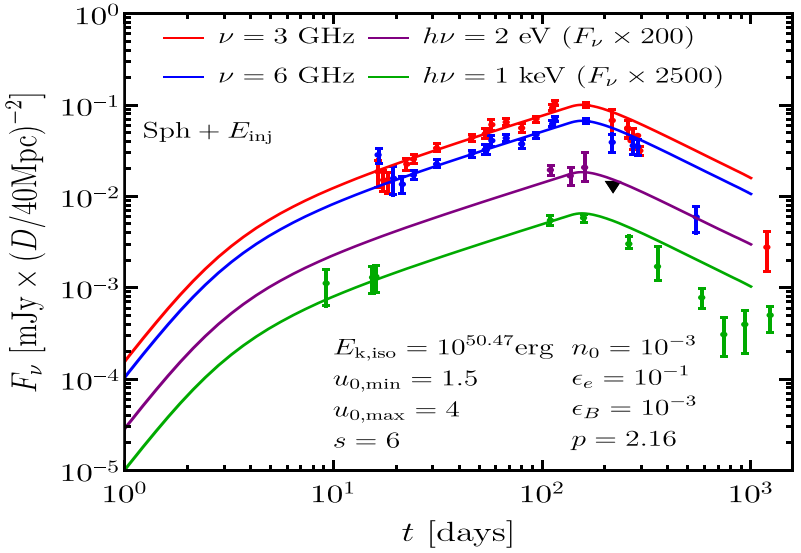


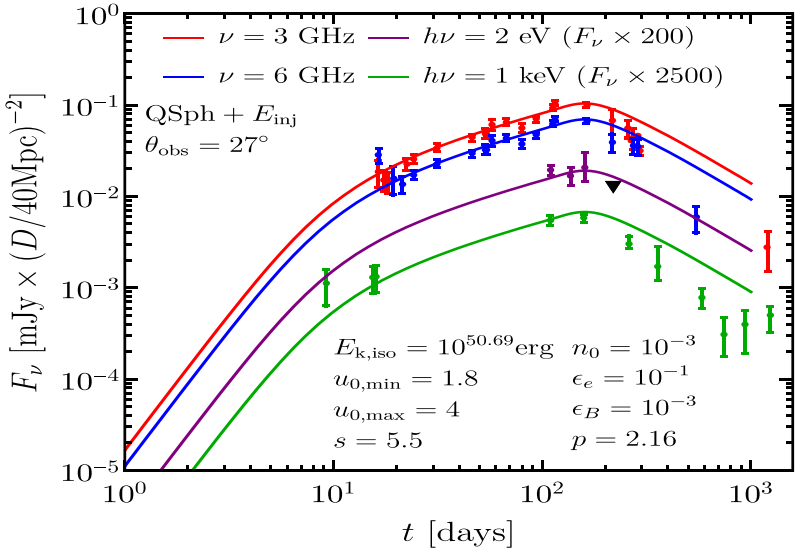


Quasi Spherical + Energy Injection

# Afterglow Images: Flux Centroid, Size, Shape

- The flux centroid motion: a potentially powerful diagnostic
- It may be hard to tell apart models based on the image size alone, but a much higher axis-ratio is expected for jet models

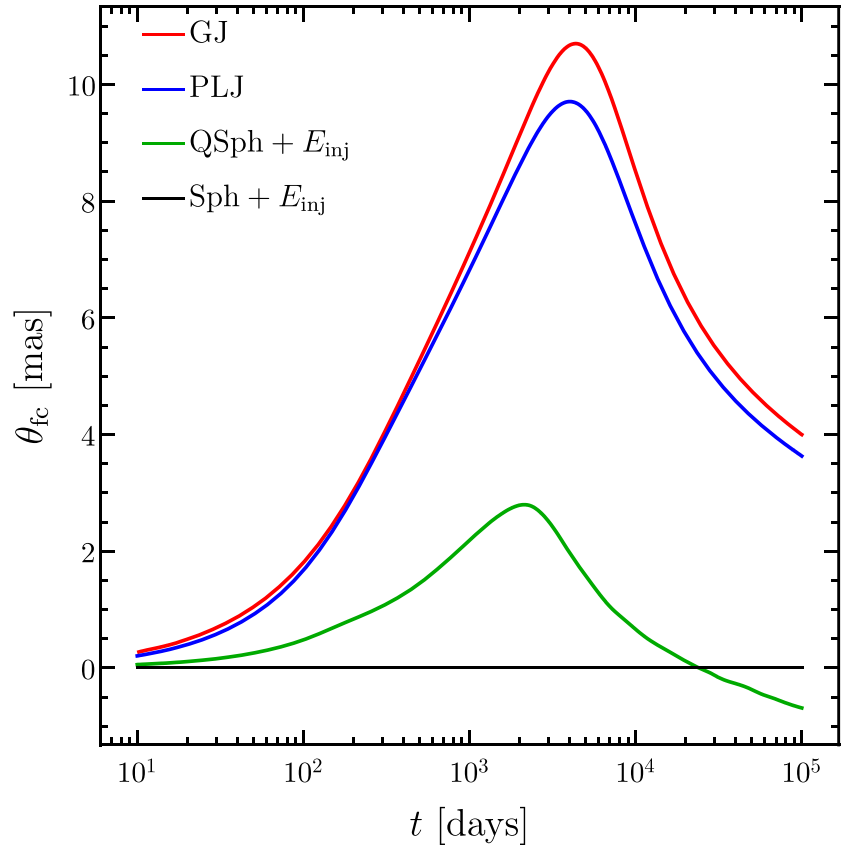


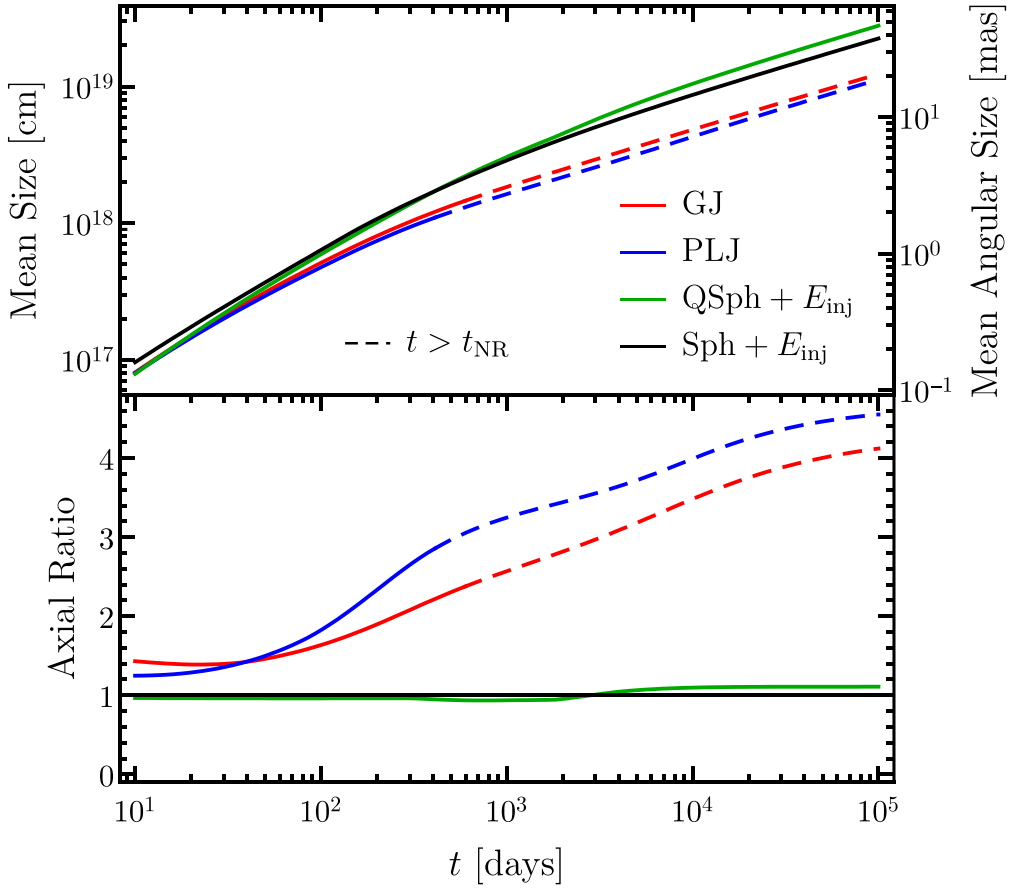

# Afterglow Images: Flux Centroid, Size, Shape

- The flux centroid motion: a potentially powerful diagnostic
- It may be hard to tell apart models based on the image size alone, but a much higher axis-ratio is expected for jet models

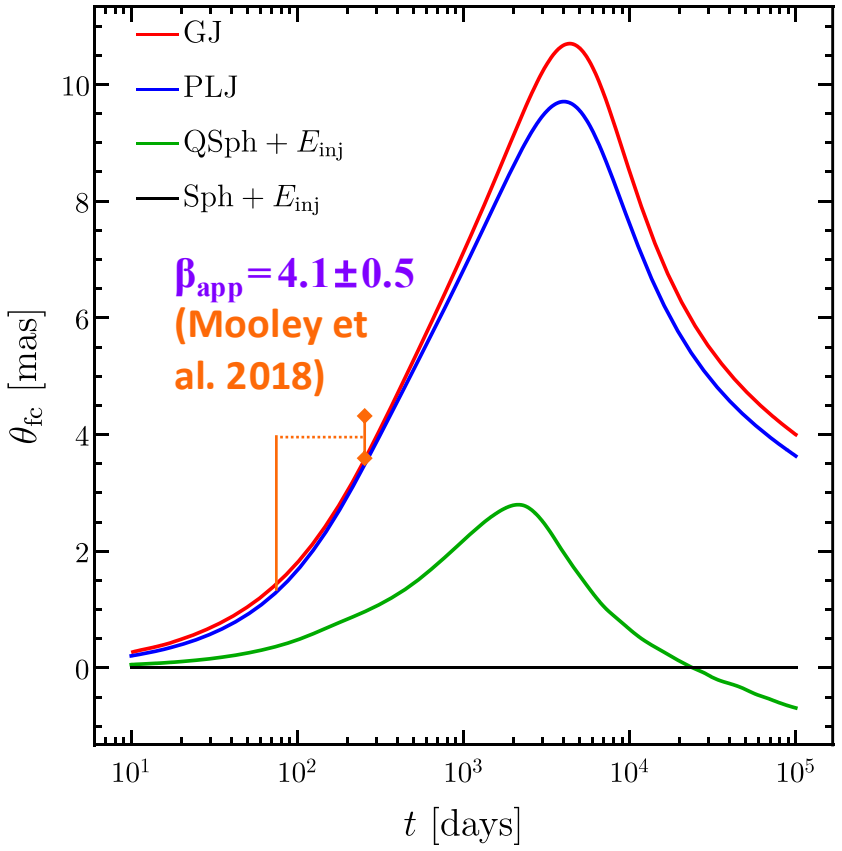


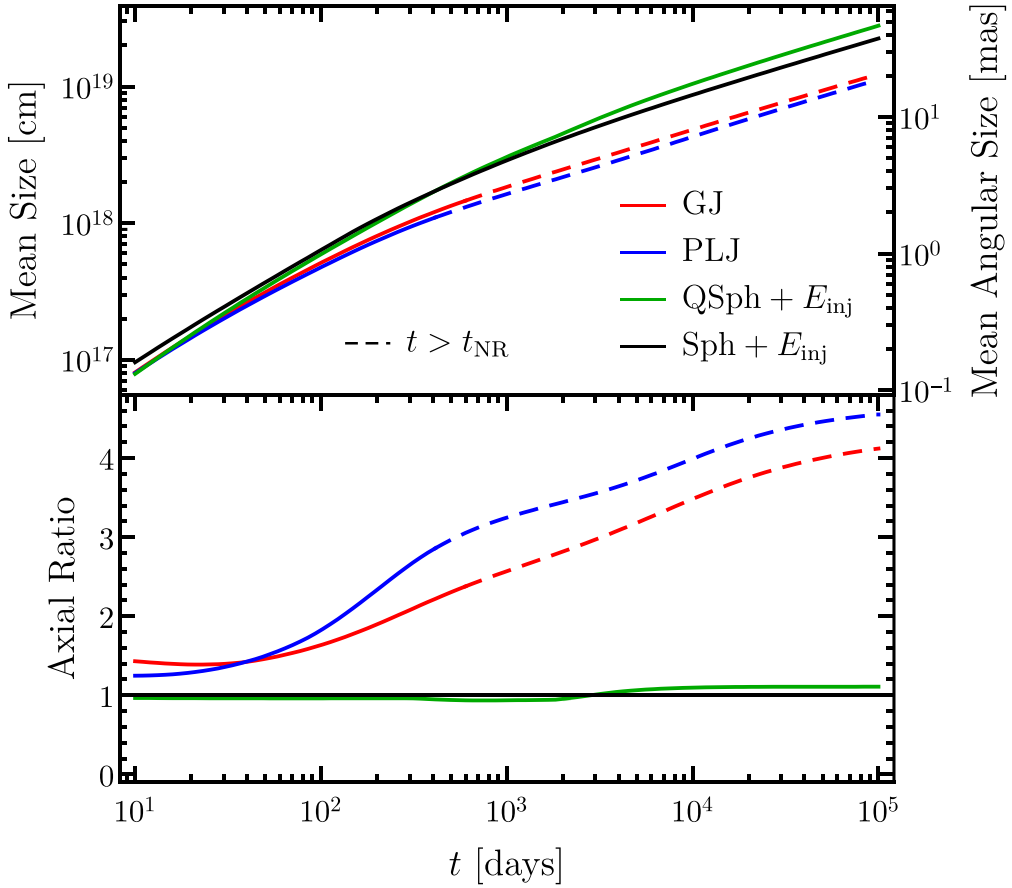

# Afterglow Images: Flux Centroid, Size, Shape

- The flux centroid motion: a potentially powerful diagnostic
- It may be hard to tell apart models based on the image size alone, but a much higher axis-ratio is expected for jet models

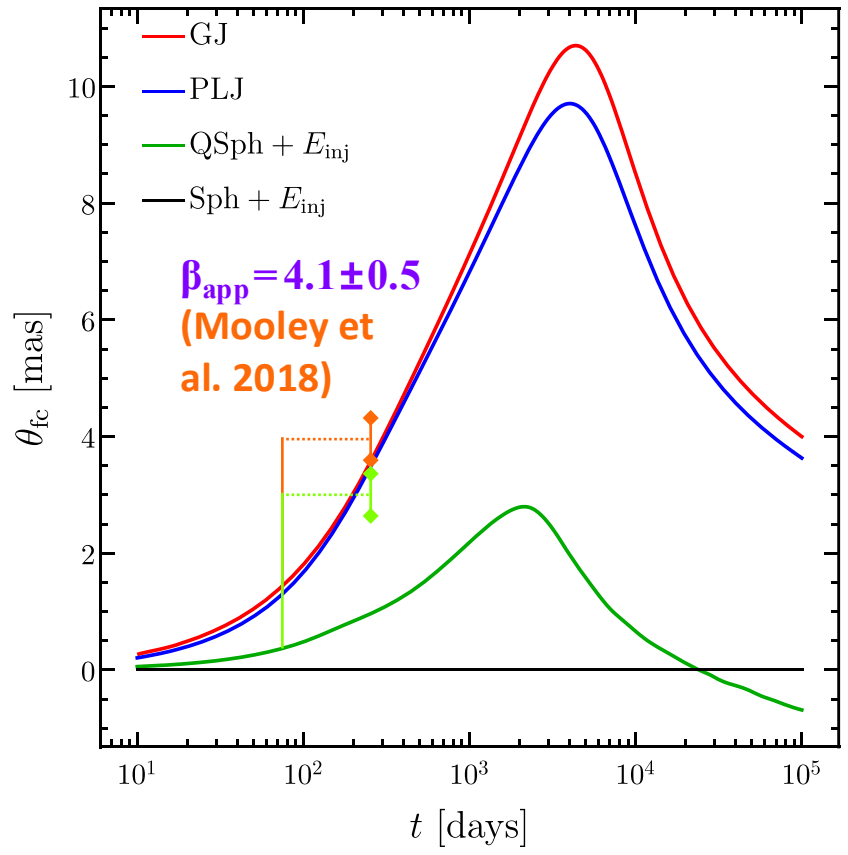


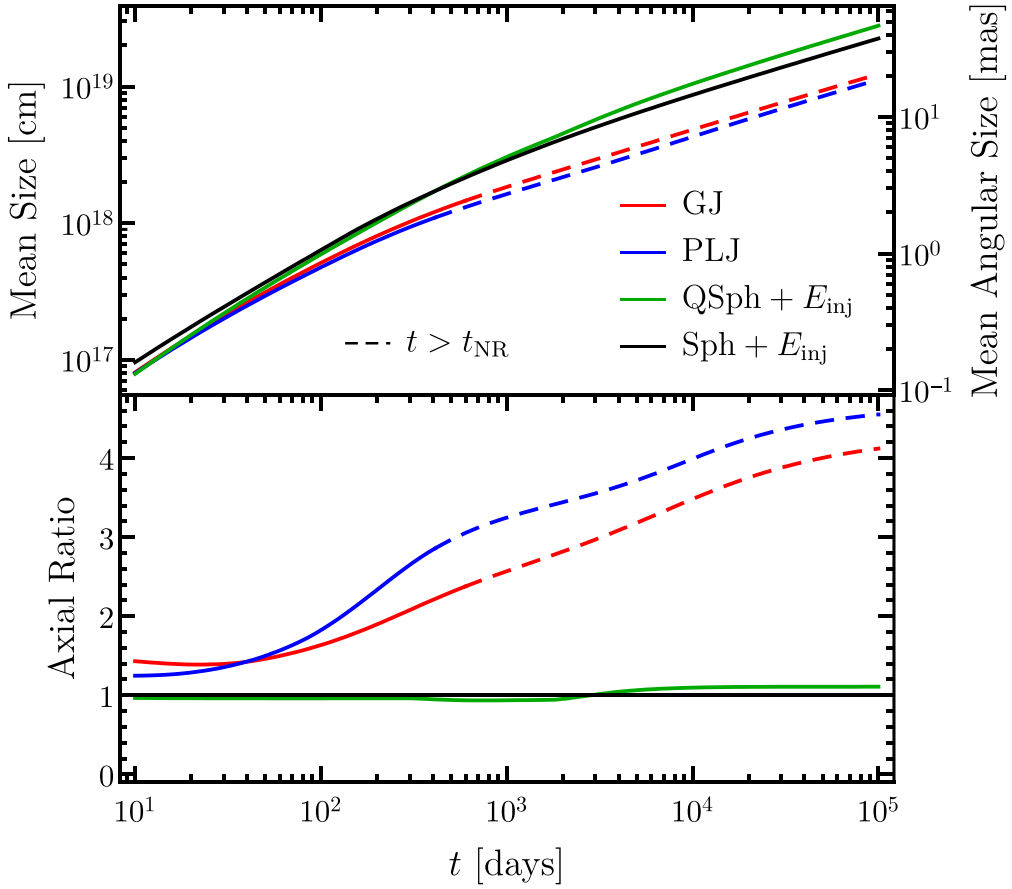

# Afterglow Images: Flux Centroid, Size, Shape

- The flux centroid motion: a potentially powerful diagnostic
- It may be hard to tell apart models based on the image size alone, but a much higher axis-ratio is expected for jet models

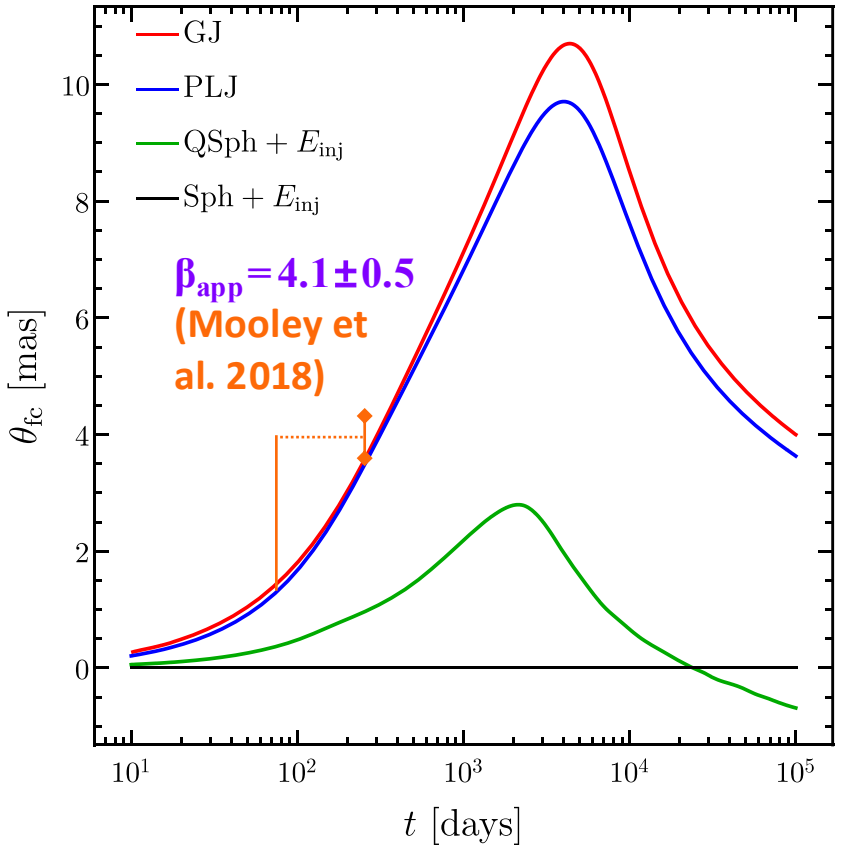


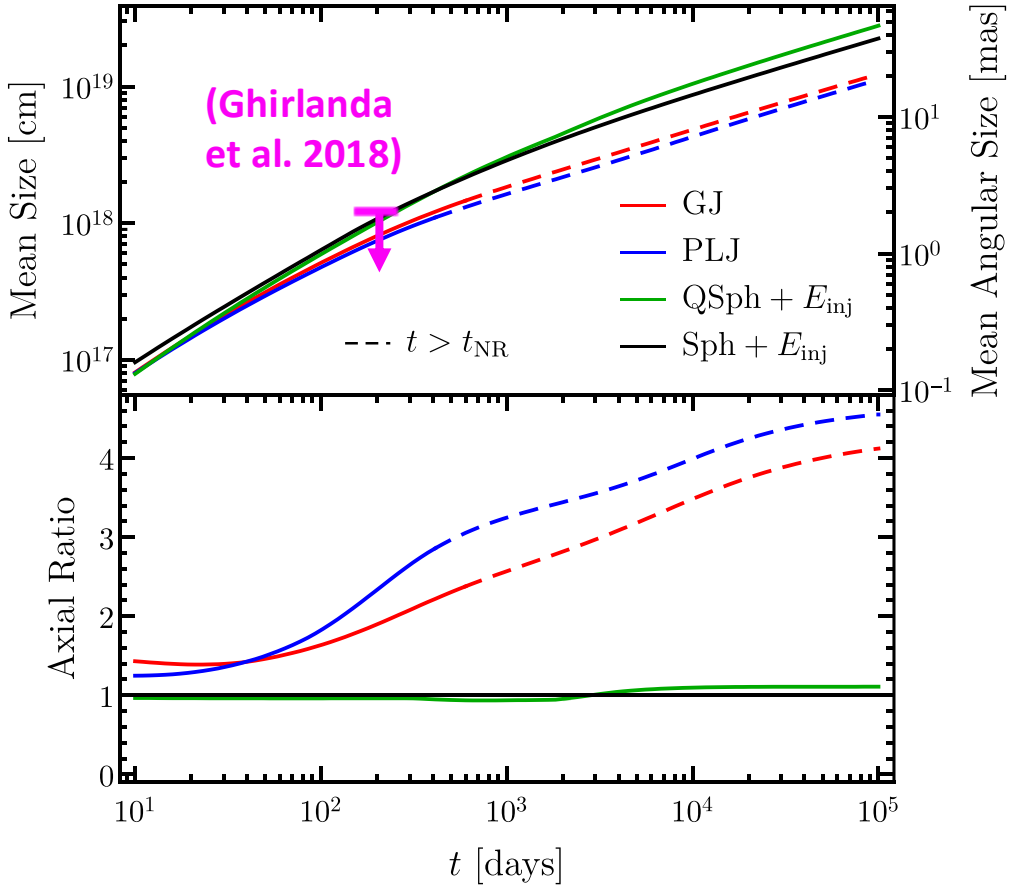

# Afterglow Images: Flux Centroid, Size, Shape

- The flux centroid motion: a potentially powerful diagnostic
- It may be hard to tell apart models based on the image size alone, but a much higher axis-ratio is expected for jet models

**Radio flux centroid motion: semi-analytic**

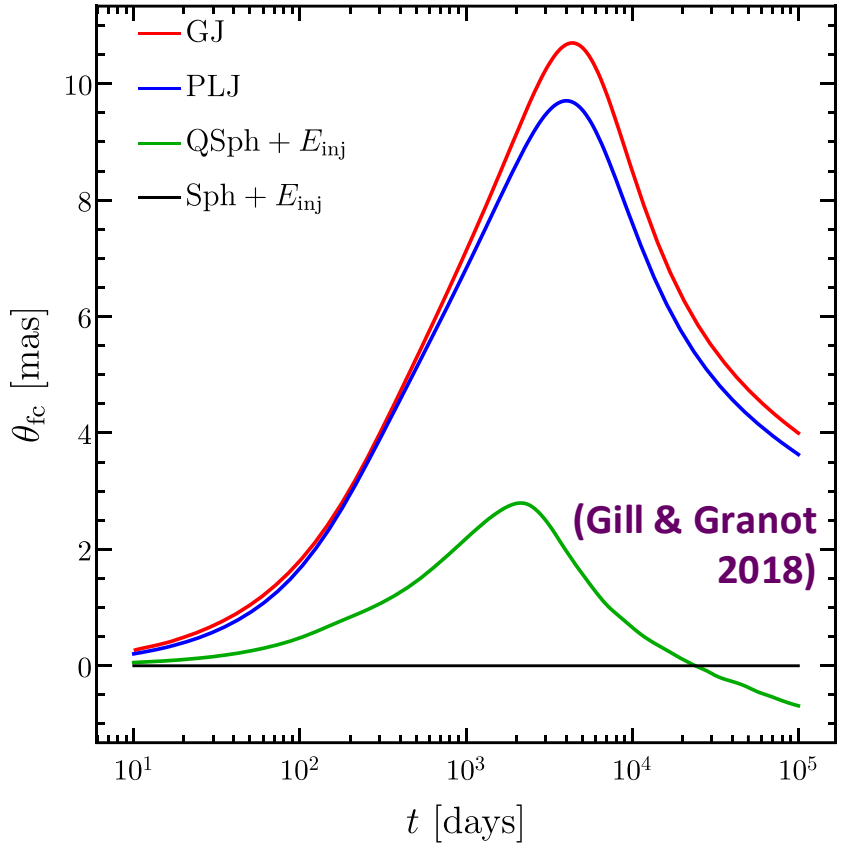


(Gill & JG 2018)

**Agree with radio afterglow images from simulations**

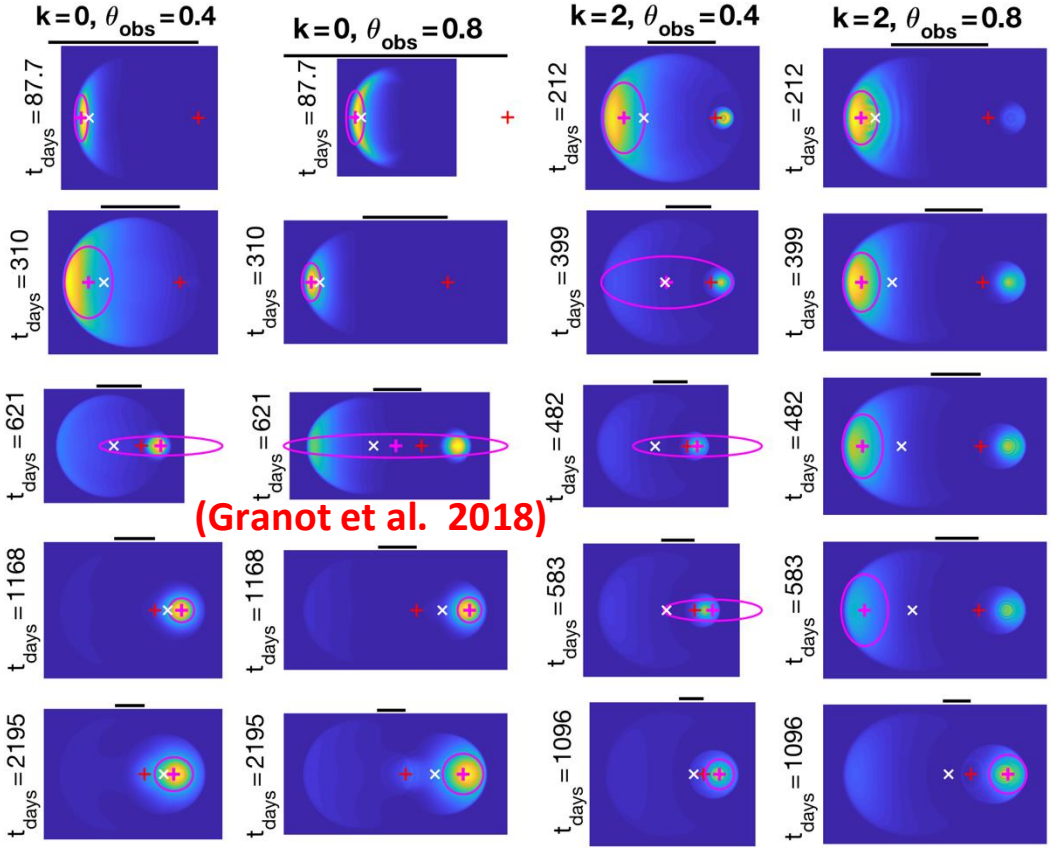


(Granot et al. 2018)

(JG, De Colle & Ramirez-Ruiz 2018)

# GRB Polarization probes the B-field & Jet structures:

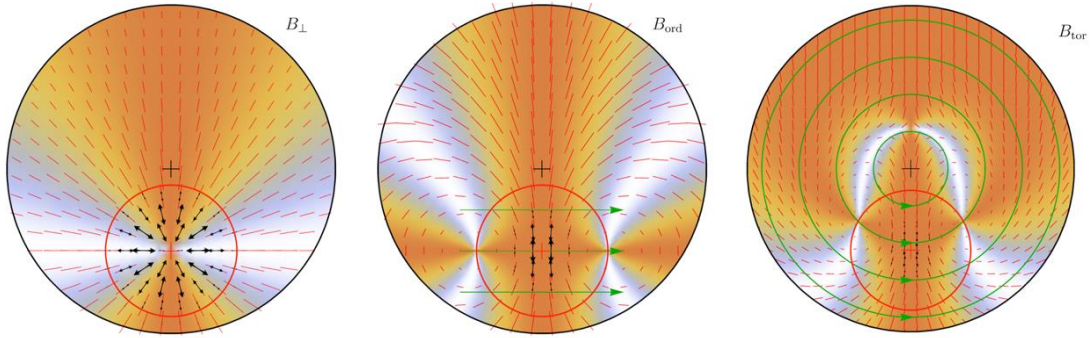


- **Prompt GRB**: hard X-ray – soft $\gamma$-ray
  ⇒ hard to measure ⇒ no clear detections
  (stay tuned: POLAR-2, LEAP, COSI, eXTP)

- **Reverse Shock**: also probes original ejecta, but in optical to radio ⇒ detections
  - ❖ Probes B-field structure & turbulence in the ejecta near the deceleration epoch
  - ❖ Radio UL $\Pi_{8.5\rm GHz}(1\,\rm day) < 7\%$ ⇒ rules out ordered B-field (coherent over $\theta_B \gtrsim 1/\Gamma$) or toroidal B-field + $dE/d\Omega \propto \theta^{-2}$ structured jet; allows $\theta_B \lesssim 10^{-2}$ patches (JG & Taylor 2005)
  - ❖ RINGO2 GRB120308A: $\Pi_{\rm opt}(240-323\,\rm s) = 28 \pm 4\%$ ⇒ ordered B-field (Mundell et al. 2013)
  - ❖ ALMA GRB190114C: $\Pi_{97.5\rm GHz}(2.2 \rightarrow 5.2\ \rm hr) = 0.9 \rightarrow 0.6\%$ with $\Delta\theta_{\rm p}(2.2 \rightarrow 5.2\ \rm hr) = 54°$ (first GRB radio polarization) ⇒ favors patches with $\theta_B \sim 10^{-3}$ (Laskar et al. 2019)

- **Afterglow**: optical & radio – probes jet angular structure & B-field structure in collisionless relativistic shocks

# GRB 170817A: polarization UL ⇒ post-shock B-field

- Jet angular structure & $\theta_{\rm obs}$ well constrained ⇒ breaks degeneracies
- Assuming a shock-produce B-field with $b \equiv 2\langle B_\parallel^2\rangle/\langle B_\perp^2\rangle$ (JG & königl 03; Gill & JG 18)

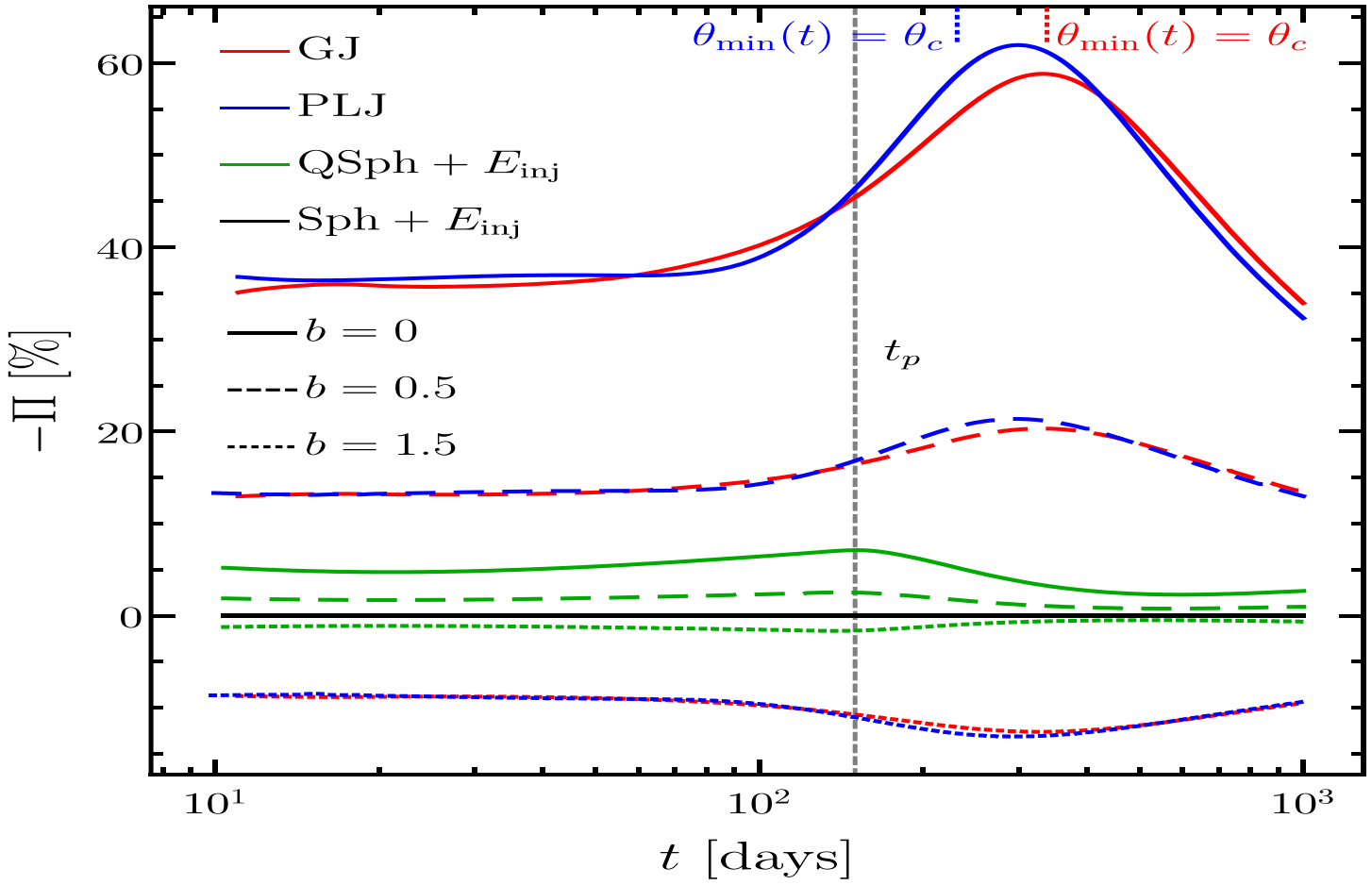

# GRB 170817A: polarization UL ⇒ post-shock B-field

- Jet angular structure & $\theta_{\rm obs}$ well constrained ⇒ breaks degeneracies
- Assuming a shock-produce B-field with $b \equiv 2\langle B_\parallel^2\rangle/\langle B_\perp^2\rangle$ (JG & königl 03; Gill & JG 18)

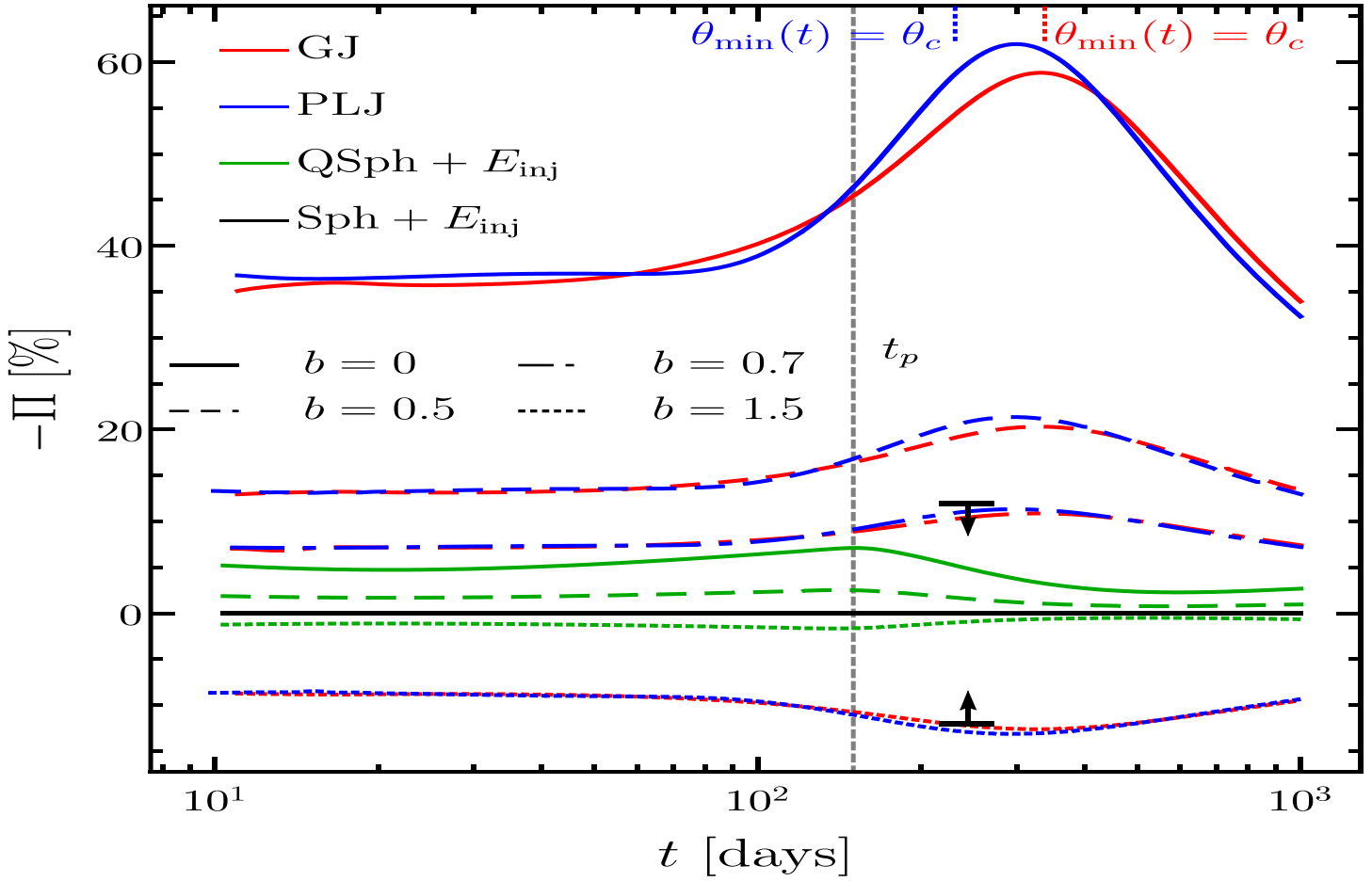


**Later: upper limit**
**$P_{\rm lin}$ < 12% @**
**ν = 2.8 GHz,**
**t = 244 days**
**(Corsi + 2018)**

# GRB 170817A: polarization UL ⇒ post-shock B-field

- Jet angular structure & $\theta_{\rm obs}$ well constrained ⇒ breaks degeneracies
- Assuming a shock-produce B-field with $b \equiv 2\langle B_\parallel^2\rangle/\langle B_\perp^2\rangle$ (JG & königl 03; Gill & JG 18)

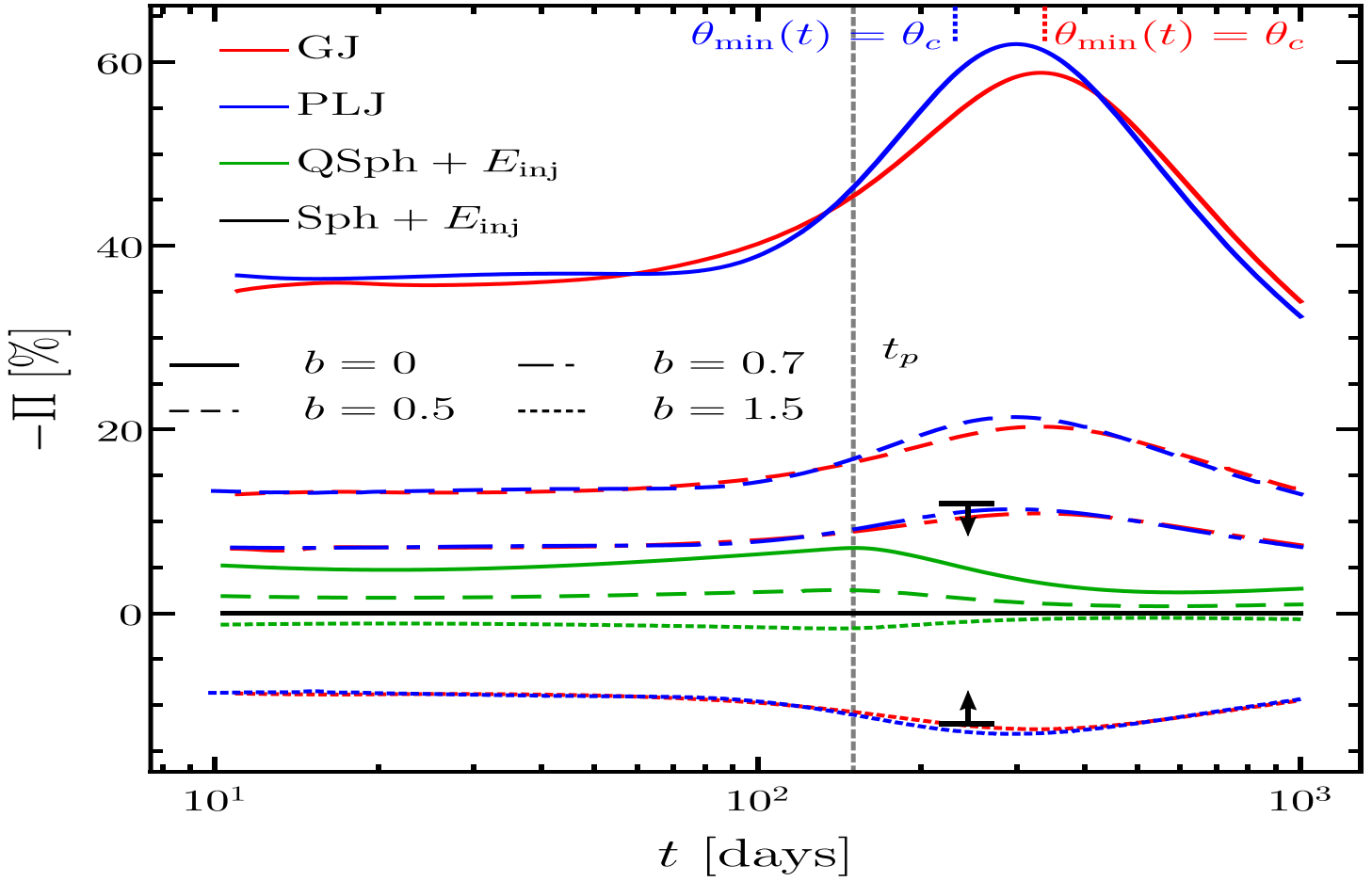


**0.7 ≲ b ≲ 1.5 for jet models**

**Later: upper limit $P_{\rm lin} < 12\%$ @ ν = 2.8 GHz, t = 244 days (Corsi + 2018)**

# GRB 170817A: polarization UL ⇒ post-shock B-field

More realistic assumptions ⇒ B-field in collisionless shocks: (Gill & JG 2020)

- 2D emitting shell ➜ 3D emitting volume (local BM76 radial profile)
- B-field evolution by faster radial expansion: $L'_r / L'_{\theta,\phi} \propto \chi^{(7-2k)/(8-2k)}$
- B-field isotropic in 3D with $B'_r \rightarrow \xi B'_r$ (Sari 1999); $\xi = \xi_f \chi^{(7-2k)/(8-2k)}$

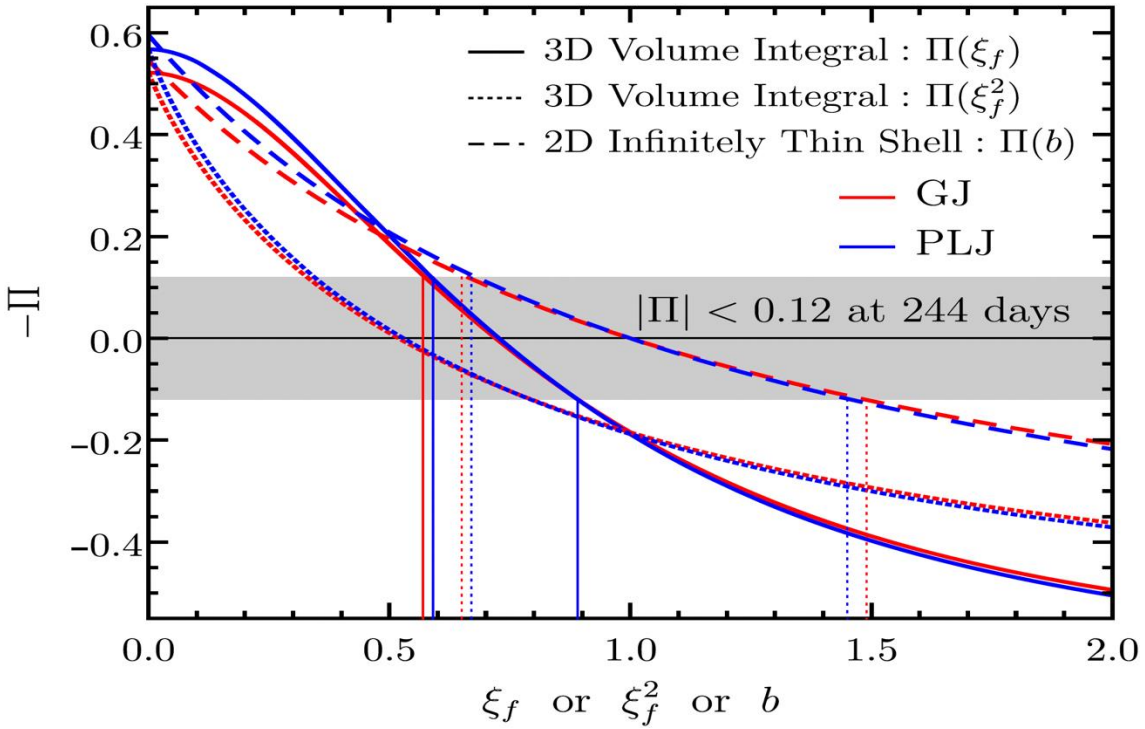


**$0.57 \lesssim \xi_f \lesssim 0.89$**

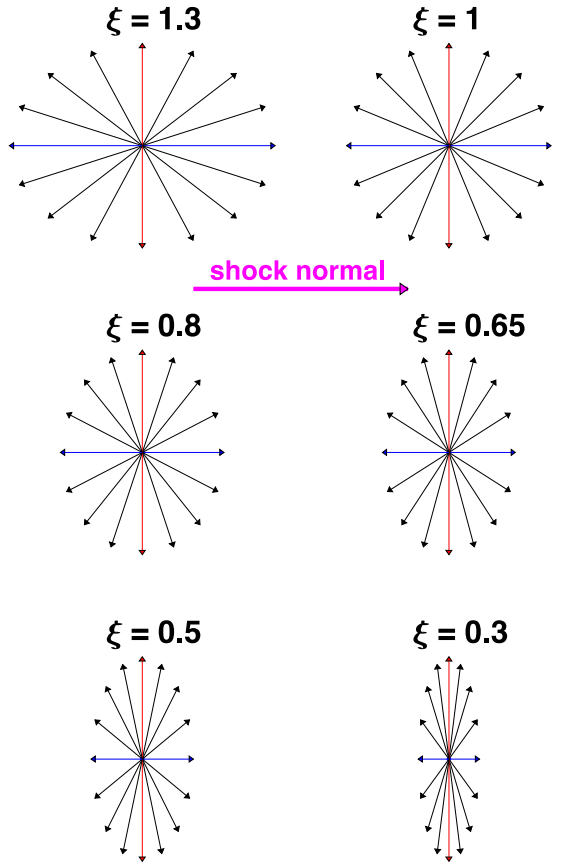

# Reverse + Forward Shock Polarization: (Arimoto et al. 2023)

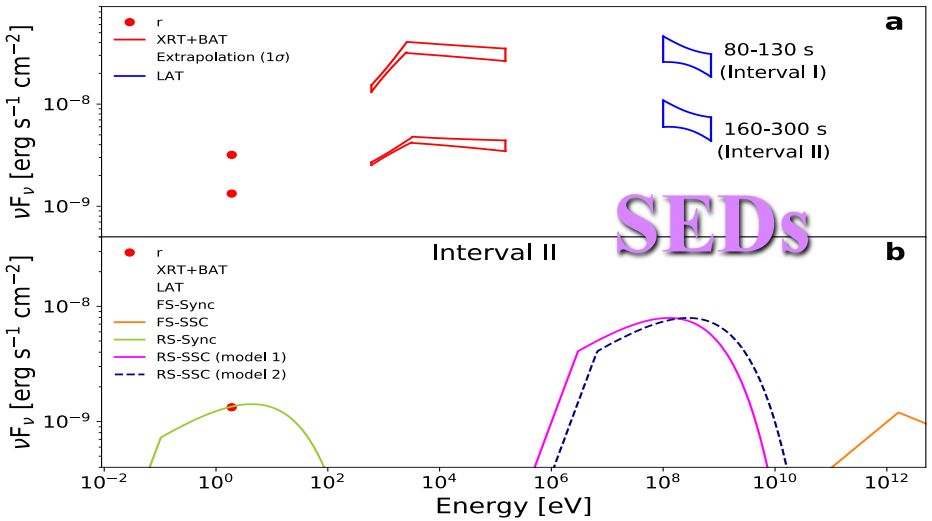


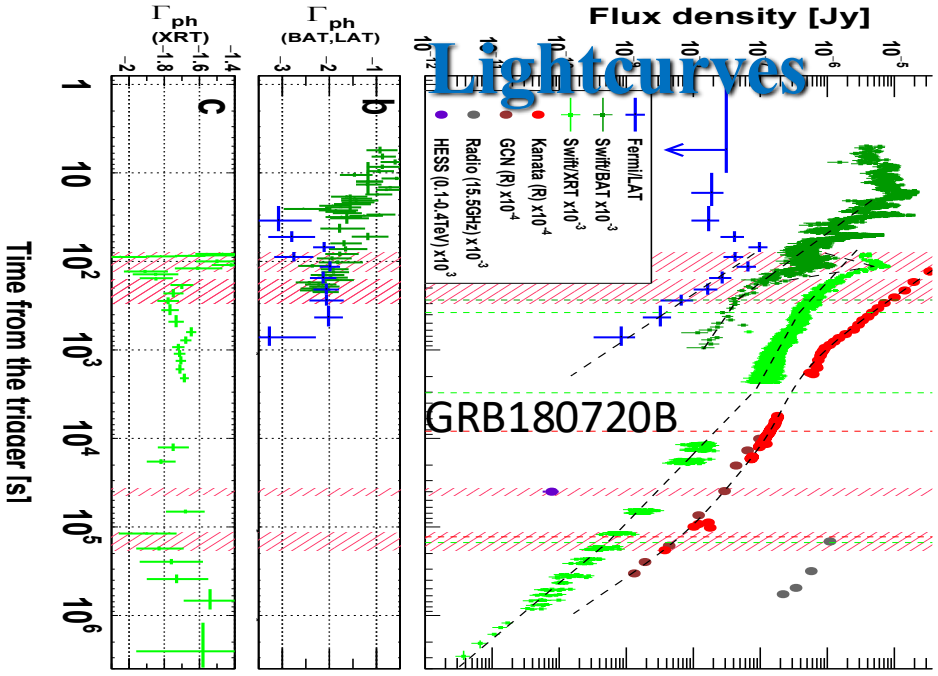


- < 300 s: RS; P: 5 → 1%, θp ≈ 70°
- 0.3-2 ks: P ~ 2-8%, $\theta_p$ varies
- 5-20 ks: FS; P ~ 0.5-2%, $\theta_p$ ≈ 160°
- RS → FS dominance @ ~$10^3$ s

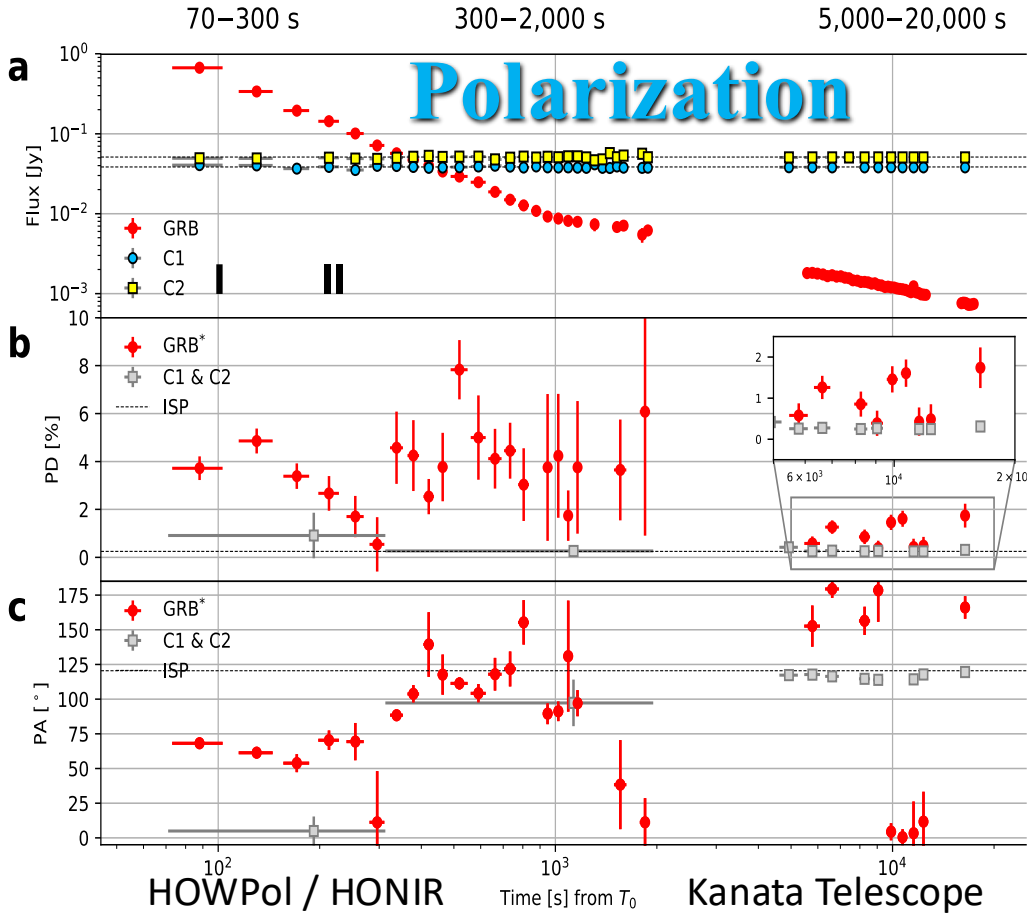

# Reverse + Forward Shock Polarization: (Arimoto et al. 2023)

- < 300 s: ejecta; $B_{tor}$ + turbulence
- 0.3-2 ks: turbulence-induced P
- 5-20 ks: CSM; radial stretching

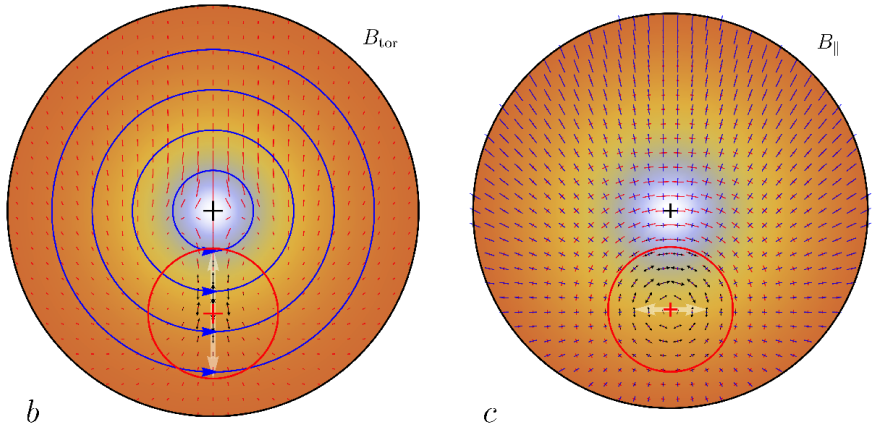


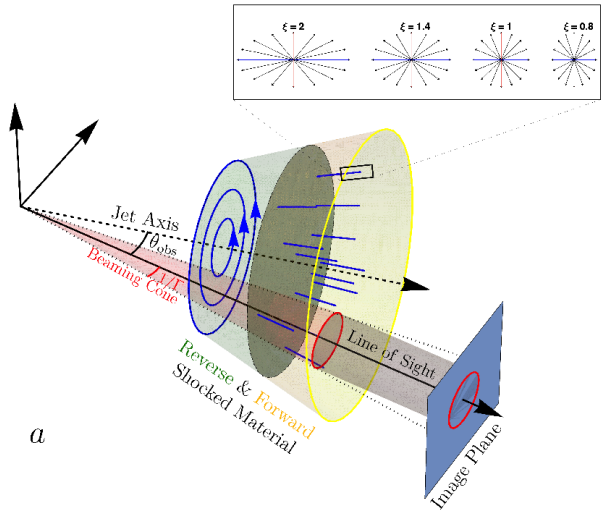


- < 300 s: RS; P: 5 → 1%, θp ≈ 70°
- 0.3-2 ks: P ~ 2-8%, $\theta_p$ varies
- 5-20 ks: FS; P ~ 0.5-2%, $\theta_p$ ≈ 160°
- RS → FS dominance @ ~$10^3$ s

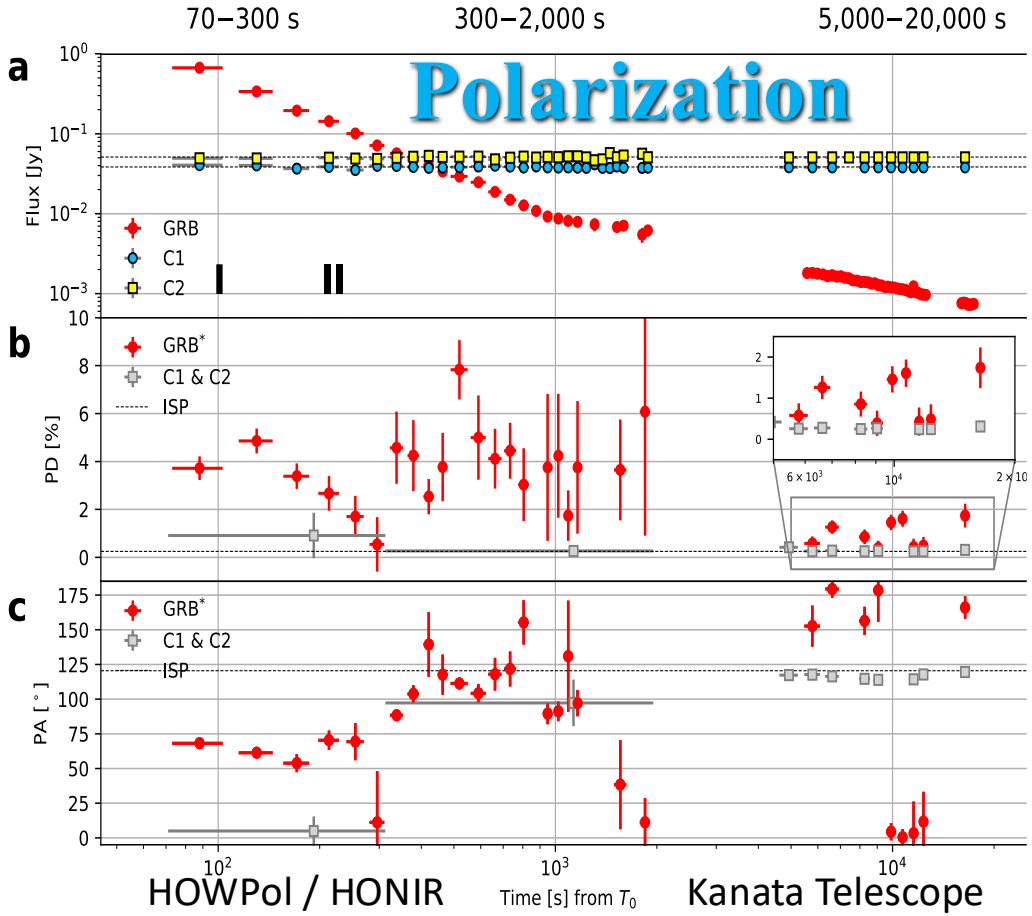

# Afterglow Polarization from Shallow Jets (Birenbaum et al. 2024)

***P*** peaks near the jet break time

$$P_{\max} \approx q a^{1.4}[0.055 \tanh(0.34 - 2.3 \log_{10} \xi) - 0.02]$$

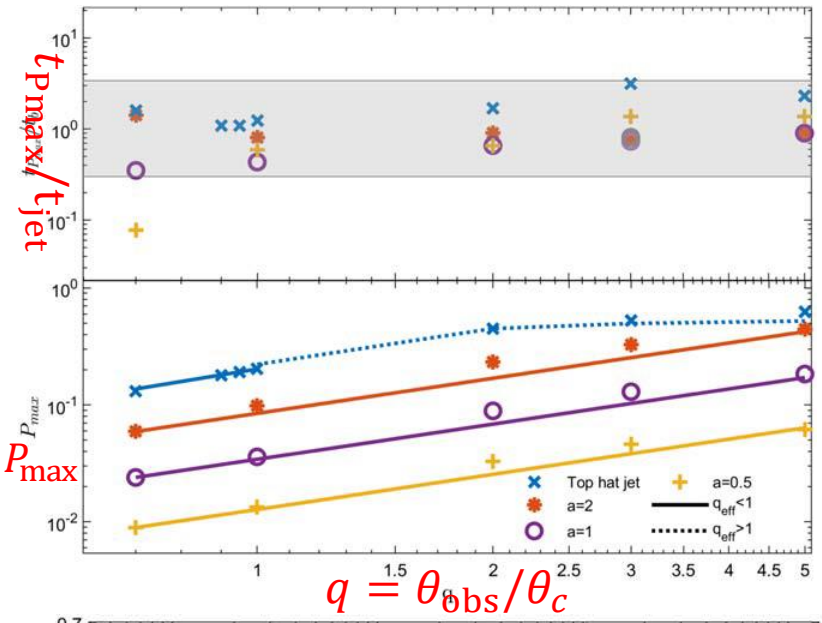


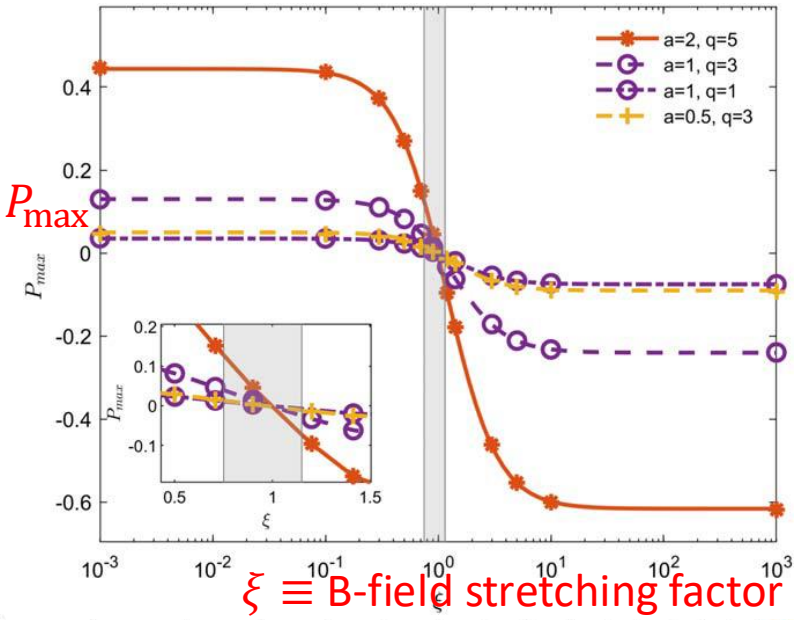


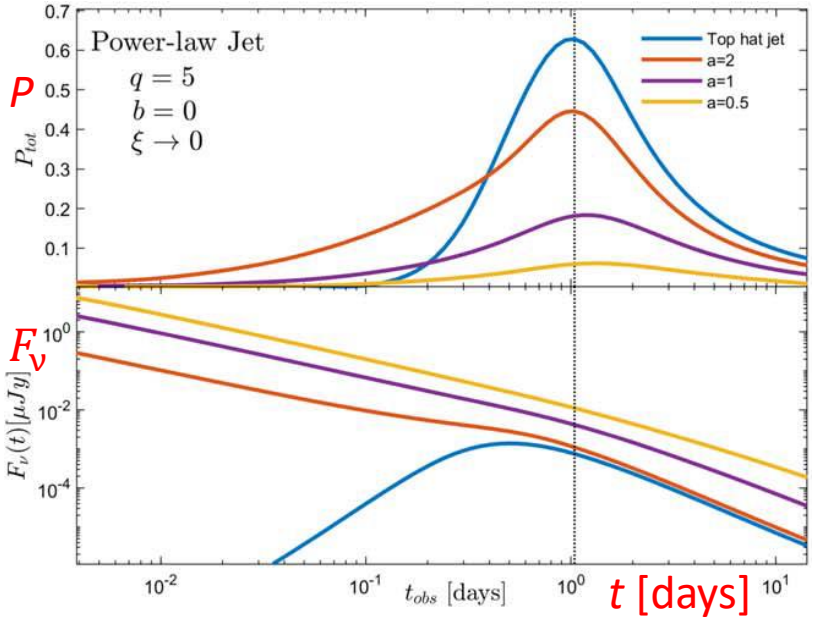


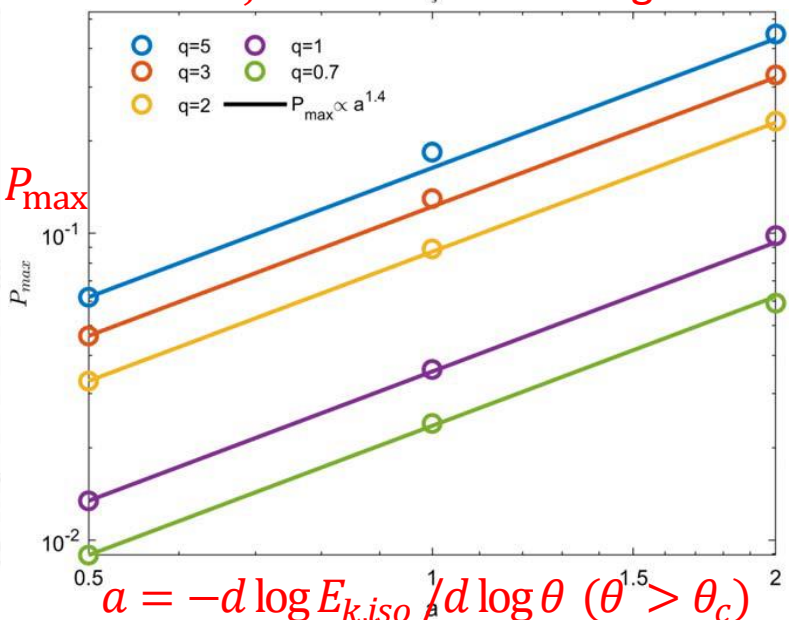


- Particularly energetic GRBs seem to have **shallow Jets**
- Earlier polarimetry of the B.O.A.T could have helped constrain its jet structure & post-shock B-field structure

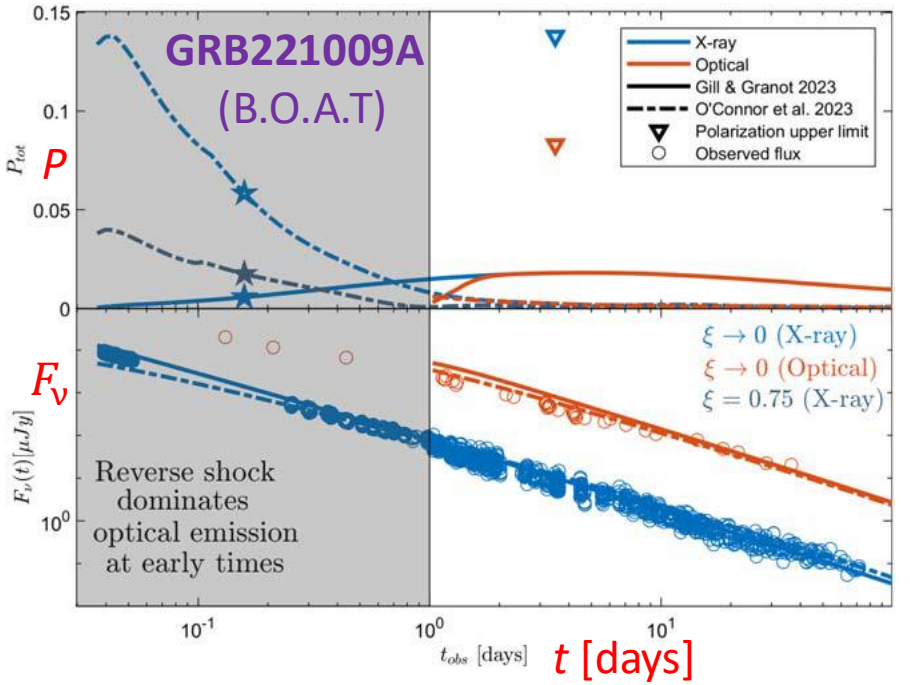

# Afterglow Polarization from Steep Jets ($a \geq 2$; Birenbaum et al. 2026)

***P*** peaks near the jet break time

$P_{\max} \approx \Psi(a,q)\,[A \tanh(-B \log_{10}\xi + C) - D]$

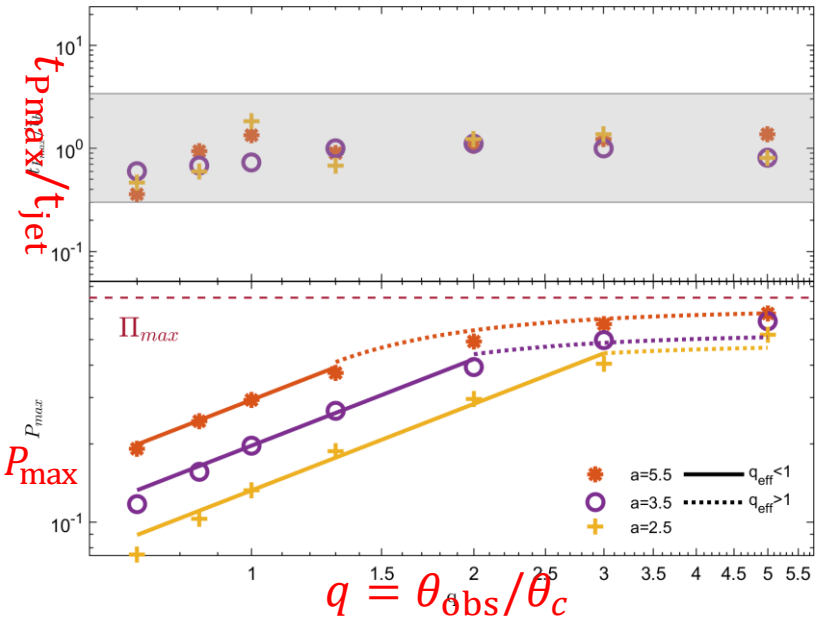


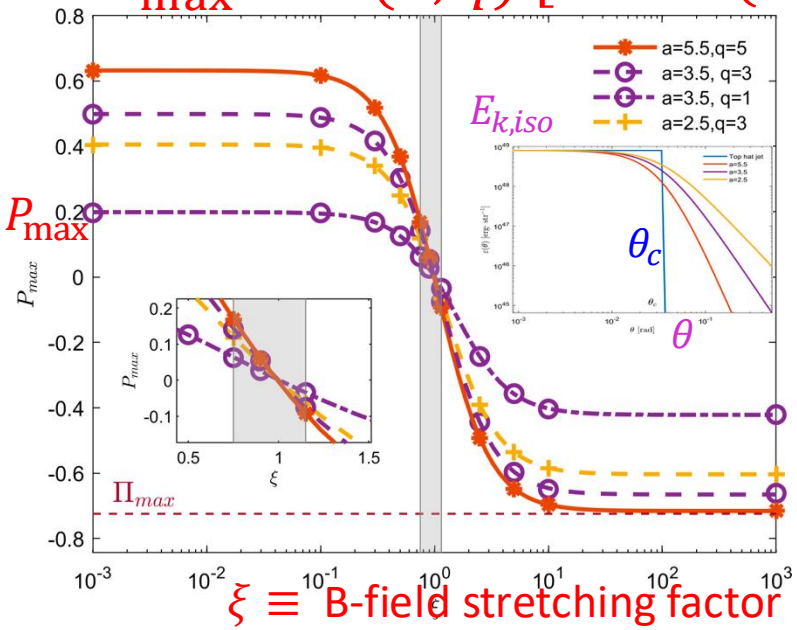


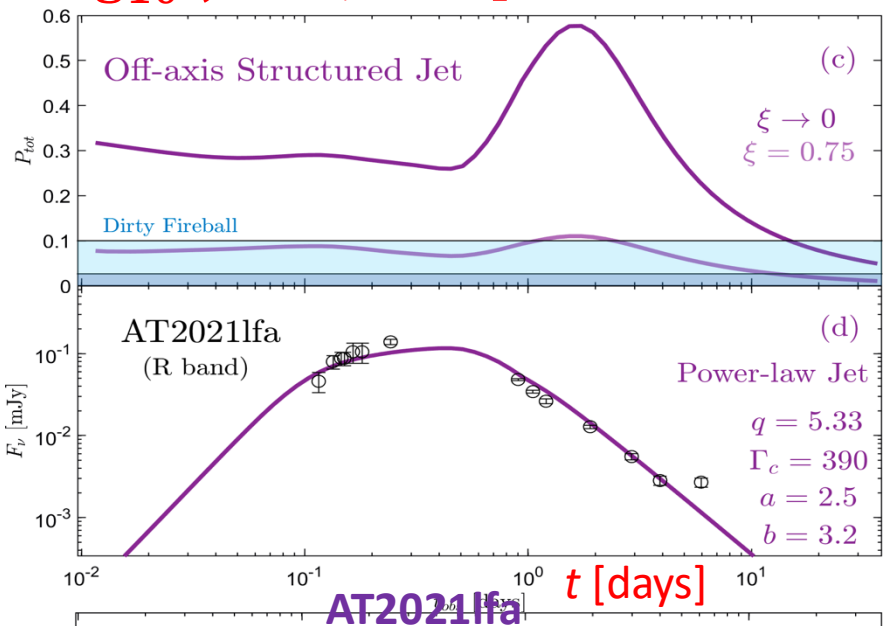


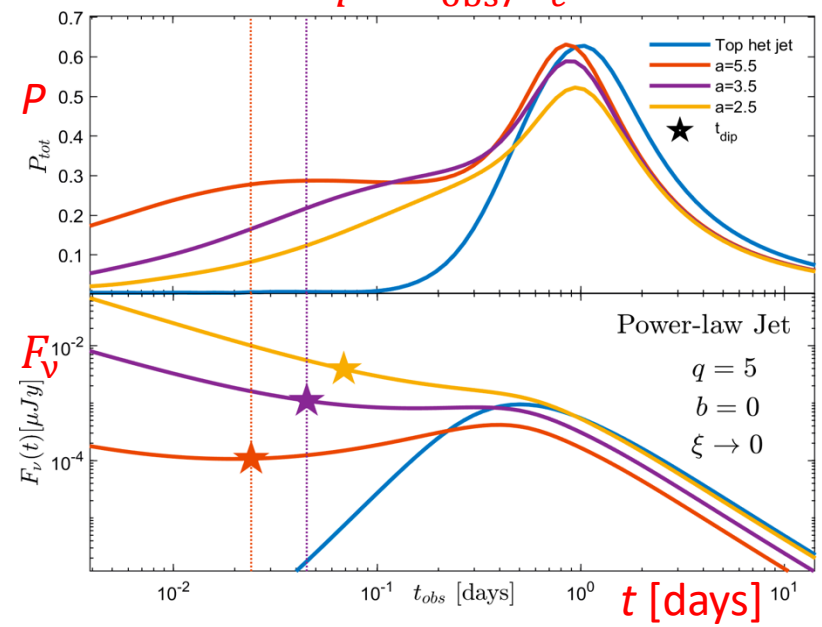


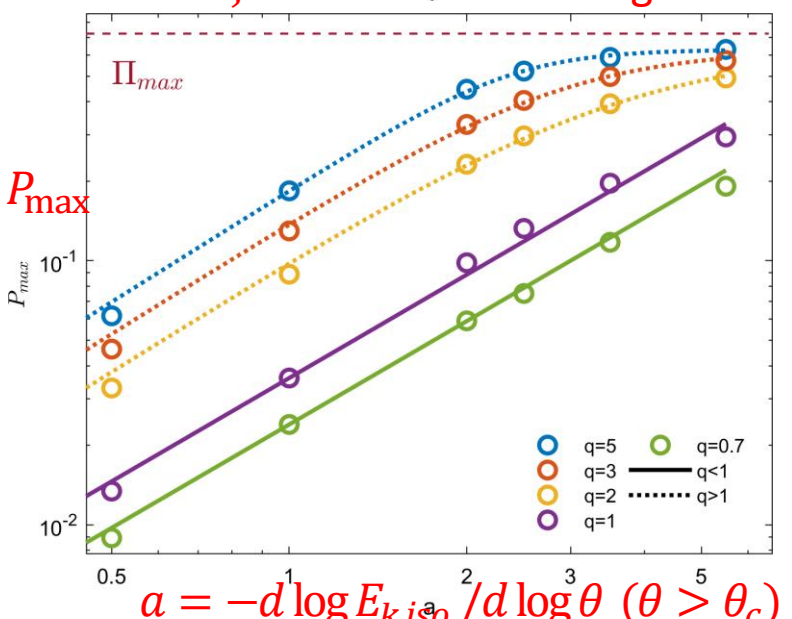


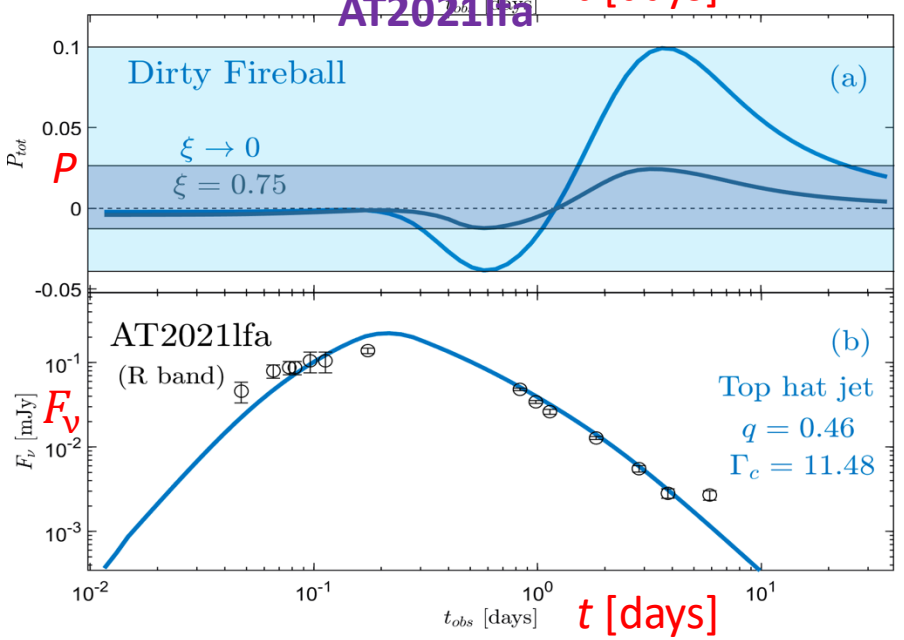

# ULGRB250702B: Prompt Emission

$T_{\rm GRB} \approx 25$ ks (longest ever)

$E_{\gamma,\rm iso} \geq 1.4 \times 10^{54}$ erg;

$L_{\gamma,\rm iso} \approx 5 \times 10^{51}$ erg/s

$E_{p,z} \sim 1.5 - 6$ MeV

$t_{\rm MV} \approx 1$s, $E_{\rm max} \approx 5$ MeV $\Longrightarrow \Gamma > 56$

$E_{\rm cut} \approx 4$ MeV $\Longrightarrow \Gamma \approx 81$

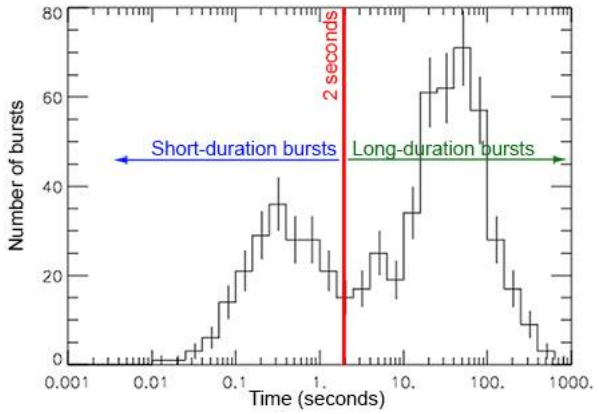


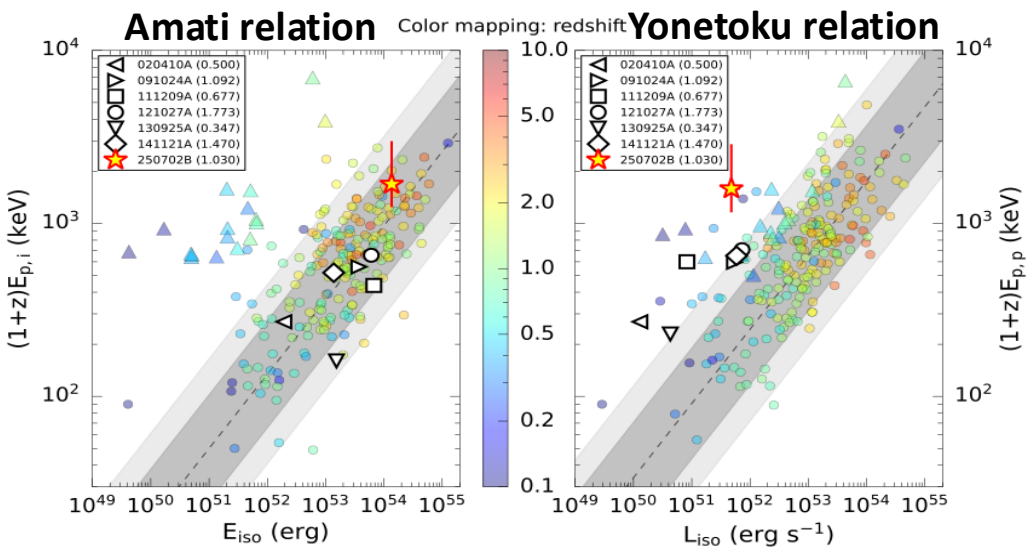


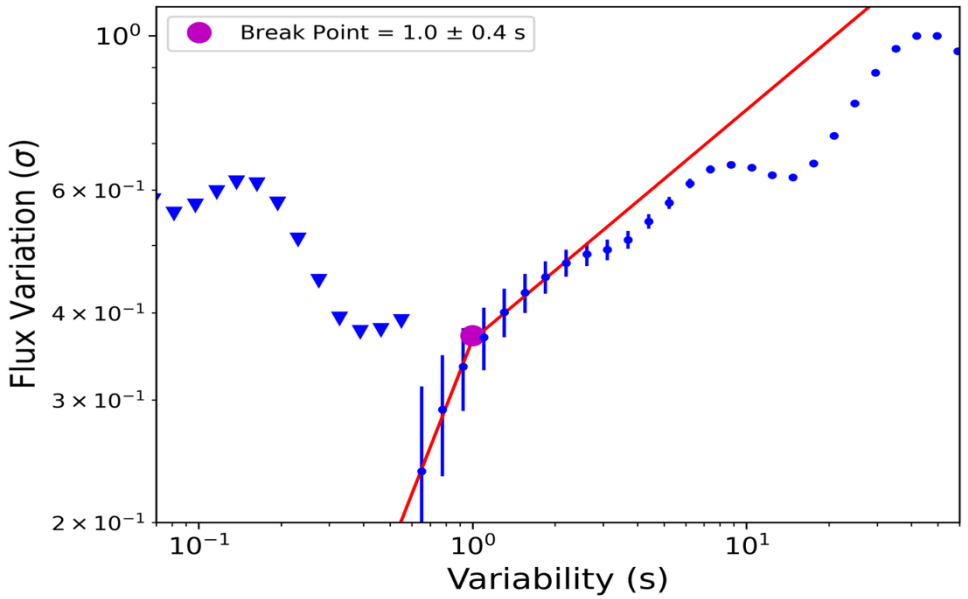


(Neights et al. 2025)

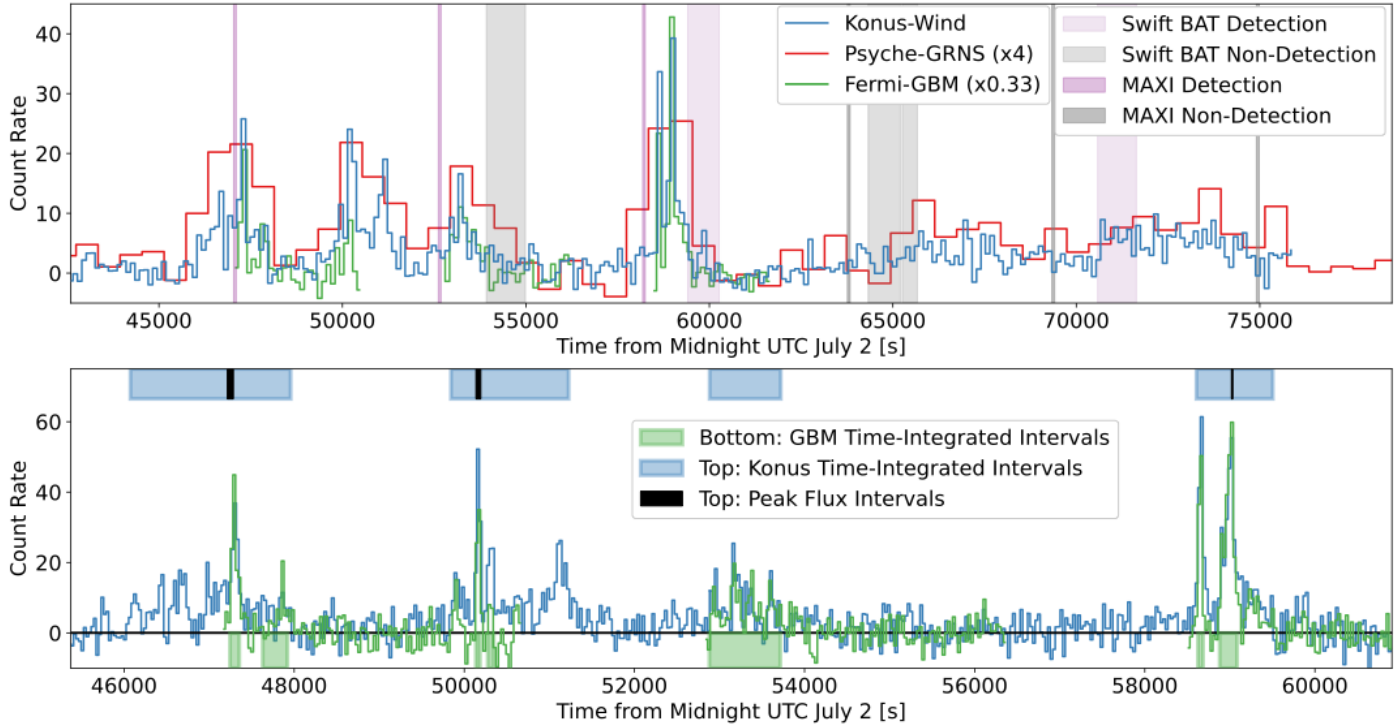

# Ultra-Long GRBs:

$T_{\rm GRB} \approx 25$ ks

$E_{\gamma,\rm iso} \geqq 1.4 \times 10^{54}$ erg

$L_{\gamma,\rm iso} \approx 5 \times 10^{51}$ erg/s

$\bar{L}_{\gamma,\rm iso} \geqq 1.1 \times 10^{50}$ erg/s

$E_{p,\rm z} \sim 1.5 - 6$ MeV

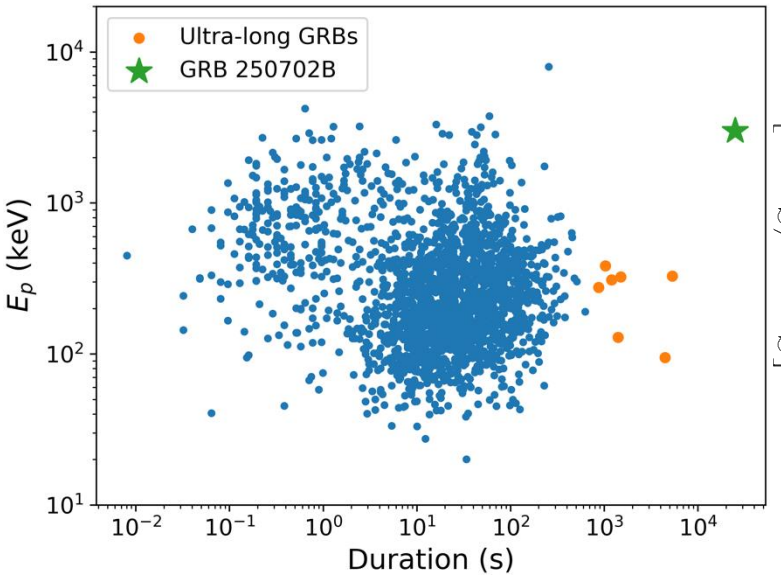


(Neights et al. 2025)

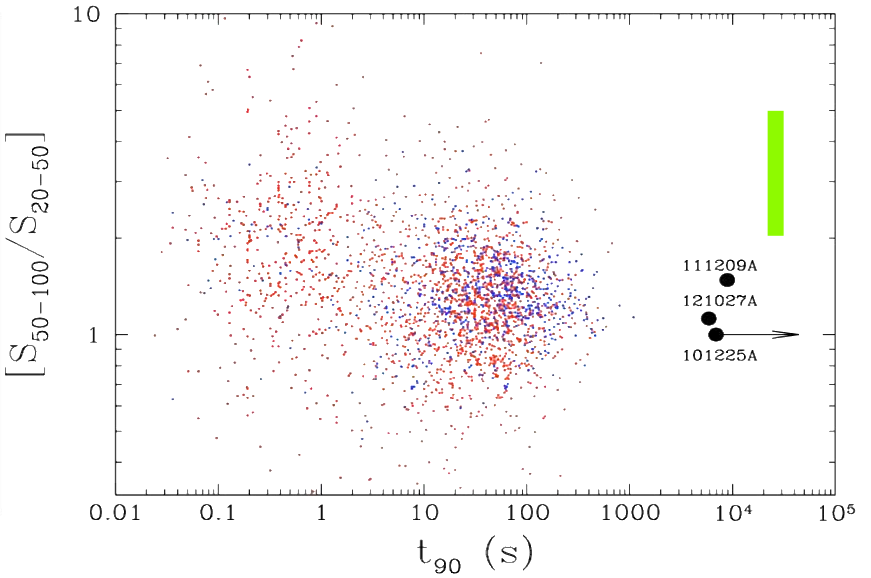


(Levan et al. 2014)

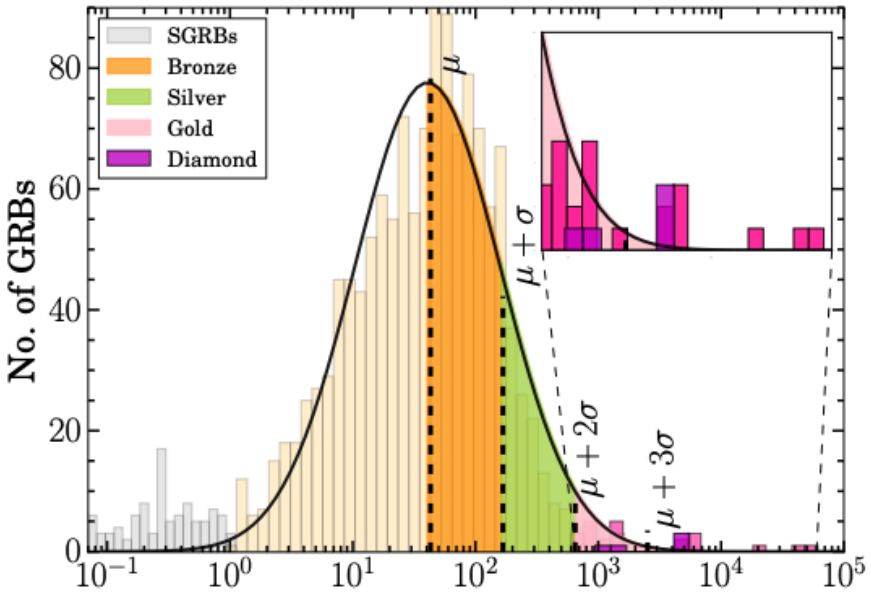


(Ror et al. 2024)

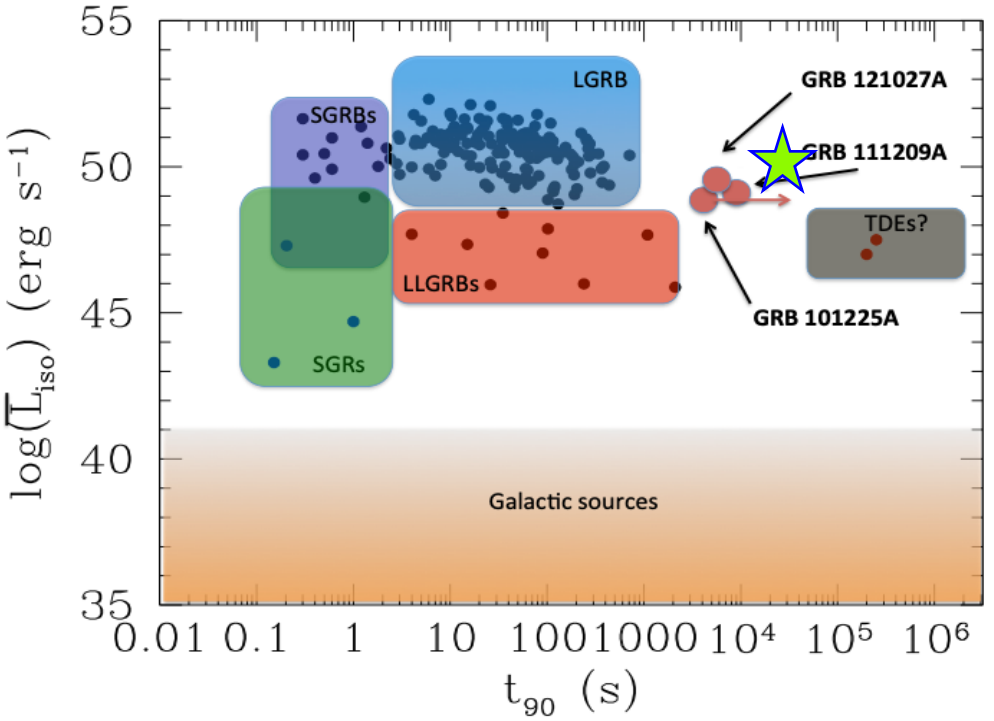

# ULGRB250702B

## Redshift & Host galaxy:

**JWST: $z = 1.036$**

Massive spiral galaxy (with dust lane?) or merger

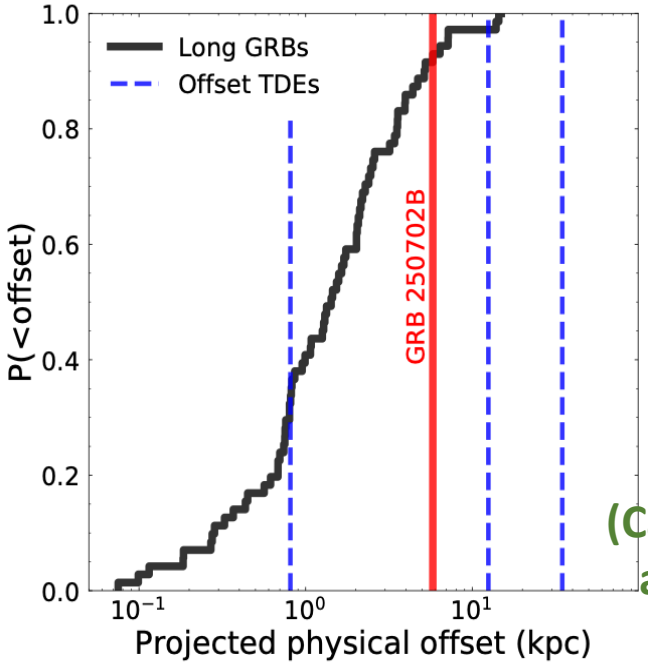


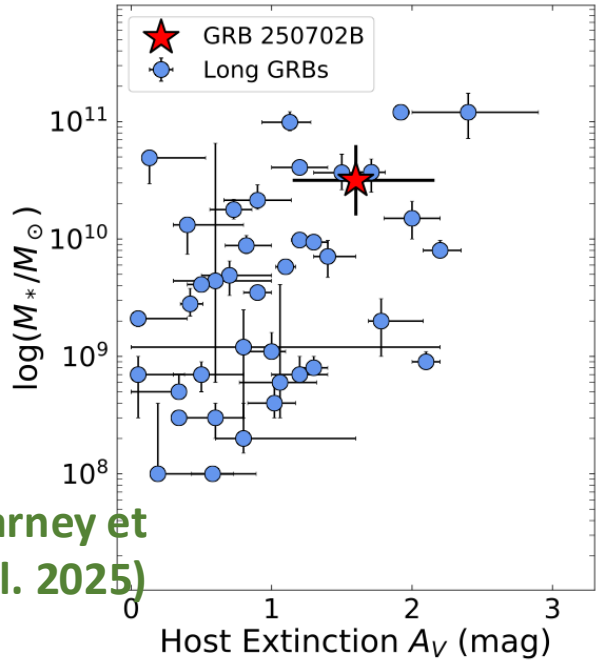


(Carney et al. 2025)

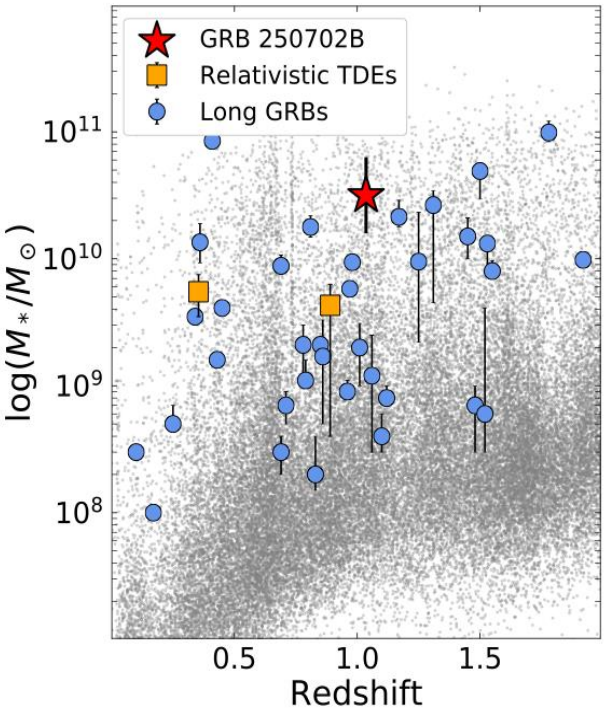


(Carney et al. 2025)

offset = 5.7 kpc

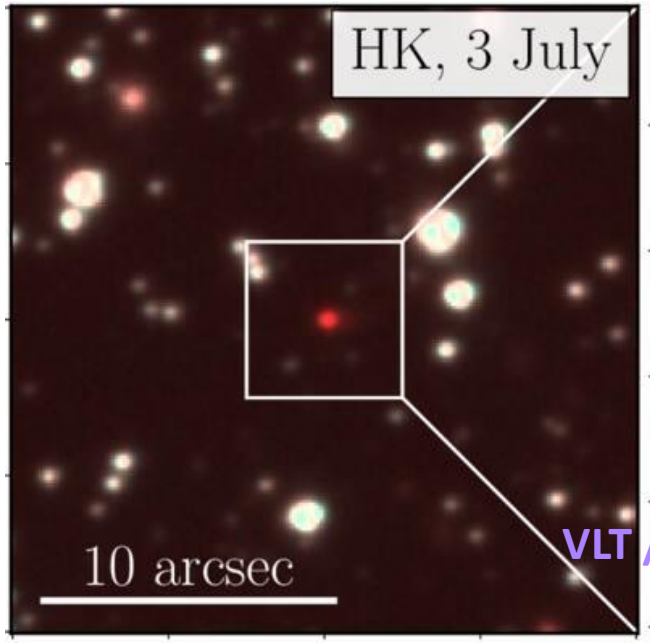


VLT / HAWK-I

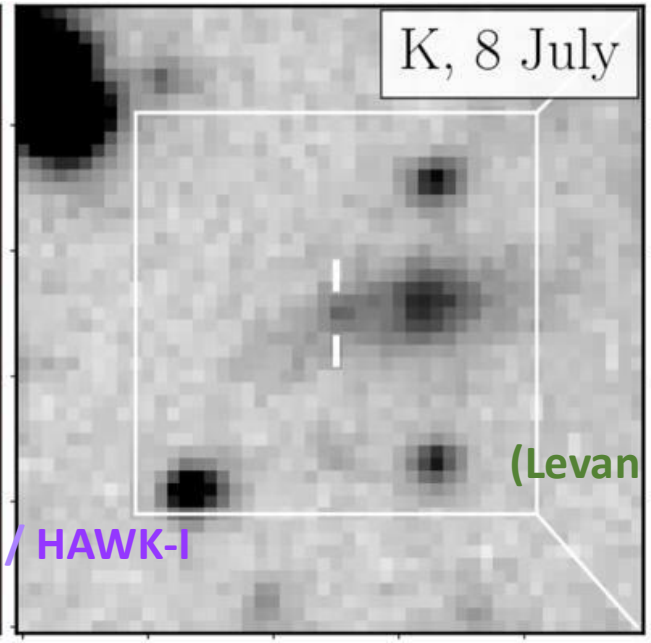


(Levan et al. 2025)

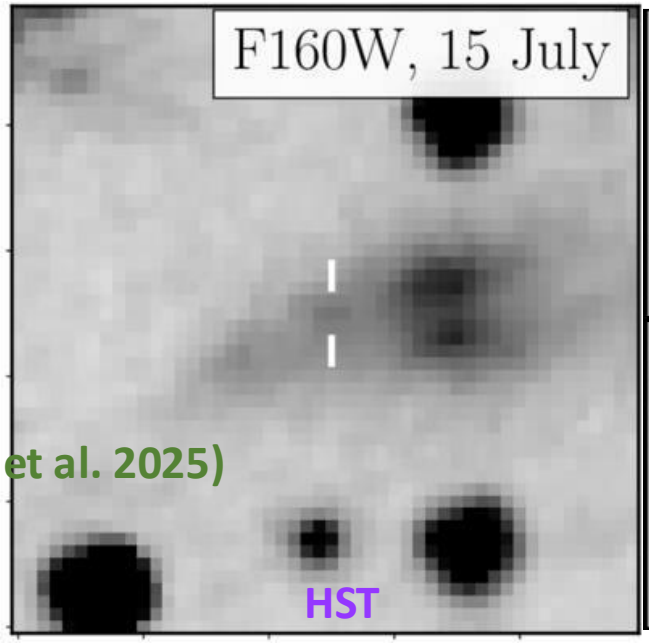


HST

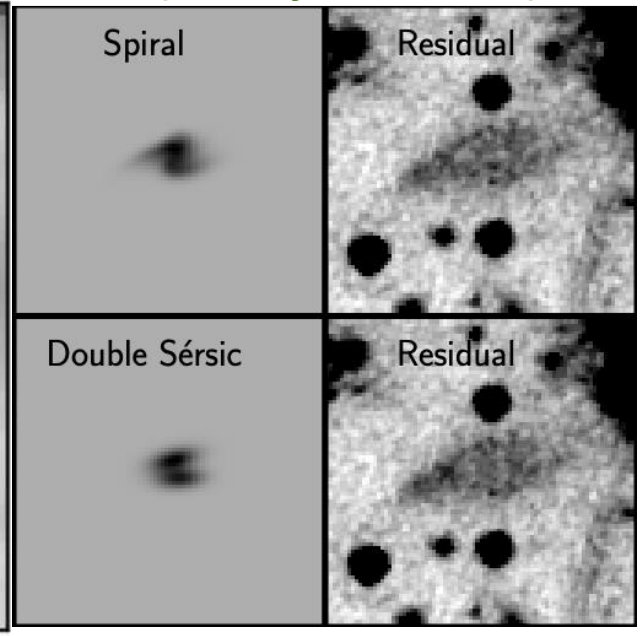

# ULGRB250702B Afterglow: X-ray, IR, radio

- **Extinction:** $A_V = 0.847$ mag (MW) + $2-9$ mag (host); $N_H \approx (3-5)\times 10^{22}$ cm$^{-2}$

(O'Connor et al. 2025)

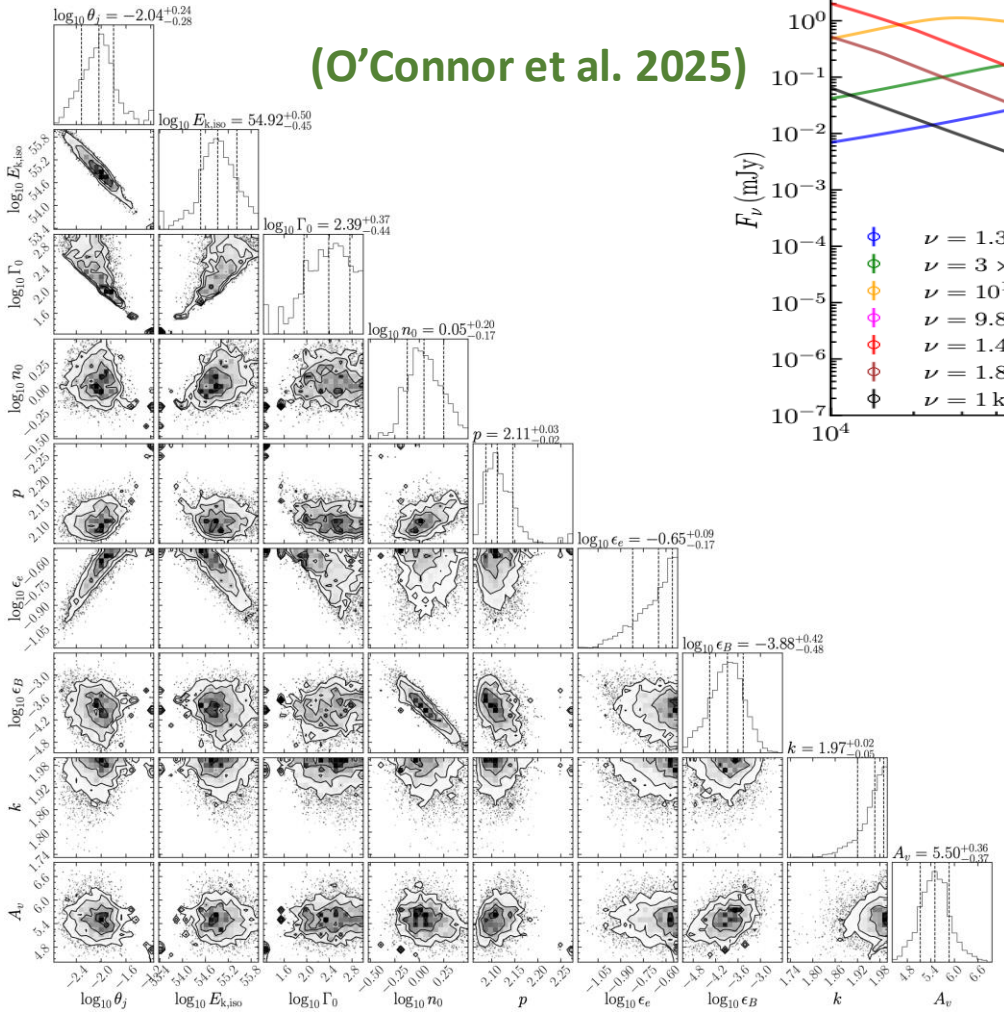


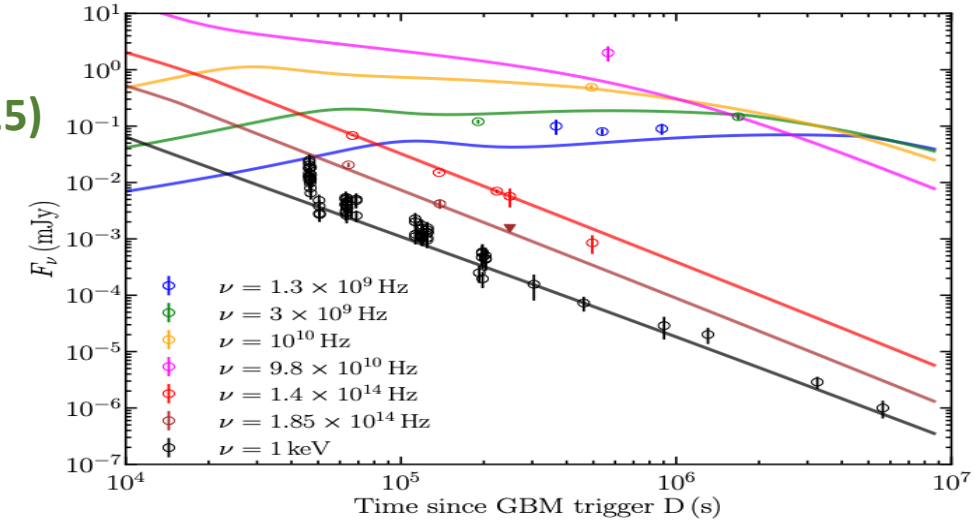


- **Stratified external medium**
- $E_{\rm k,iso} \sim$ few $\times$ $E_{\gamma,\rm iso}$
- **Narrow jet:** $\theta_{\rm jet} \sim 10^{-2}$ rad
- **Still many degeneracies; more data expected**

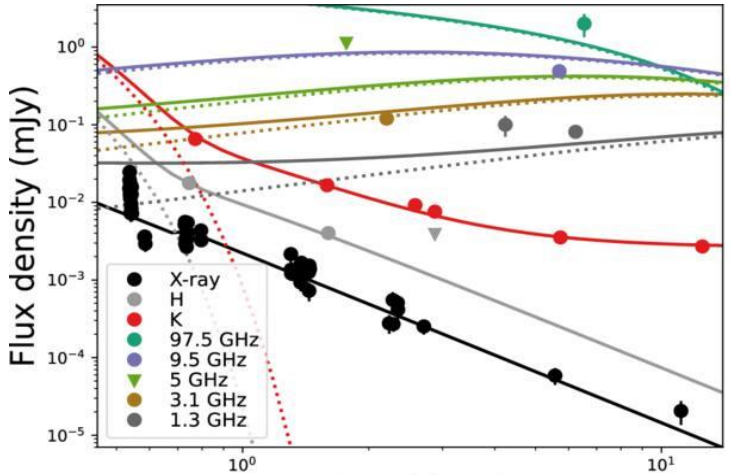


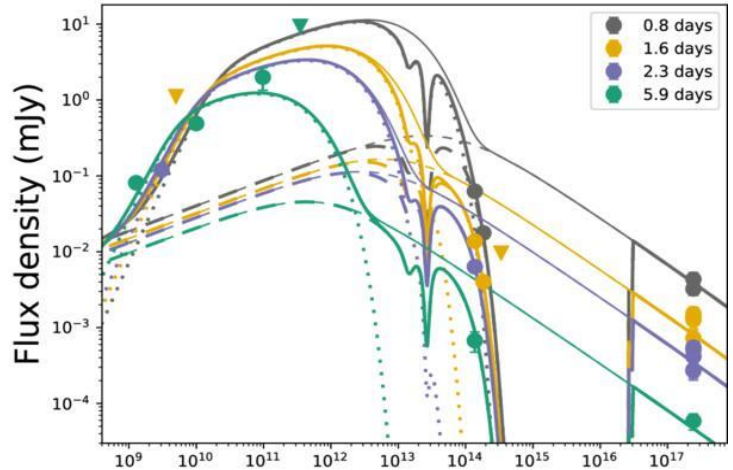


(Levan et al. 2025)

# ULGRB250702B
# X-ray Afterglow:

- Very rapid variability in first few days: $\Delta t/t \sim 10^{-2.5}$
  $\Longrightarrow$ rules out afterglow origin
- Likely late time residual source activity (accretion powered jet)
- Decay slope broadly consistent with TDE expectations

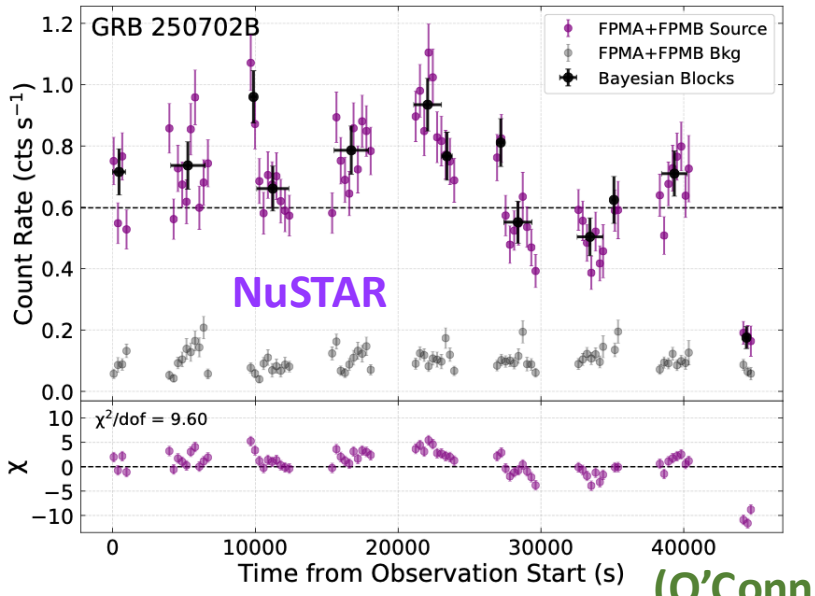


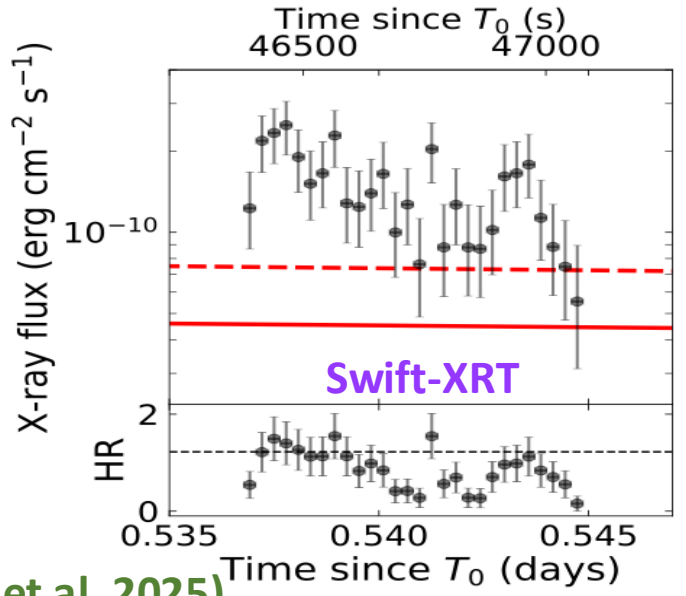


(O'Connor et al. 2025)

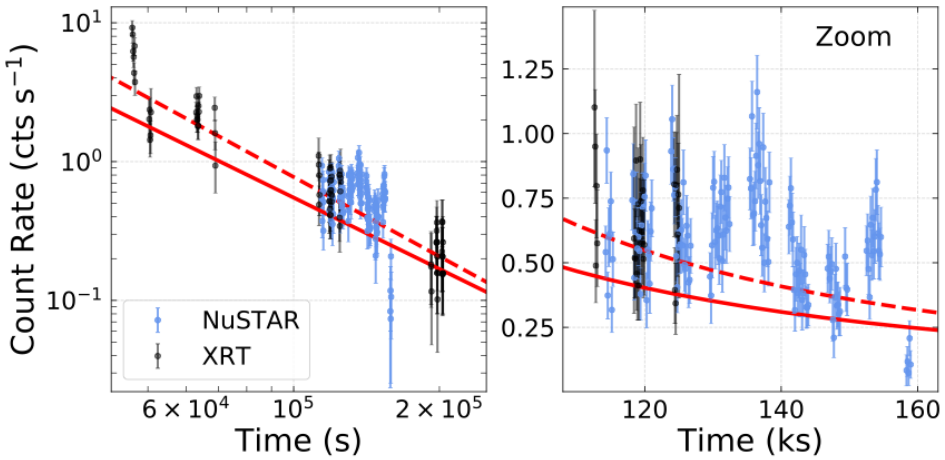


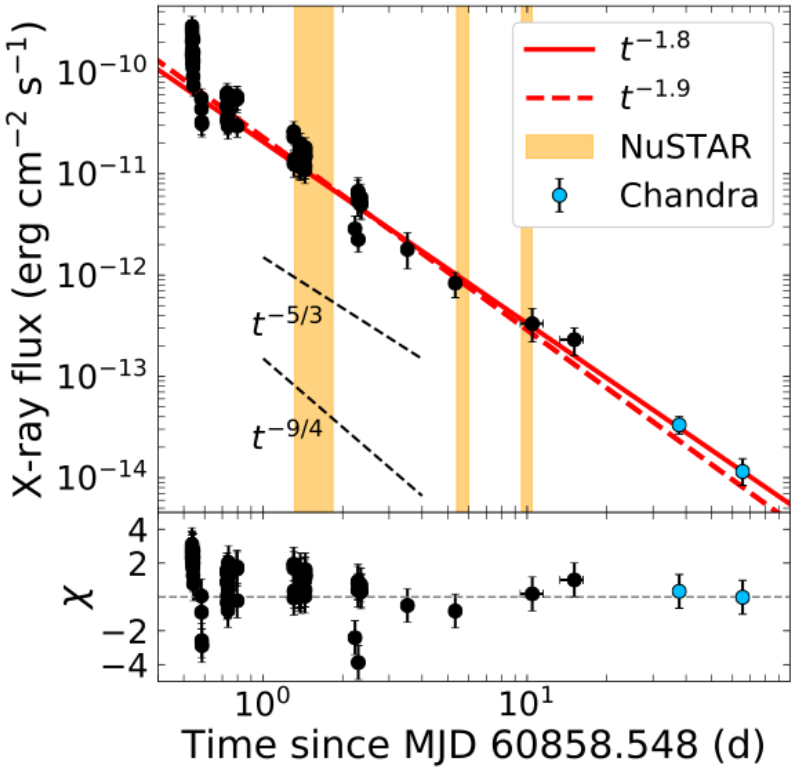


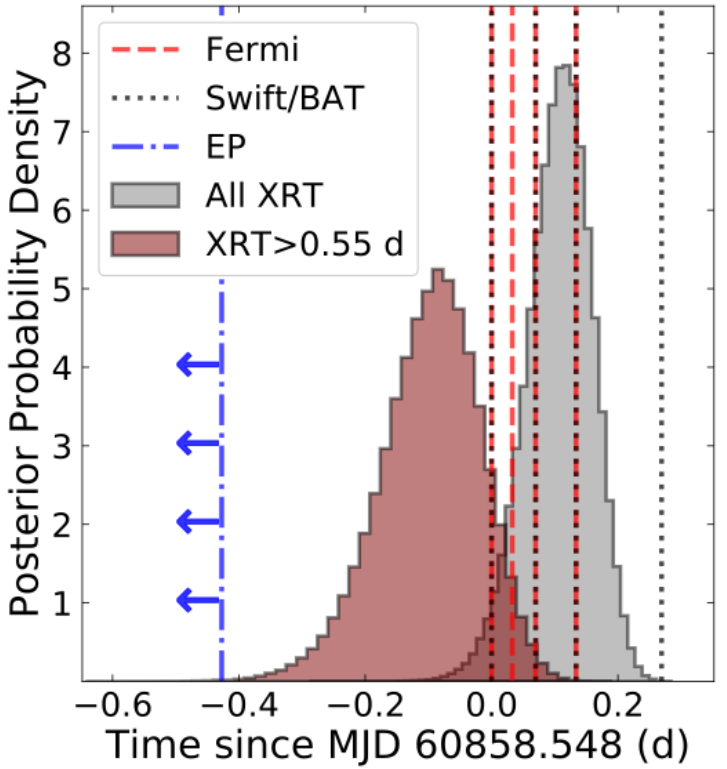

# ULGRB250702B: GRB or TDE?

(O'Connor et al. 2025)

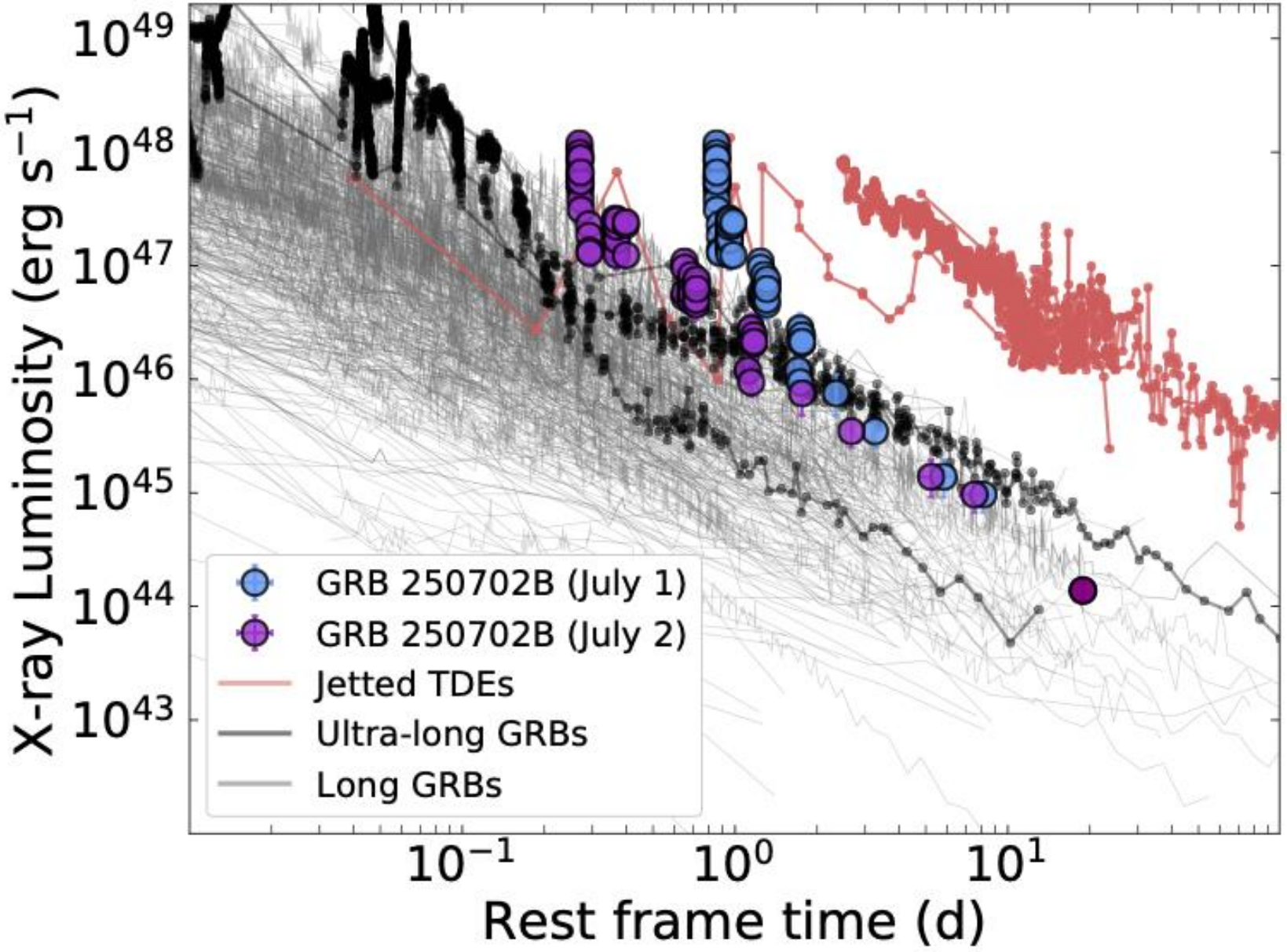


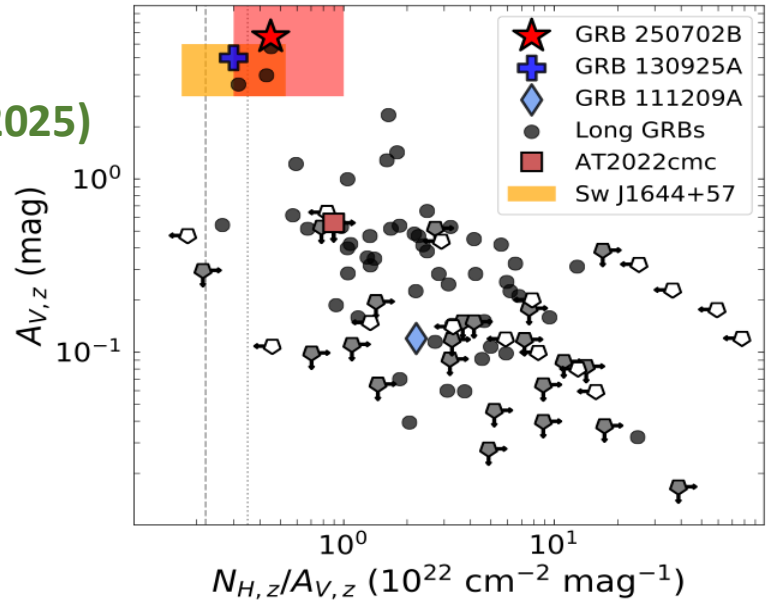


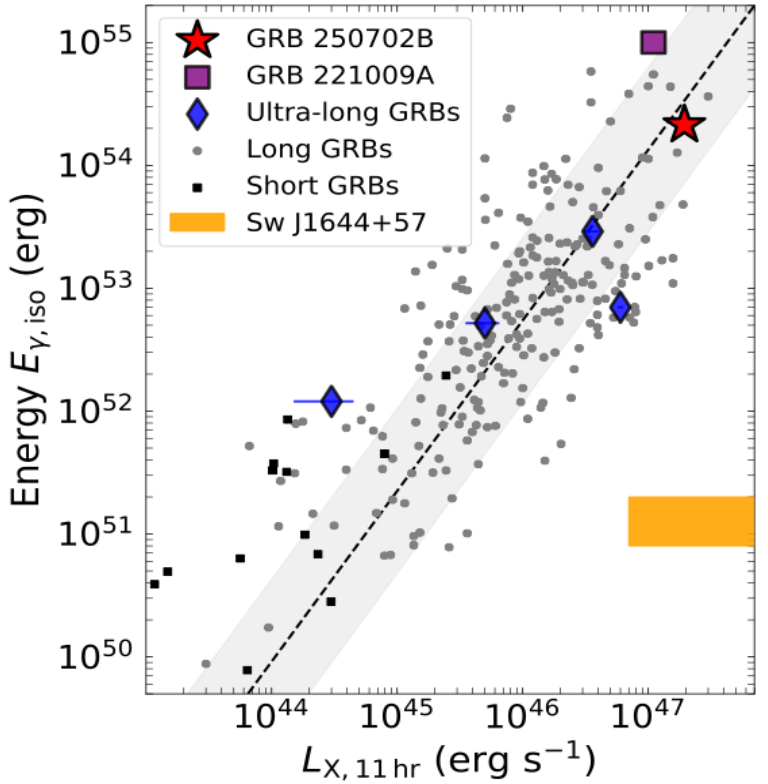

# ULGRB250702B: Einstein Probe: X-ray starts 1 day earlier

$E_{X,\mathrm{iso}}(\mathrm{pre\text{-}peak}) \sim 10^{52.5}$ erg

$E_{X,\mathrm{iso}}(\mathrm{peak}) \sim 10^{53}$ erg

$E_{\gamma,\mathrm{iso}}\ (\mathrm{peak}) \geq 1.4 \times 10^{54}$ erg

**$\Longrightarrow$ likely beamed relativistic jet**

- Insight-HXMT/HE + Fermi /GBM: ~50 s precursor found ~25 hr before the main peak (Zhang+26)

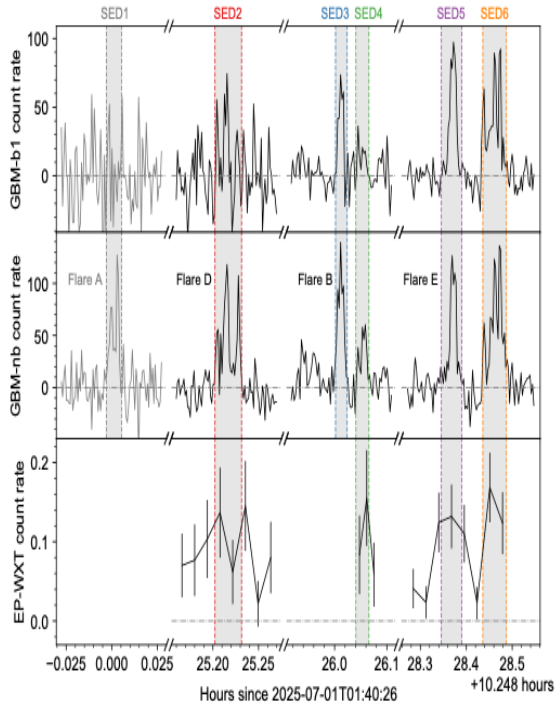


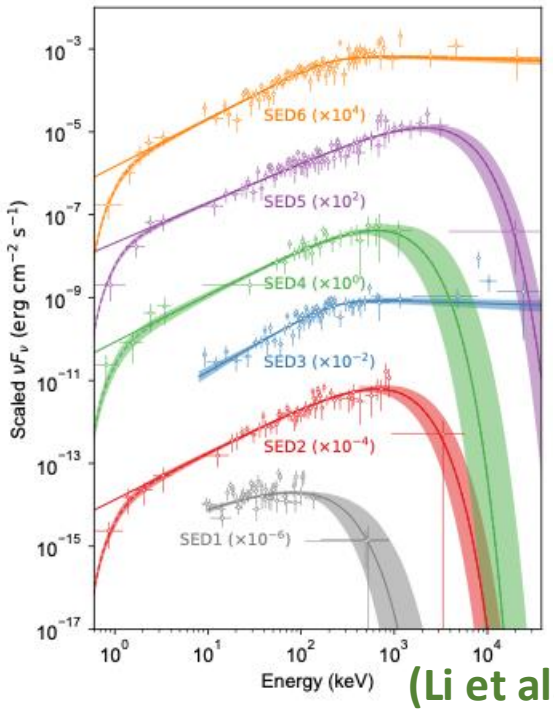


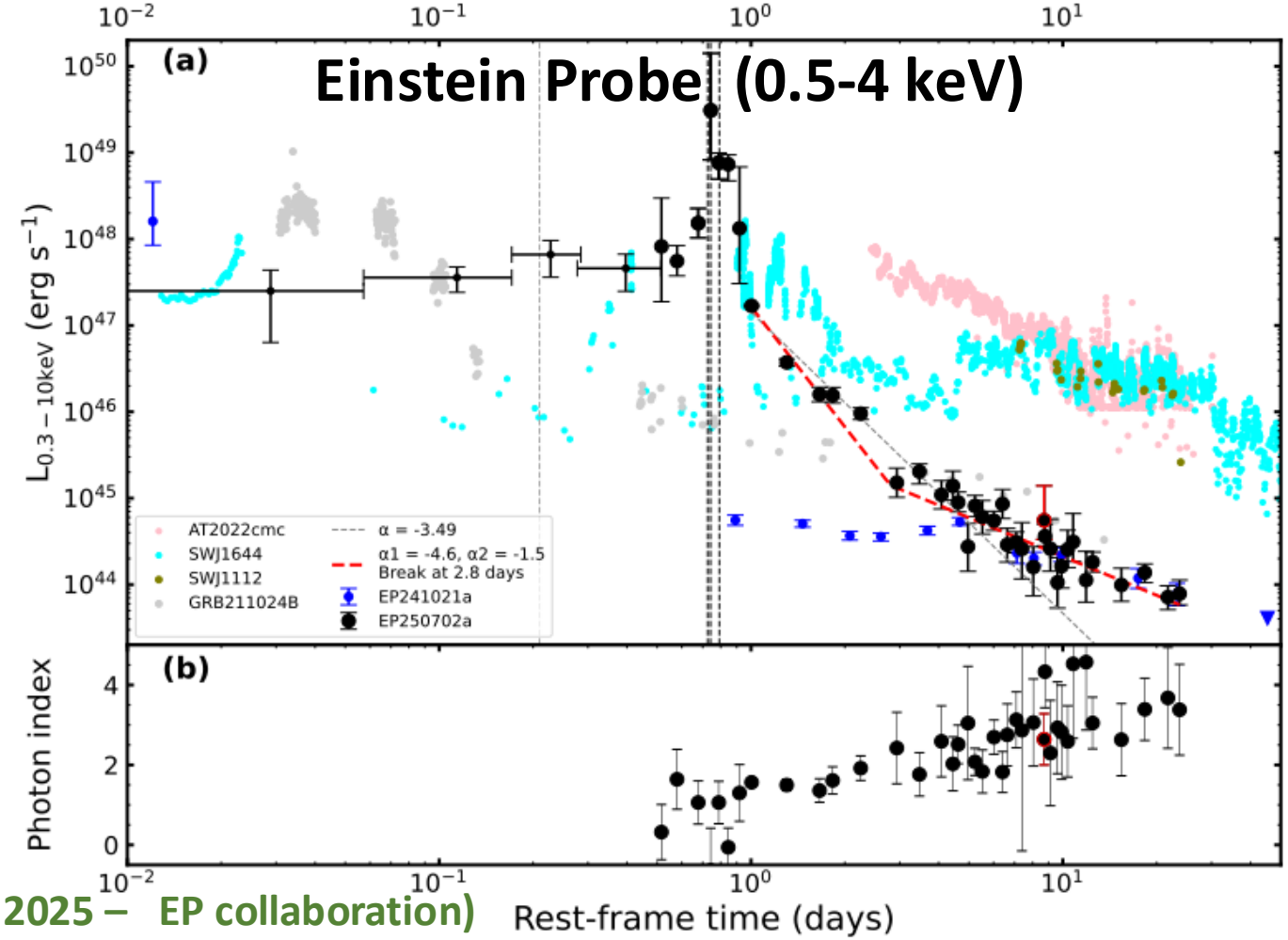


(Li et al. 2025 – EP collaboration)

# What can it be?

- **Unusual type of collapsar (variant of long GRBs)? He-core + NS/BH? (JWST rules out a typical broad-line SN Ic, associated with LGRSs)**
- **Extreme Ultra-Long GRB?** (maybe, but unclear what ULGRBs are…)
- **TDE-SMBH:** offset from host + $t_{\mathrm{MV,z}} \approx 0.5\,\mathrm{s} > \frac{r_g}{c} \Longrightarrow M_{\mathrm{BH}} < 5 \times 10^4 M_\odot$
- **TDE-stelar-mass-BH (micro-TDE): possible (Beniamini, Perets & JG 2025)**
- **TDE-IMBH: possible (MS or WD?);** $t_{\mathrm{MV,z}} \approx 0.5\,\mathrm{s}$ & $\Gamma > 56$ still favor a stellar-mass BH engine

**TDE-IMBH of WD:**
Timescales & lightcurve shape don't quite match

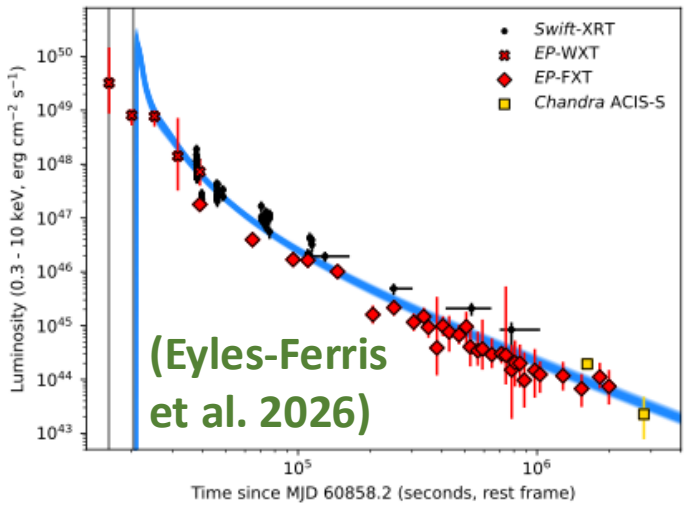


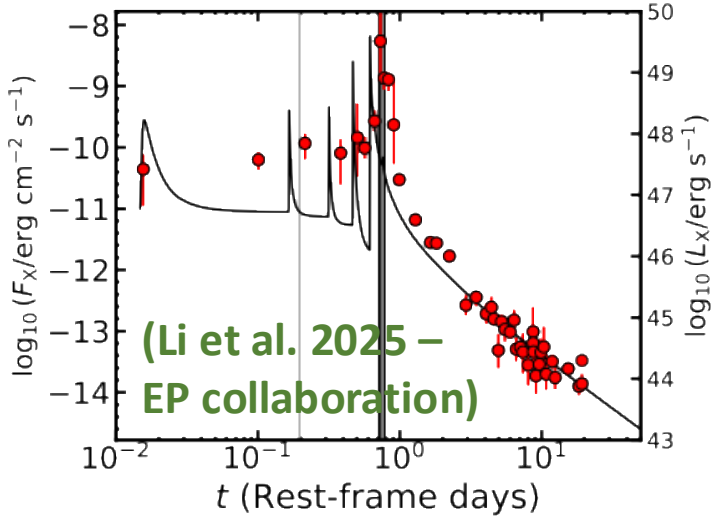

# A milli-TDE Model for GRB250702B: MS Star Disrupted by IMBH

## (JG, Peters, Gill, Beniamini, O'Connor 2025)

### GRB250702B Afterglow Fit:

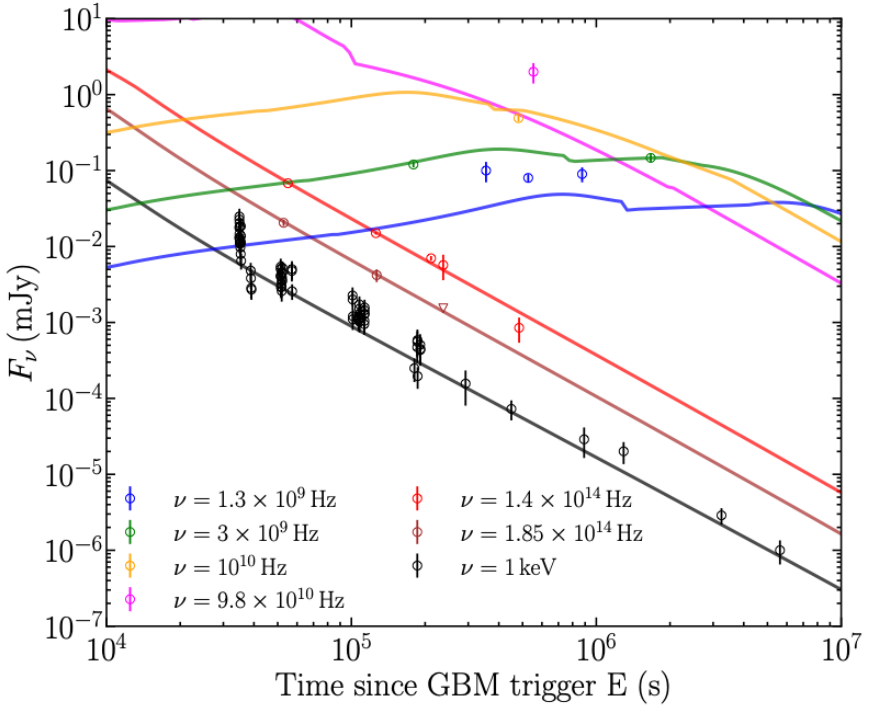


$k = -1.60 \pm 0.17$ (consistent with -3/2)

$n(r) = n_d (r/R_d)^{-k}, R_d = 10^{18}$ cm

$\log_{10} n_{d,0} = 0.36 \pm 0.28$

($\log_{10} \theta_j = -1.99^{+0.33}_{-0.27}$; $\log_{10} E_{\rm k,iso} = 54.99^{+0.53}_{-0.57}$

$50 \lesssim \log_{10} E_{\rm k} \lesssim 51$)

### Bondi Accretion:

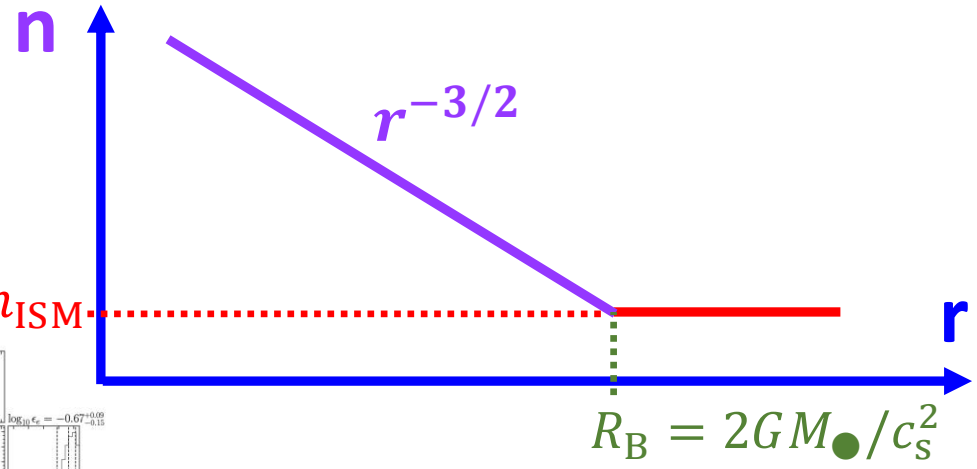

# A milli-TDE Model for GRB250702B: MS Star Disrupted by IMBH

## (JG, Peters, Gill, Beniamini, O'Connor 2025)

### Inferred Bondi Radius:

$$R_{\rm B} = R_d\,(n_{\rm d}/n_{\rm ISM})^{2/3} = 0.56^{+0.31}_{-0.19}\,n_0^{-2/3}\ {\rm pc}$$

### Inferred IMBH Mass:

$$M_\bullet = 6.55^{+3.51}_{-2.29}\times 10^3 n_0^{-2/3} c_{\rm s,6}^2\,M_\odot$$

$k = -1.60 \pm 0.17$ (consistent with -3/2)

$n(r) = n_d(r/R_d)^{-k}, R_d = 10^{18}$ cm

$\log_{10} n_{d,0} = 0.36 \pm 0.28$

### Bondi Accretion:

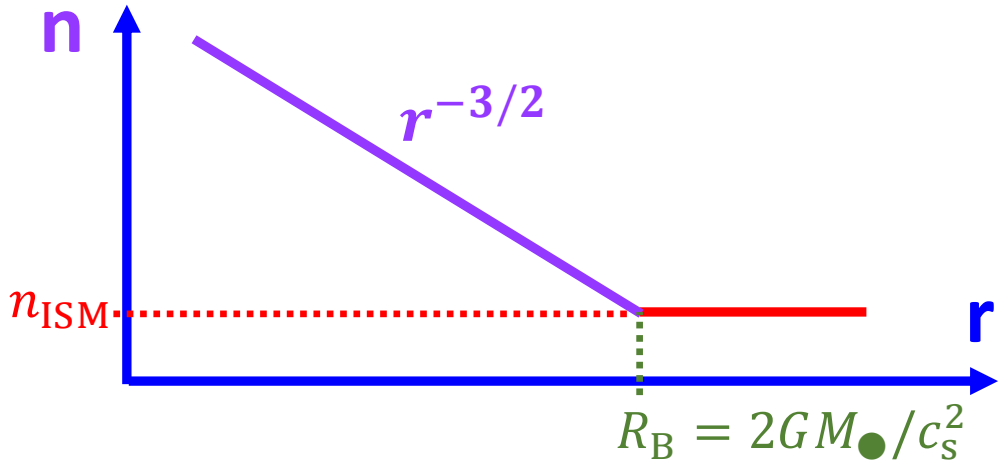


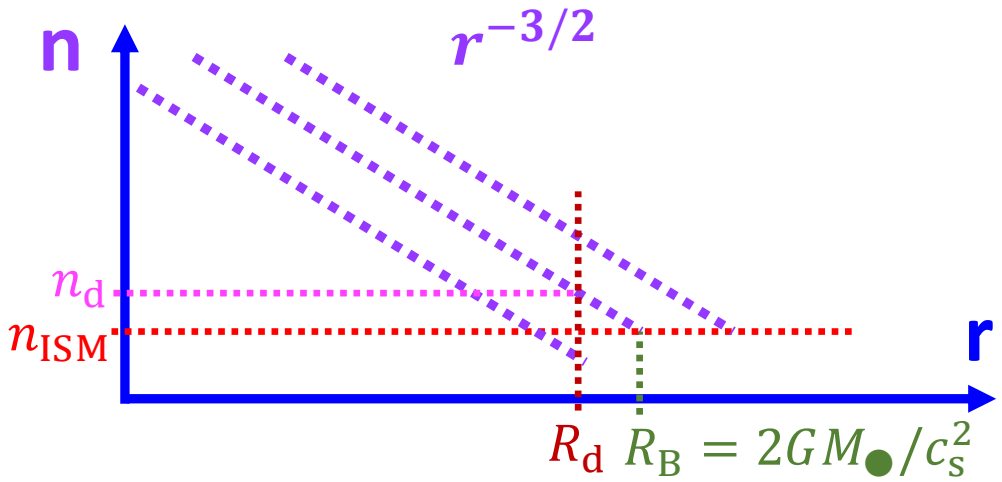

# A milli-TDE Model for GRB250702B: MS Star Disrupted by IMBH

## (JG, Peters, Gill, Beniamini, O'Connor 2025)

### Inferred Bondi Radius:

$$R_{\rm B} = R_d\,(n_{\rm d}/n_{\rm ISM})^{2/3} = 0.56^{+0.31}_{-0.19}\,n_0^{-2/3}\ {\rm pc}$$

### Inferred IMBH Mass:

$$M_\bullet = 6.55^{+3.51}_{-2.29}\times 10^3 n_0^{-2/3} c_{s,6}^2\,M_\odot$$

- **Also consistent with the observed afterglow emission coming from $r < R_B$**

$k = -1.60 \pm 0.17$ (consistent with -3/2)

$n(r) = n_d(r/R_d)^{-k}, R_d = 10^{18}$ cm

$\log_{10} n_{d,0} = 0.36 \pm 0.28$

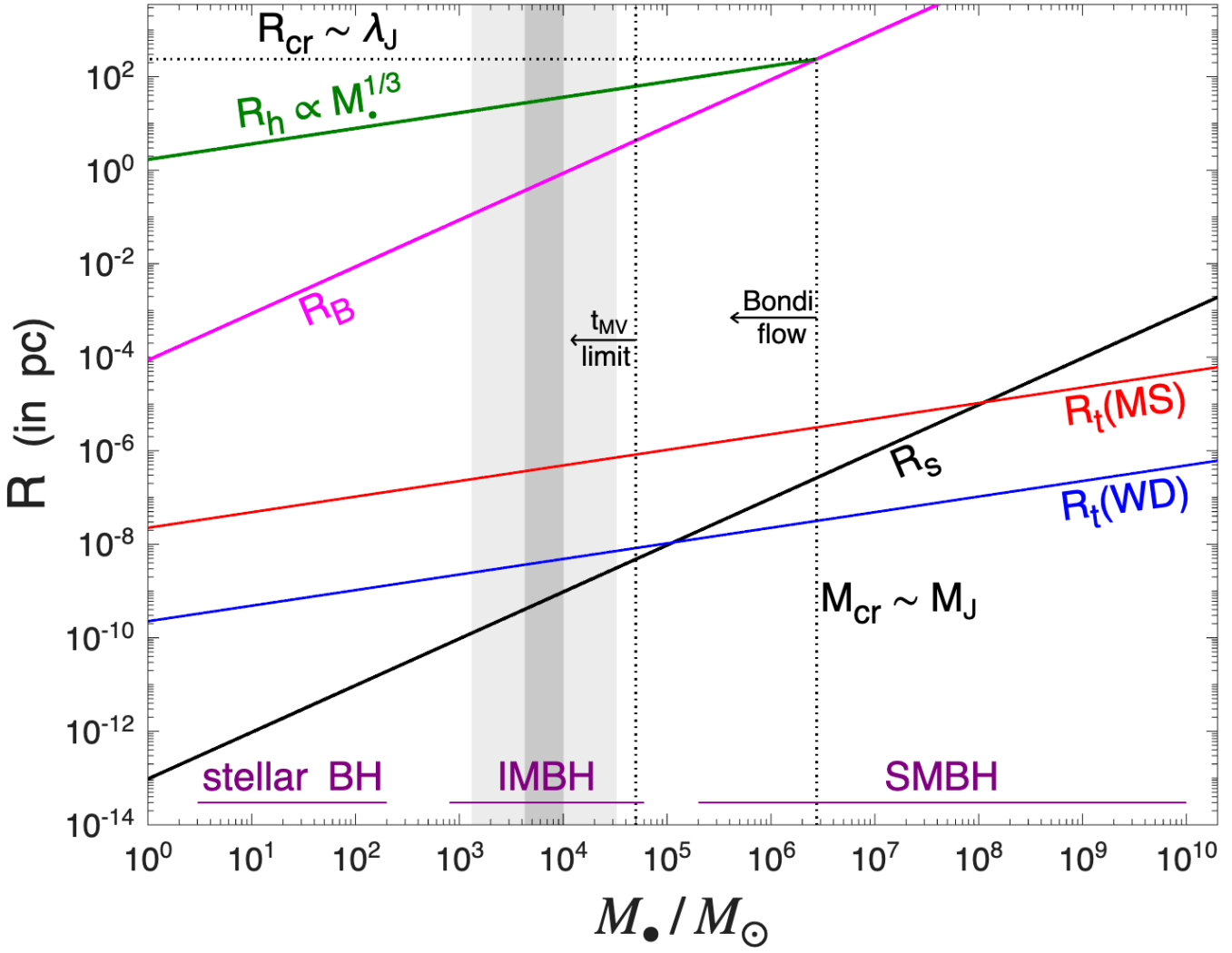

# Bondi Hoyle Lyttleton Accretion:

## Modified Bondi Radius ($v_{\rm BH}$ added):

$$R_{\rm BHL} \approx \frac{R_{\rm B}}{1+\mathcal{M}^2} = \frac{2GM_\bullet}{c_{\rm s}^2(1+\mathcal{M}^2)}; \quad \mathcal{M} \equiv \frac{v_{\rm BH}}{c_{\rm s}}$$

## Modified infered IMBH Mass:

$$M_\bullet = 6.55^{+3.51}_{-2.29} \times 10^3 n_0^{-2/3} c_{\rm s,6}^2 (1+\mathcal{M}^2)\, M_\odot$$

$$t_{\rm MV,z} > \frac{r_g}{c} \Longrightarrow \frac{M_{\rm BH}}{M_\odot} < 5\times 10^4 \Longrightarrow v_{\rm BH} \lesssim 28 n_0^{1/3} \rm km/s$$

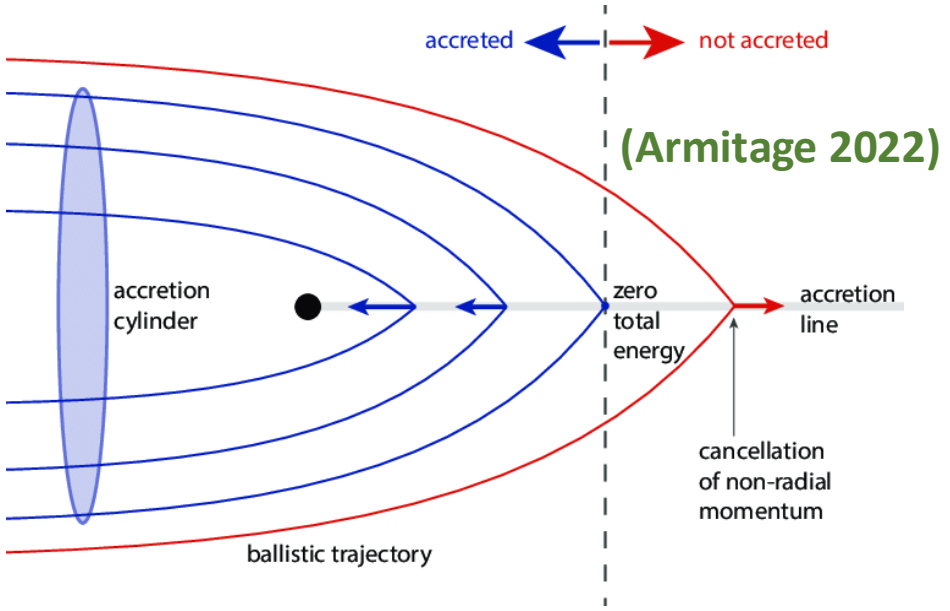


(Armitage 2022)

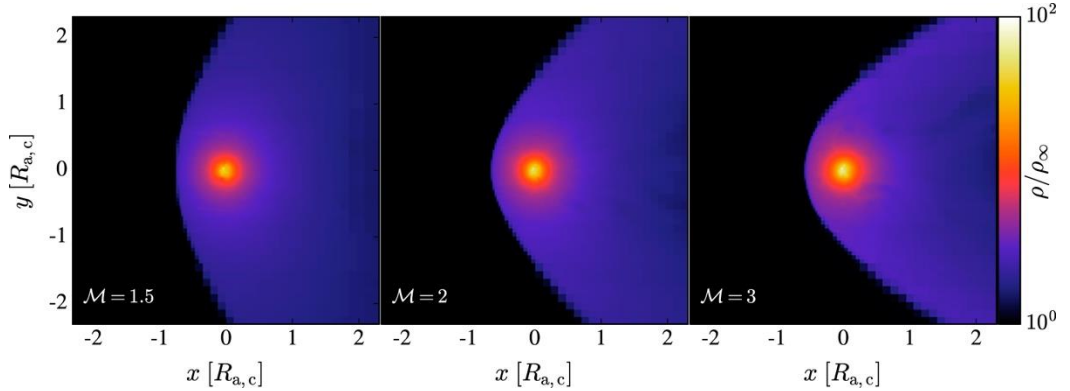


(Kaaz, Antoni & Ramirez-Ruiz 2019)

# Relevant Timescales: Main Sequence vs. White Dwarf

## Disruption to 1st periastron passage ($r_t \rightarrow r_p$):

$$t_1 = \sqrt{\frac{\pi^2 R_*^3}{2GM_*}} = \begin{cases} 3.54\times10^3 R_{*,0}^{3/2} M_{*,0}^{-1/2}\ \mathrm{s} & (\mathrm{MS})\ , \\ 3.54\, R_{*,-2}^{3/2} M_{*,0}^{-1/2}\ \mathrm{s} & (\mathrm{WD})\ . \end{cases}$$

## Orbital time of the most bound debris:

$$t_{\min} \approx \begin{cases} 3.5\times10^4\, A_{\beta,-1}\, \eta^2\, M_{\bullet,4}^{1/2} R_{*,0}^{3/2} M_{*,0}^{-1}\ \mathrm{s} & (\mathrm{MS})\ , \\ 3.5\times10^1\, A_{\beta,-1}\, \eta^2\, M_{\bullet,4}^{1/2} R_{*,0}^{3/2} M_{*,0}^{-1}\ \mathrm{s} & (\mathrm{WD})\ . \end{cases}$$

Where $A_\beta \sim 1$ for frozen in approx, or $\sim \beta^{-3}$ for efficient dissiption near $r_p$
($\beta \equiv r_t/r_p$ = penetration factor)

- **The observed timescales greatly prefer a MS star over a WD**
- **For a WD $r_p \lesssim r_{\rm ISCO}$ is possible, in which case no accretion disk or jet would form**

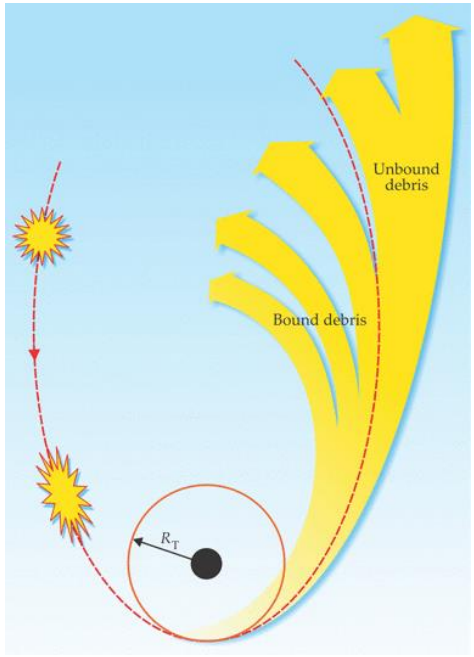


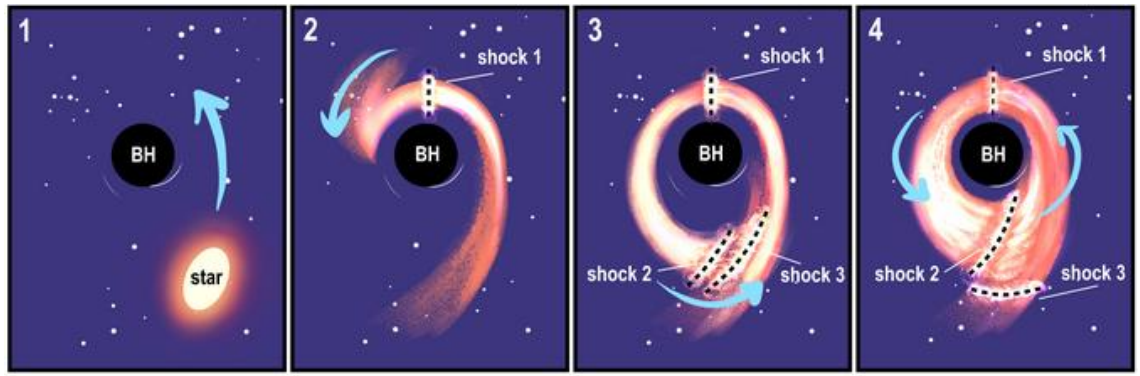


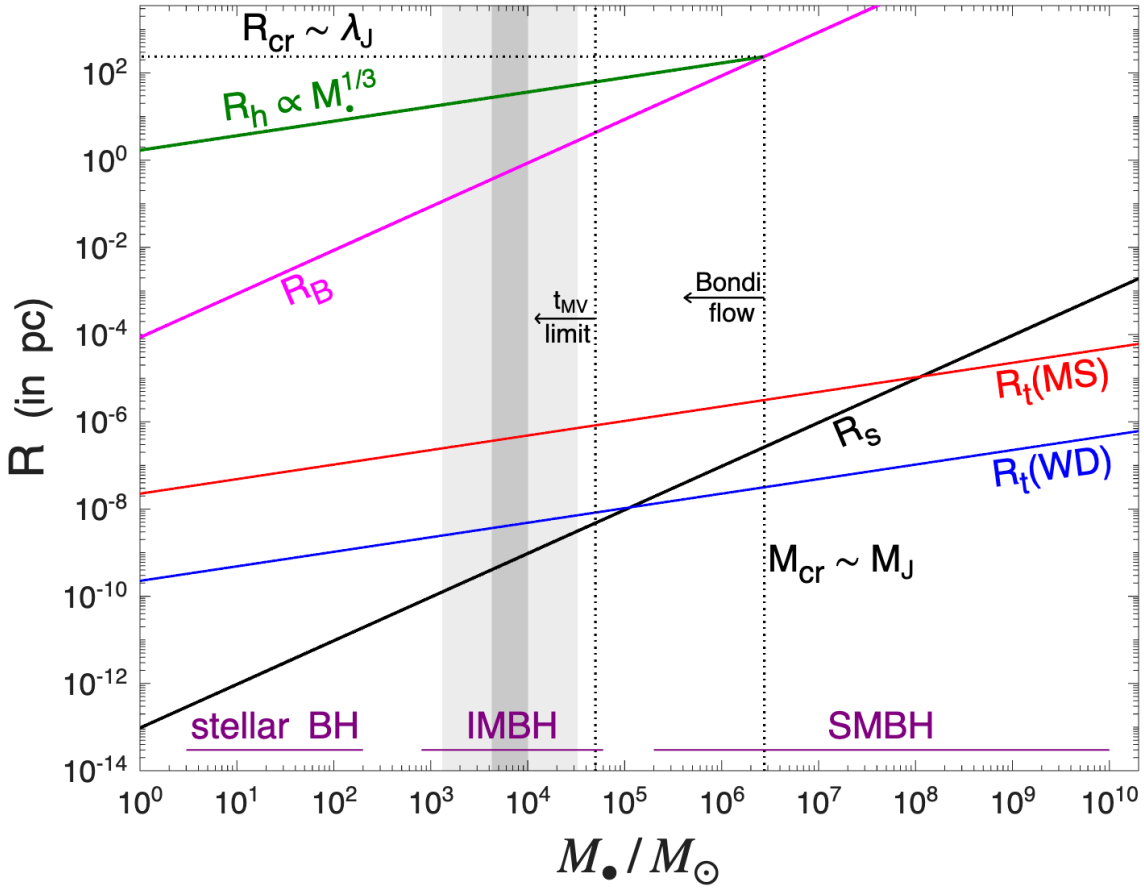

# Relevant Timescales: Main Sequence vs. White Dwarf

## Disruption to 1st periastron passage ($r_t \rightarrow r_p$):

$$t_1 = \sqrt{\frac{\pi^2 R_*^3}{2GM_*}} = \begin{cases} 3.54\times10^3 R_{*,0}^{3/2} M_{*,0}^{-1/2}\ \mathrm{s} & (\mathrm{MS})\ , \\ 3.54\, R_{*,-2}^{3/2} M_{*,0}^{-1/2}\ \mathrm{s} & (\mathrm{WD})\ . \end{cases}$$

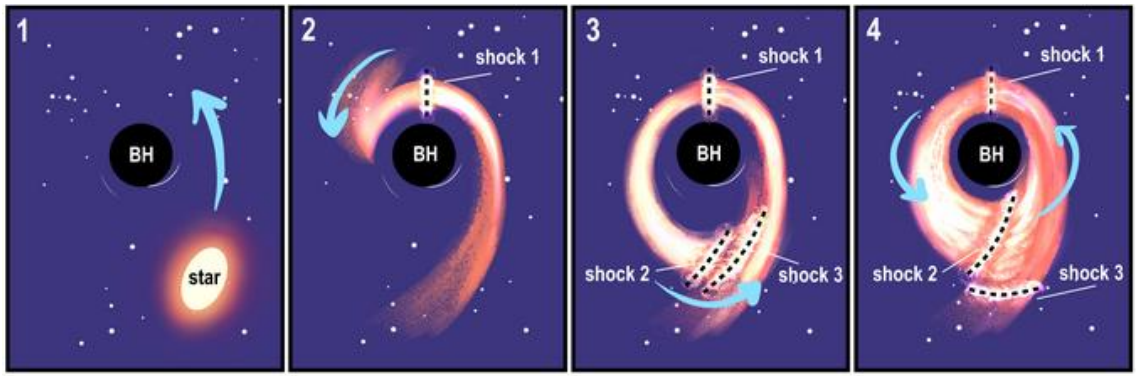


## Orbital time of the most bound debris:

$$t_{\min} \approx \begin{cases} 3.5\times10^4\, A_{\beta,-1}\, \eta^2\, M_{\bullet,4}^{1/2}\, R_{*,0}^{3/2}\, M_{*,0}^{-1}\ \mathrm{s} & (\mathrm{MS})\ , \\ 3.5\times10^1\, A_{\beta,-1}\, \eta^2\, M_{\bullet,4}^{1/2}\, R_{*,0}^{3/2}\, M_{*,0}^{-1}\ \mathrm{s} & (\mathrm{WD})\ . \end{cases}$$

## For $R_{\rm circ} \approx 2r_p = 2r_t/\beta$, $t_{\rm acc} \approx t_{vis}(R_{\rm circ})$:

$$t_{\rm acc} \approx\ 4.5\times10^4\, \beta^{-3/2}\, \alpha_{-1}^{-1}\, h^{-2}\, M_{*,0}^{-\frac{1}{2}}\, R_{*,0}^{3/2}\ \mathrm{s}$$

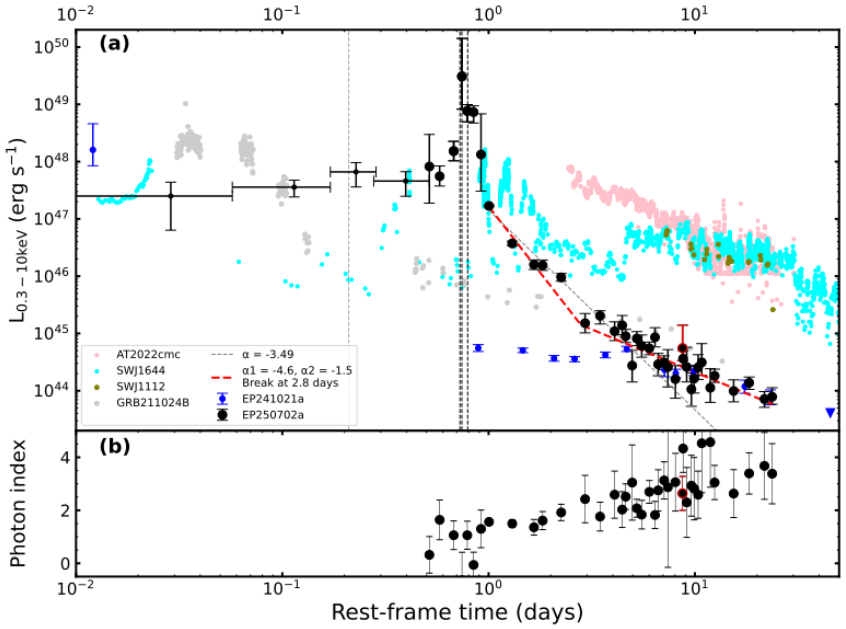


(Li et al. 2025 EP collaboration)

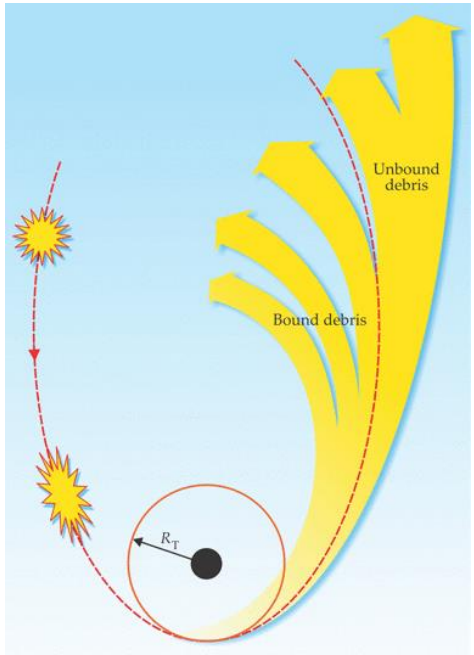


## Approximate rise and peak timescales:

$$t_{\rm X,rise} \sim t_{\rm circ} + t_{\rm acc}\ , \qquad t_{\rm main} \sim t_{\rm min} + t_{\rm acc}\ ,$$

$$t_{\rm circ} \approx 3.5\times10^4 f_{0.5}\beta_{0.5}^{-3}\, \eta^2\, M_{\bullet,4}^{1/2}\, R_{*,0}^{3/2}\, M_{*,0}^{-1}\ \mathrm{s}\ ,$$

$$t_{\rm min} \approx 1.1\times10^4 \beta_{0.5}^{-3}\, \eta^2\, M_{\bullet,4}^{1/2}\, R_{*,0}^{3/2}\, M_{*,0}^{-1}\ \mathrm{s}\ ,$$

$$t_{\rm acc} \approx\ 3.2\times10^4\, \beta_{0.5}^{-3/2}\, \alpha_{-1}^{-1}\, h_{-0.3}^{-2}\, M_{*,0}^{-\frac{1}{2}}\, R_{*,0}^{3/2}\ \mathrm{s}\ ,$$

## Energetics limit on the jet beamin factor:

$$f_b \le 6.4\times10^{-4} \eta_{j,-2}\eta_{\gamma,-1} M_{*,0} \left(\frac{f_{\rm fb}}{0.5}\right)\left(\frac{1.4\times10^{54}\,\mathrm{erg}}{E_{\gamma,\rm iso}}\right)$$

# Persistent Radio Sources (PRSs) of Repeating FRBs: Implications for Magnetar Progenitors (Rahaman, Acharia, Beniamini & JG 2025)

- A handful of confirmed/candidate PRSs associated with repeating FRBs
- Appear to have large $DM_{host}$, large + variable R, low-Z high-SFR hosts
- Model: synchrotron emission from a compact Magnetar Wind Nebula (MWN)

| Property | FRB 20121102A | FRB 20190417A | FRB 20190520B | FRB 20201124A | FRB 20240114A |
|---|---|---|---|---|---|
| $z$ (redshift) | 0.193 | 0.128 | 0.241 | 0.098 | 0.130 |
| Host galaxy | Dwarf | Dwarf | Dwarf | Spiral | Dwarf |
| DM $[\mathrm{pc\ cm^{-3}}]$ | 558 | 1379 | 1204 | 413 | 528 |
| $DM_{host,rest}$ | $\lesssim 203$ | $> 1228$ | $137 - 707$ | $150 - 220$ | $142 \pm 107$ |
| $RM_{rest}$ $[\mathrm{rad\ m^{-2}}]$ | $(0.44 - 1.5) \cdot 10^5$ | $(5.04 - 6.44) \cdot 10^3$ | $(-3.6 - 2.0) \cdot 10^4$ | $-661 \pm 42$ | $449 \pm 13$ |
| $offset_{PRS-FRB}$ [pc] | $< 40$ | $< 26$ | $< 80$ | $< 188$ | $\lesssim 28$ |
| $R_{proj}$ [pc] | $< 0.7$ (at 5 GHz) | $< 23$ | $< 9$ | $< 700$ | $< 0.4$ |
| $\nu_{obs}$ [GHz] | $1 - 26$ | 1.4 | 1.5, 3, 5.5 | 6, 15, 22 | 0.65, 1.3, 5 |
| $F_\nu$ $[\mu\mathrm{Jy}]$ | 180 (at 3 GHz) | 190 (at 1.4 GHz) | 202 (at 3 GHz) | 8,20,30 (6,15,22) | 66,72,46 (.65,1.3,5) |
| $\alpha$ (spectral index) | $-0.2 - -1$ | $-1.2 \pm 0.4$ | $-0.41 \pm 0.04$ | $1.00 \pm 0.43$ | $-0.34 \pm 0.21$ |
| $L_\nu$ $[\mathrm{erg\ s^{-1}\ Hz^{-1}}]$ | $2 \times 10^{29}$ (1.4 GHz) | $8 \times 10^{28}$ (1.4 GHz) | $3 \times 10^{29}$ (1.7 GHz) | $2 \times 10^{27}$ (6 GHz) | $2 \times 10^{28}$ (5 GHz) |

PRS of FRB 121102A

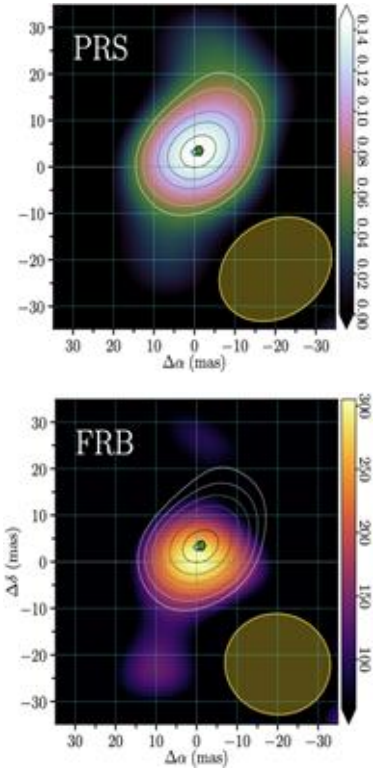


(Snelders et al. 2025) Co-spatiality confirmed

# One Known Galactic Magnetar Wind Nebula: Swift J1834–0846

- Quite rare (1 out of over 30 Galactic magnetars)
- MWN size: diffusion-dominated cooling length of X-ray emitting $e^{\pm}$
- Spindown power or $B_{\rm dipole}$ decay cannot power the MWN
- $B_{\rm int}$ decay can power the MWN for a current $B_{\rm int} \gtrsim 10^{15.5}$ G through outflows associated with bursting activity (e.g. giant flares)

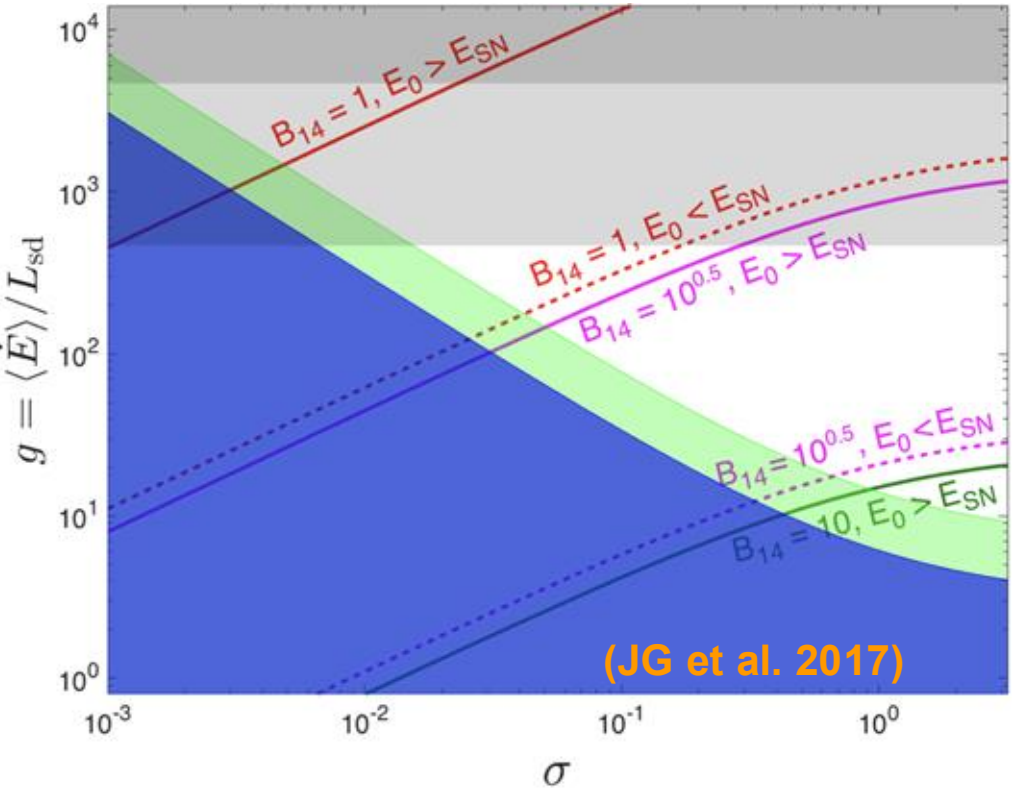


$$P = 2.48 \text{ s}$$
$$\dot{P} = 7.96 \times 10^{-12} \text{ s s}^{-1}$$
$$\tau_c = 4.9 \text{ kyr} \quad (n = 3)$$
$$t = \tau_c - 10^5 \text{ yr}$$
$$B_{\rm d} = 10^{14} \text{ G}$$
$$L_{\rm sd} = 2 \times 10^{34} \text{ erg s}^{-1}$$

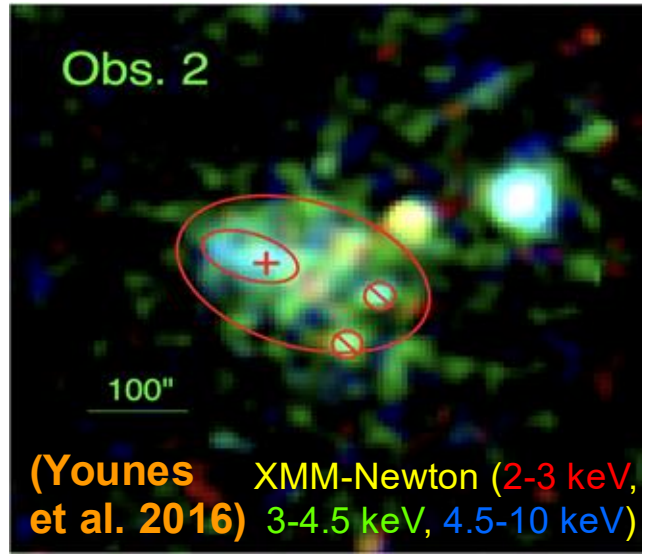


**Associated with SNR W41**

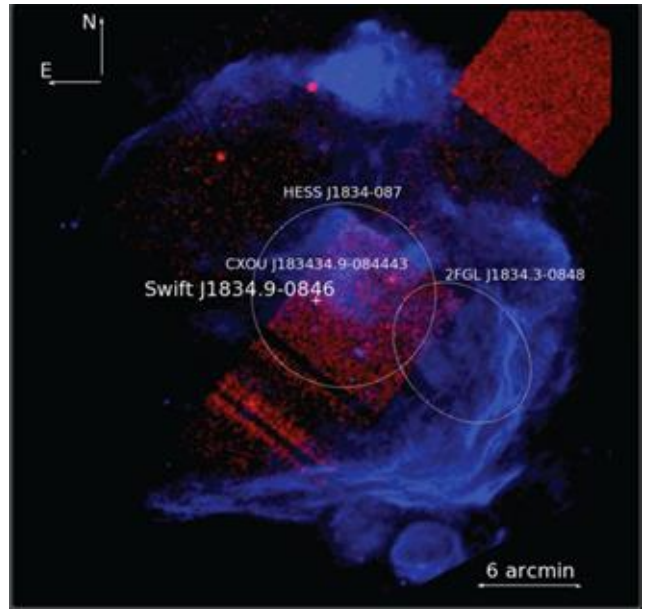

# Persistent Radio Sources (PRSs) of Repeating FRBs: Implications for Magnetar Progenitors (Rahaman, Acharia, Beniamini & JG 2025)

## PRS of FRB 121102A: the best constrained source

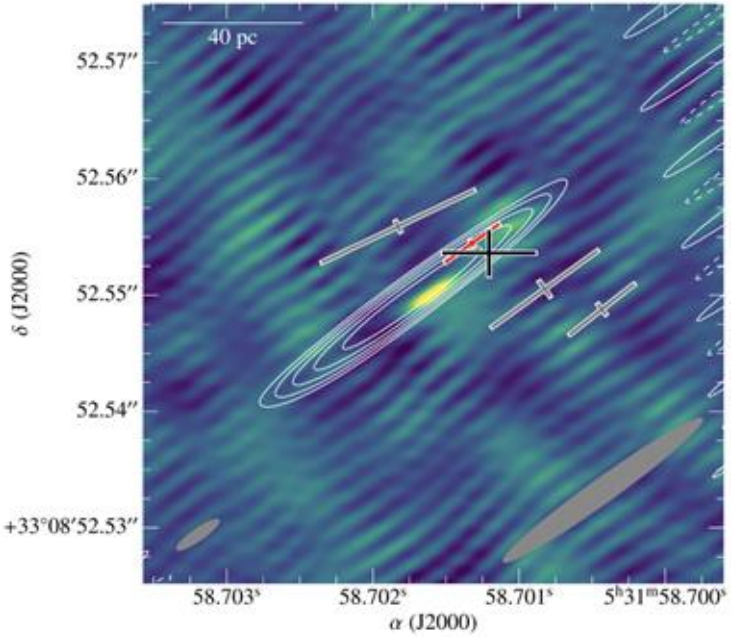


$R_{\rm max} = 0.7$ pc (imaging)
(Marcote et al. 2017)

$R_{\rm eq} \sim 0.1$ pc (equipartition)

$R_{\rm min} = 0.03$ pc (scintillation)
(Chen et al. 2023)

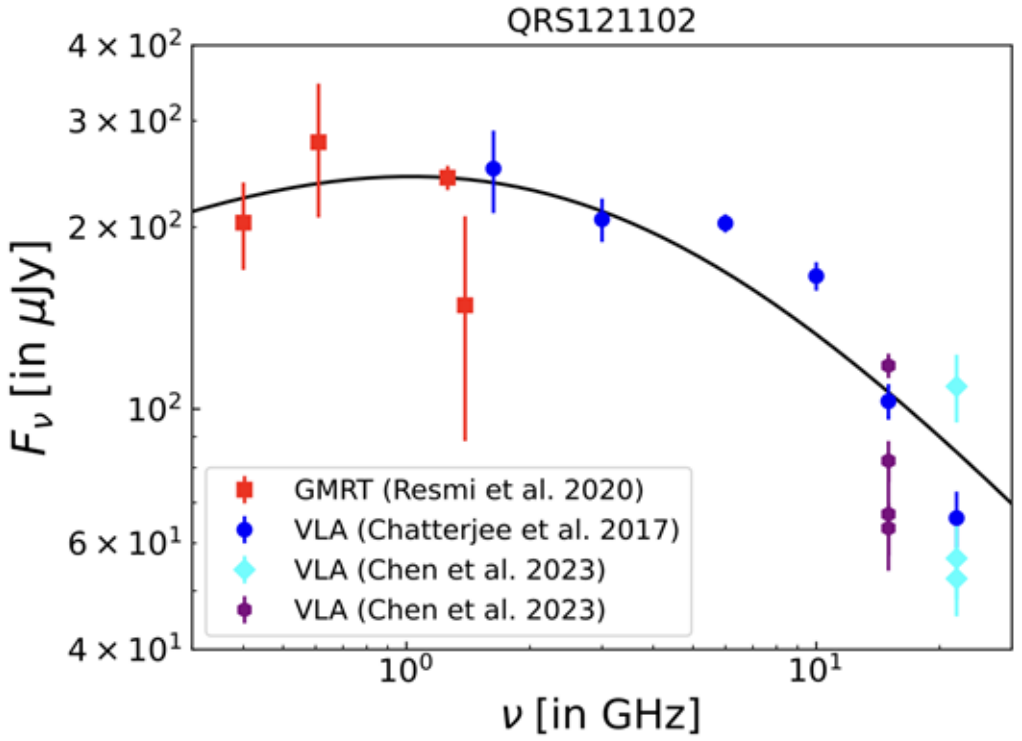


$L_\nu \sim 2 \times 10^{29} \frac{\rm erg}{\rm s\ Hz}$

$\nu_{\rm sa} < 0.5$ GHz

$\nu_{\rm m} < 3$ GHz

$\nu_{\rm c} > 22$ GHz

$R_{\rm min} < R_{\rm eq} < R_{\rm max}$

**PRS is very compact**

# Persistent Radio Sources (PRSs) of Repeating FRBs: Implications for Magnetar Progenitors (Rahaman, Acharia, Beniamini & JG 2025)

- Magnetar Wind Nebula (**MWN** = PRS candidate) is **confined** in a SuperNova Remnant (**SNR**)
- **Can a millisecond-magnetar work?** (Murase et al. 2016; Metzgar et al. 2017; Margalit & Metzgar 2018; Omand et al. 2018; Murase et al. 2021; Bhattacharya et al. 2024)
- **No** – the **compact size** and **minimal age** exclude this!!!

$$t = \frac{R_{\rm SNR}}{v_{\rm SNR}} = R_{\rm SNR}\sqrt{\frac{M_{\rm SNR}}{2(E_{\rm rot}+E_{\rm SN})}}$$

$$\approx \begin{cases} 2.5\ R_{17.3}\ M_3^{\frac{1}{2}}\ P_{\rm i,-3}\ {\rm yr} & \text{for } E_{\rm rot} > E_{\rm SN}, \\ 63.4\ R_{17.3}\ M_{10}^{\frac{1}{2}}\ E_{50}^{-\frac{1}{2}}\ {\rm yr} & \text{for } E_{\rm rot} < E_{\rm SN}. \end{cases}$$

$$E = E_{\rm SN} + E_{\rm rot}$$ (Total SNR Energy)

**This source is already observed for over 13 years**

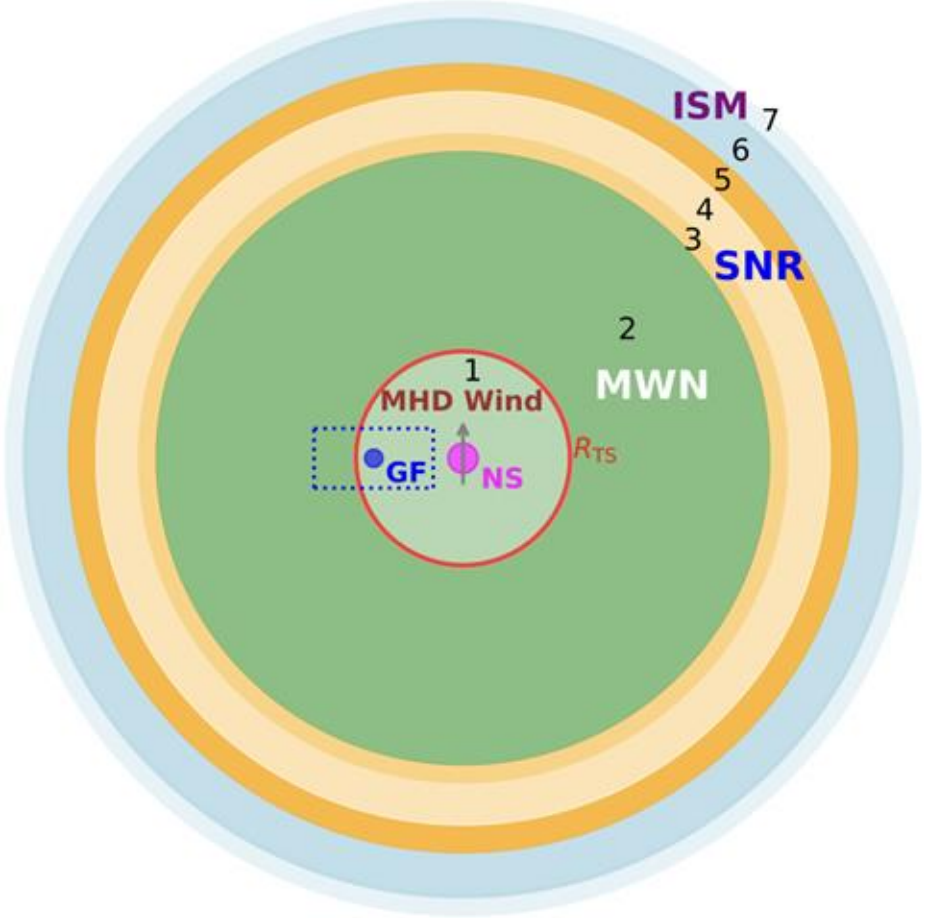

# Persistent Radio Sources (PRSs) of Repeating FRBs: Implications for Magnetar Progenitors (Rahaman, Acharia, Beniamini & JG 2025)

- Equipartition/minimum nebular energy: $E_{\rm eq} \sim 10^{49}$ erg
- To power the FRB: $B_{\rm dip} \geq 10^{14}$ G (Lu & Kumar 2018, Beniamini & Kumar 2025)
- For an age of t > 13 years spindown cannot power the MWN

- After a characteristic time, $t_{\rm switch}$, the nebular energy input is dominated by $B_{\rm int}$ decay
- We require $B_{\rm int}$ decay time: $t_{\rm d} \sim 10^{2.5}$ yr $\gg t_{\rm sd}$ (Other B-powered models need months: Murase+16, Metzger+17, Margalit & Metzgar 18, Omand+18, Murase+21, Bhattacharya+24)

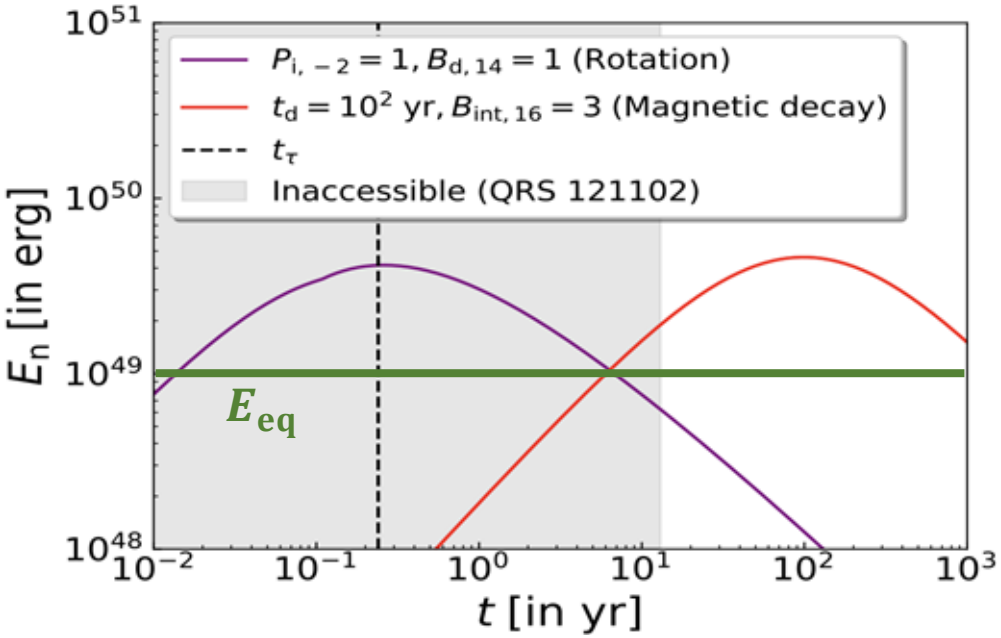


Nebular energy

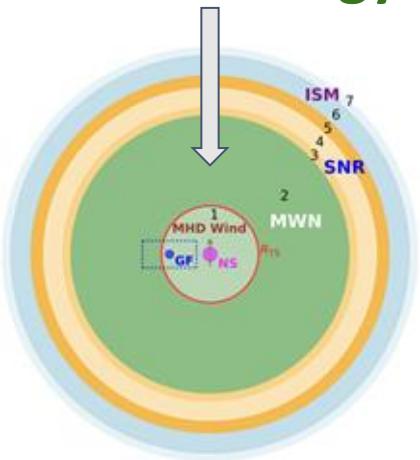


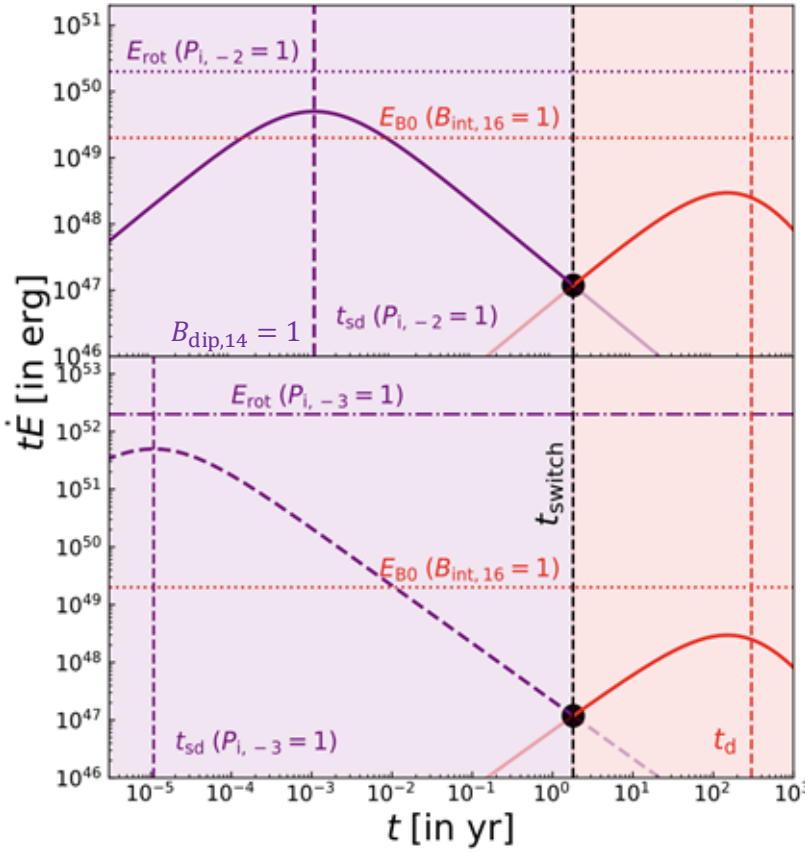

# Persistent Radio Sources (PRSs) of Repeating FRBs: Implications for Magnetar Progenitors (Rahaman, Acharia, Beniamini & JG 2025)

## Model favored by all of the observations: Extreme magnetar & weak SN explosion

- Extreme initial internal B-field: $B_{\rm int} \sim (1-3) \times 10^{16}\,{\rm G}$ with a rather small decay time $t_{\rm d} \sim 10^{2} - 10^{2.5}\,{\rm yr}$
- Weak SN explosion: $E_{\rm SN} \sim 10^{50} - 10^{51}\,{\rm erg}$ given to an an ejected mass of $M_{\rm ej} \sim (3-10) M_{\odot}$
- Age of PRS/FRB source: $13\,{\rm yr} < t \lesssim 100\,{\rm yr}$
- The slowest allowed $B_{\rm int}$ decay time $t_{\rm d,max} \sim 500\,{\rm yr}$ favors a sub-energetic SN explosion $E_{\rm SN} \sim 10^{50}\,{\rm erg}$ with $M_{\rm ej} \gtrsim 10\,M_{\odot}$ & a low-ionization fraction (~3%)
- Similar results hold for the PRS of FRB 20190520B
- PRS of FRB 20201124A is rather poorly constrained

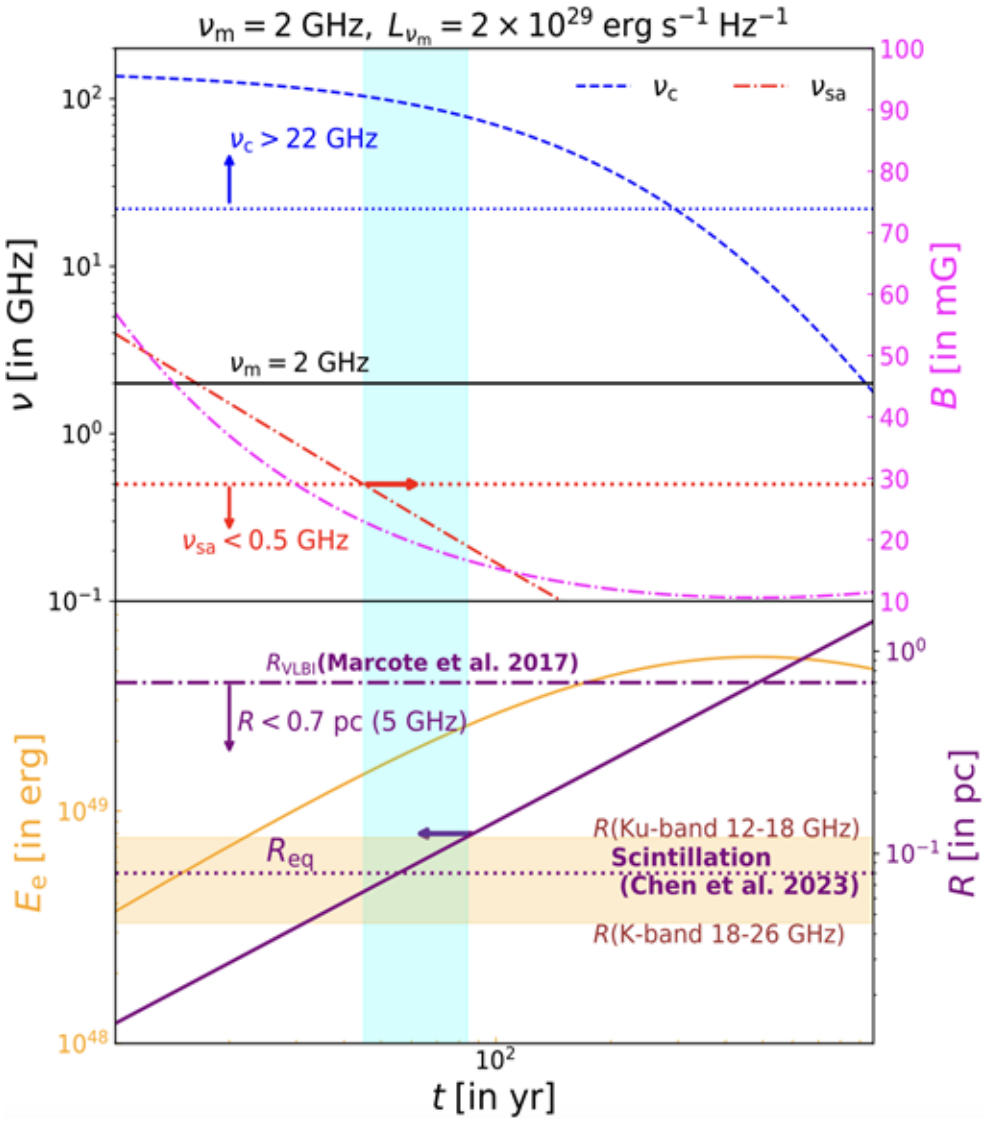

# Extragalactic Magnetar Giant Flares (GFs)

- There are **3 known Galactic GFs** (including the 5.3.1979 GF from SGR 0526-66 in the **LMC**)
- Similar energy in pulsating tail ($\sim 10^{44}$erg ): $e^+e^-\gamma$ that is trapped on closed field lines
- The initial spike energy varies greatly ($E_{\rm spike}/E_{\rm tail} \sim 1-10^{2.5}$): what cannot be trapped
- 2 of the 3 Galactic GFs created a radio nebula, implying $u=\Gamma\beta\sim 1$ outflow: $E_{\rm k}\sim E_{\rm spike}$
- Recently: 10 good candidates for extragalactic GFs (only the initial spike is detectable)
- **Sculptor galaxy** (3.5 Mpc): $\Gamma\sim 100$, $E_{\rm k}\sim E_{\rm spike}\sim 10^{46.5}$erg (similar to SGR 1806−20)

**Observed delay of emission from outflow collision with an external bow-shock sell:** $\Delta t_{\rm obs,r}=\frac{R_{\rm ext}(1-\beta)}{\beta c}\sim\frac{R_{\rm ext}}{2c\Gamma^2}\sim 17 R_{16}\Gamma_2^{-2}$ s

(LAT ~GeV photons at 19, 180, 284 s)

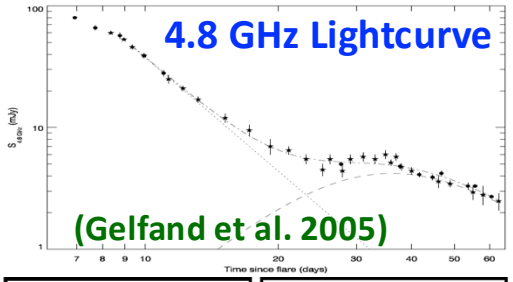


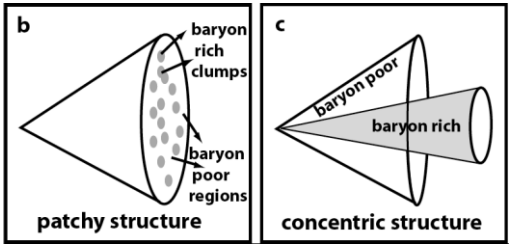


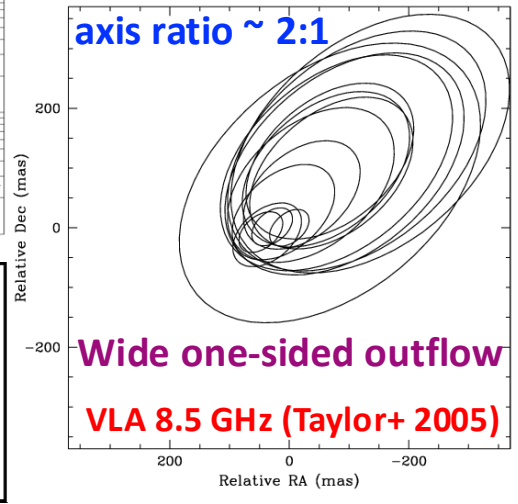


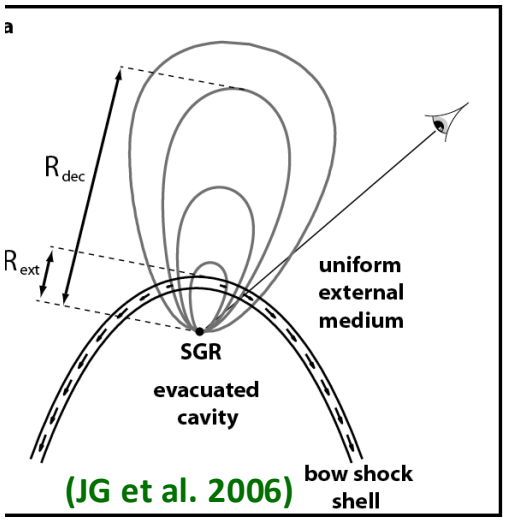


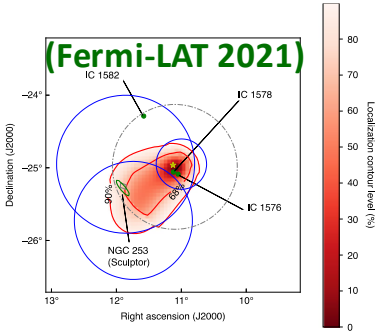


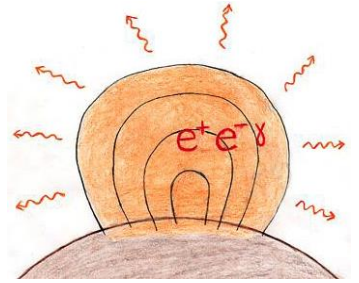


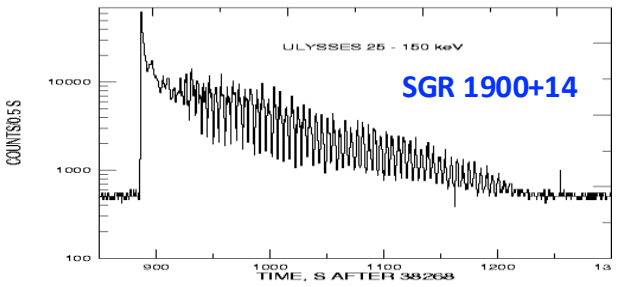


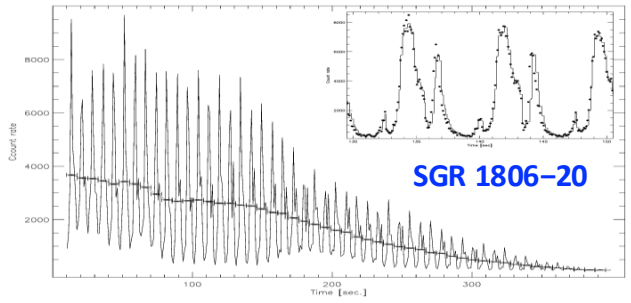

# Extragalactic Magnetar Giant Flares (GFs) (Beniamini et al. 2025)

- Each magnetar is born with initial B-field $B_0$ of energy $E_{B,0}$, which decays on timescale $\tau_{\rm d,0}$ and powers the GFs: $\int dE_t E_t \frac{\partial^2 N}{\partial E_t \partial \tau} = f_{fl}\left|\dot{E}_B\right|$
- Power law energy distribution: $\frac{\partial^2 N}{\partial E_t \partial \tau} \propto E_t^{-s} e^{-E_t/E_{c,t}}$ ($s \approx 1.7$ from obs.) with cutoff energy: $E_{c,t} = f_E f_{\rm dip} E_B(\tau)$, $f_{\rm dip} = E_{\rm dip}/E_B$, $f_{\rm E} = E_{c,t}/E_{\rm dip}$
- Allow beaming: observed isotropic energy $E = E_t/f_b$ ($E_t$ = true energy)
- Allow for a distribution in $B_0$: $\mathrm{P}(B_0) \propto B_0^{-\beta}$ $\quad B_{\rm min} < B_0 < B_{\rm max}$
- Detailed predictions: can constrain magnetar properties by fits to data

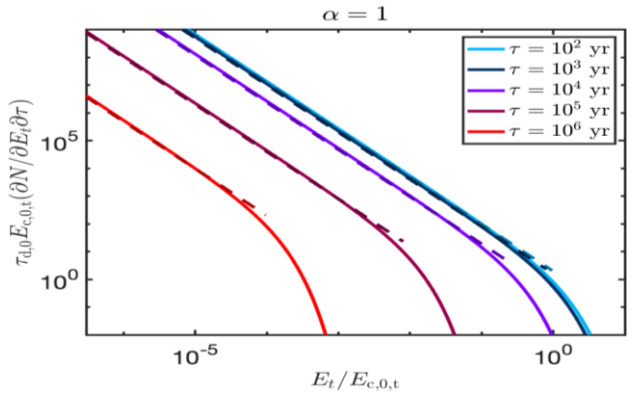


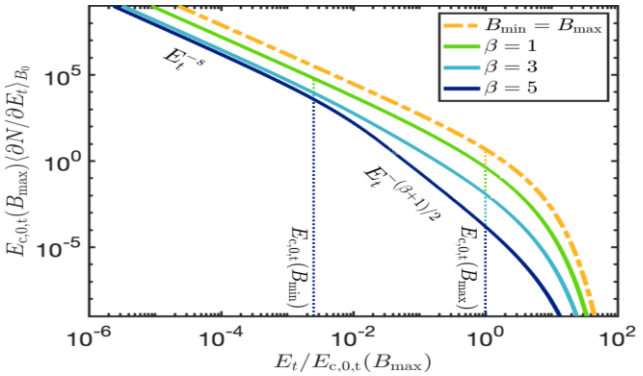


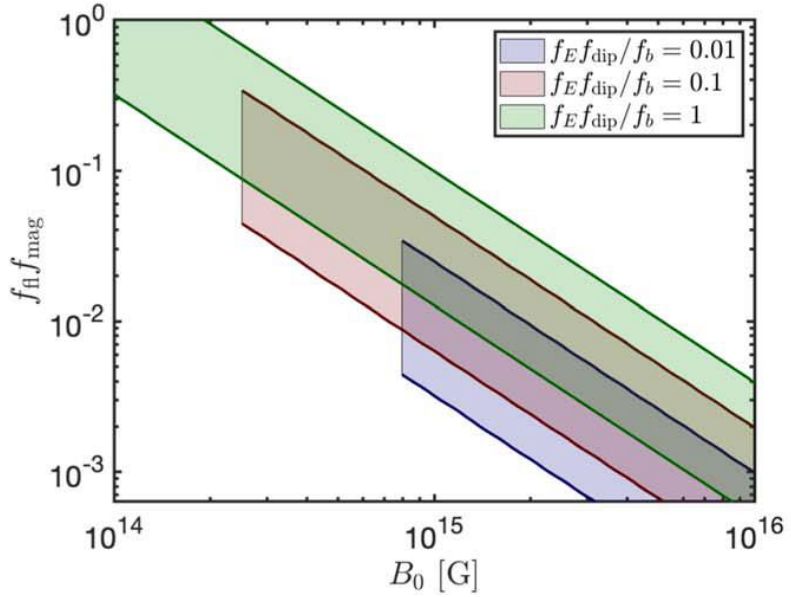


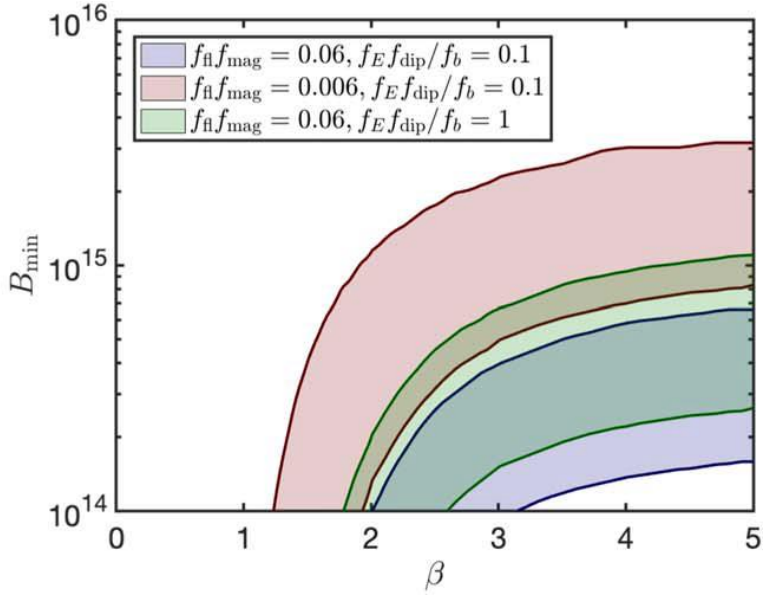


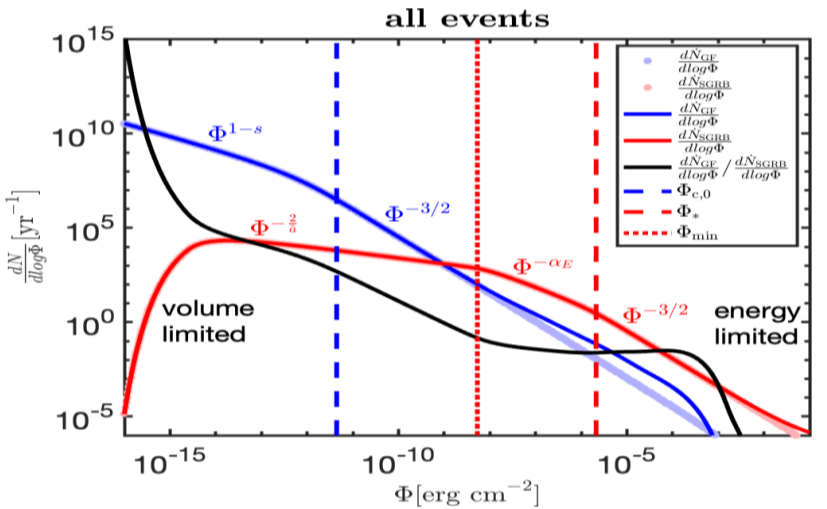

# The End